

AD-A048 966 AIR FORCE INST OF TECH WRIGHT-PATTERSON AFB OHIO SCH--ETC F/G 19/4  
MAGNUS EFFECTS ON BALLISTIC TRAJECTORIES. (U)  
DEC 77 J D SCHNEIDER

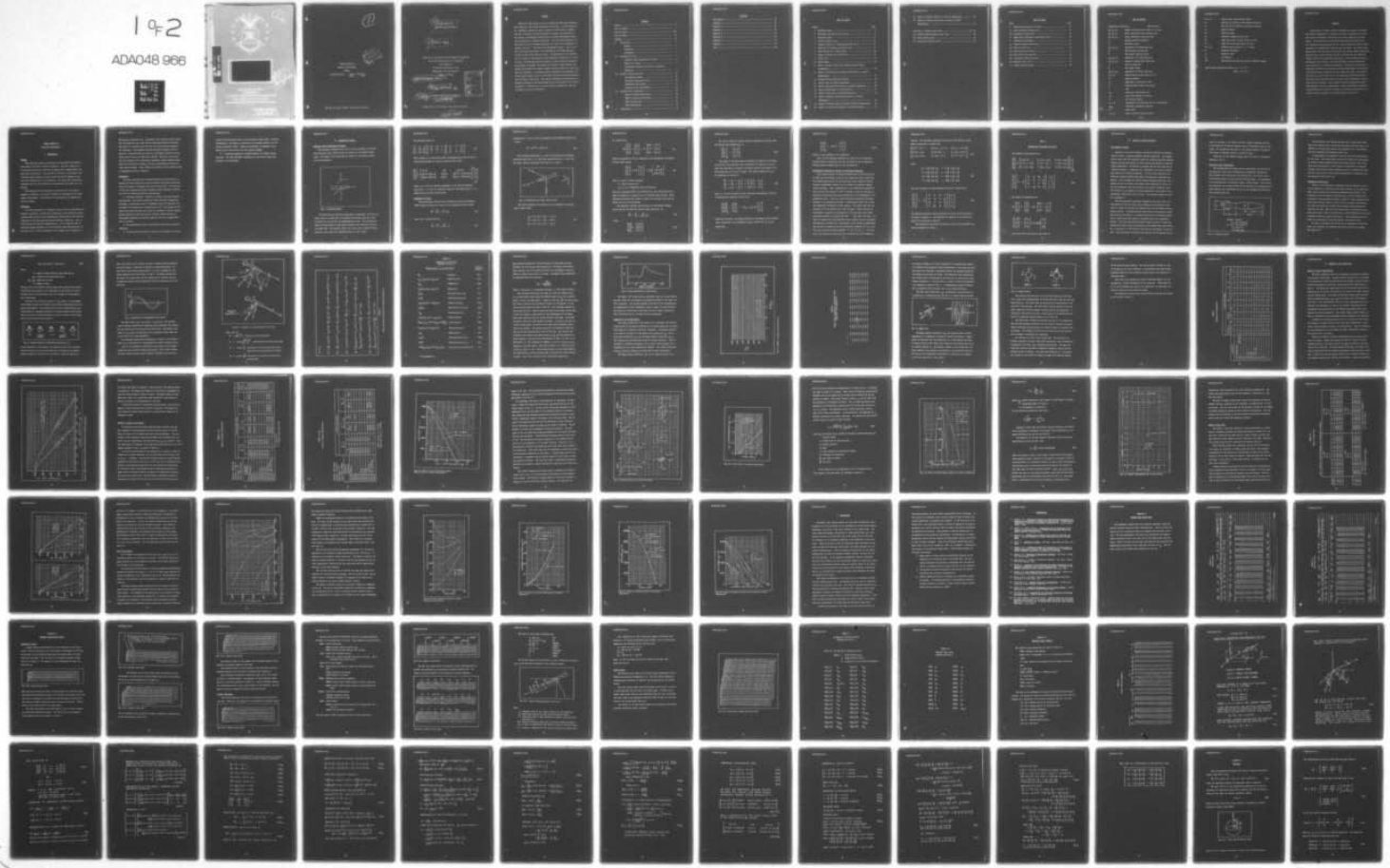
UNCLASSIFIED

AFIT/GA/AA-77D-8

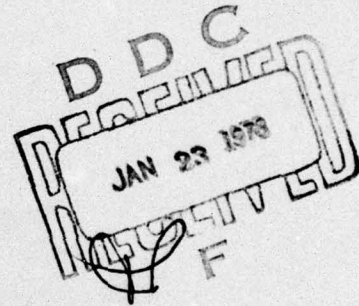
NL

1 of 2

ADA048 966



1



MAGNUS EFFECTS ON  
BALLISTIC TRAJECTORIES

THESIS IS

AFIT/GA/AA-77D-8

James D. Schneider  
Major USAF

Approved for public release, distribution unlimited.

⑨ MAGNUS EFFECTS ON  
BALLISTIC TRAJECTORIES .

⑨ Master's THESIS

Presented to the Faculty of the School of Engineering  
of the Air Force Institute of Technology  
Air University

in Partial Fulfillment of the  
Requirements for the Degree of

Master of Science

⑯ AFIT/GA/AA-77D-8

by

⑩ James D. Schneider  
Major

B.S.  
USAF

⑫ 118P. Graduate Astronautical Engineering

⑪ Dec. - 1977

ACCESSION for	
NTIS	White Section <input checked="" type="checkbox"/>
DDC	Buff Section <input type="checkbox"/>
UNANNOUNCED	
JUSTIFICATION	
BY	
DISTRIBUTION/AVAILABILITY	
Distr.	A
A	

Approved for public release, distribution unlimited.

1473  
012 225

LB

Preface

Most of my time during the past six months has been spent preparing for, working at, and finally completing this project. As time progressed, I managed to develop at least a measure of proficiency in working with the six degree of freedom equations of motion, was introduced to the utility of aerodynamic coefficients, and gained considerable experience working with a computer simulation. This learning experience, unlike most of my rote textbook encounters, was found to be satisfying, rewarding, and real. I also found the professional people I came in contact with during the project to be knowledgeable, motivated engineers willing to share their time and talent. My association with my advisor, Dr. D.W. Breuer of the Aeronautics and Astronautics department, Air Force Institute of Technology; Major Ed Mirmak, Air Force Avionics Laboratory who proposed the project; and Captain Bill Miklos, Flight Dynamics Laboratory who provided the computer program, made the project not only possible but enjoyable. An enormous amount of expertise was available to me through these people as well as from those who have previously documented their efforts in this field. This project represents the conclusion to a personal challenge of the first degree with its own reward at the time of completion. If any part of it is ever useful to anyone else, then all the effort is even more worthwhile.

Contents

Preface .....	ii
List of Figures .....	v
List of Tables .....	viii
List of Symbols .....	ix
Abstract .....	xi
I. Introduction .....	1
Purpose .....	1
Background .....	1
Assumptions .....	2
II. Mathematical Theory .....	4
Reference Frame Transformation Matrix .....	4
Equation of Motion .....	5
Differential Equations of Motion in Rotational Parameters .....	9
III. Method of Problem Solution .....	12
The Computer Program .....	12
Projectile Model Description.....	13
Aerodynamic Coefficients .....	14
Approach to the Investigation .....	23
IV. Results of the Simulations .....	28
Effect of Magnus Coefficients .....	28
Effect of Initial Pitch Motion .....	30
Effect of Spin Rate .....	41
Other Observations .....	44
V. Conclusions .....	51

Contents

Bibliography .....	53
Appendix A .....	54
Appendix B .....	57
Appendix C .....	67
Appendix D .....	69
Appendix E .....	83
Appendix F .....	85
Appendix G .....	99
Vita .....	105

List of Figures

Figure	Page
1 Reference Frames .....	4
2 Rotational and Linear Velocity Axes .....	6
3 Projectile Model .....	13
4 Periodic Change in $C_{l_0}$ .....	15
5 Typical Theoretical vs Experimental Data Curves .....	16
6 Definition of Cross-Spin/Velocity Terms .....	17
7 Force Coefficient vs Mach Number .....	21
8 Change in Magnus Force Coefficient .....	22
9 Magnus Lift .....	24
10 Magnus Moment .....	25
11 Effect of Magnus & Side Force Coefficients on Lateral Displacement .....	29
12 Effect of Pitch Motion and Magnus Coefficients on Lateral Displacement .....	33
13 Projectile Nose Track after Release .....	35
14 Initial Rate of Lateral Displacement .....	36
15 Effect of Initial Side Velocity on Lateral Progression .....	38
16 Lateral Displacement vs Yaw Oscillation .....	40
17 Effect of Spin Rate on Lateral Displacement .....	43
18 Effect of Release Velocity and Altitude on Velocity Progression .....	45
19 Effect of Release Velocity on Total Projectile Acceleration ..	47
20 Effect of Initial Pitch Motion on Lateral Deflection .....	48

21	Effect of Release Velocity on Altitude Progression .....	49
22	Effect of Release Velocity and Altitude on Lateral Displacement .....	50
B-1a thru g Computer Input Cards .....		57 - 61
B-2	Flight Path/Perturbation Angle Input .....	62
B-3	Scale Factor Inputs .....	64
E-1	Local Level Reference Frame .....	83

List of Tables

Table	Page
I Differential Equations of Motion .....	11
II Force and Moment Coefficients .....	18
III Aerodynamic Coefficients .....	19
IV Magnus Force Aerodynamic Coefficient Array .....	23
V Parameters Investigated .....	27
VI Effect of Magnus Coefficients.....	31
VII Effect of Spin Rate .....	42
A-I Wind Tunnel Spin Up Data .....	55
A-II Wind Tunnel Spin Down Data .....	56
B-I Aerodynamic Coefficient Array .....	65
B-II Computer Input Array .....	66
C-I Sample Computer Readout .....	68

List of Symbols

Aerodynamic coefficients	(See Table 3)
$C_L, C_M, C_N$	Moment coefficient about body X, Y, Z axes
$C_x, C_y, C_z$	Force coefficient along inertial axes
$C_X, C_Y, C_Z$	Force coefficient along body axes
$d$	Maximum projectile diameter
$\mathbf{F}$	Net force vector
$F_x, F_y, F_z$	Components of $\mathbf{F}$ along body axes
$g$	Gravitational acceleration
$\bar{h}$	Net angular momentum vector
$h_x, h_y, h_z$	Components of $\bar{h}$ along body axes
$I_x, I_y, I_z$	Moment of inertia about body axes
$m$	Mass of projectile
$\bar{M}$	Net moment vector
$M_x, M_y, M_z$	Components of $\bar{M}$ about body axes
$p, q, r$	Rate of rotation about body X, Y, Z
$Q$	Dynamic pressure
$q''$	Magnitude of cross-spin vector
$S$	Cross-sectional area of projectile
$t$	Time
$t_E$	Simulation termination time
$v_a$	Speed with respect to air mass
$\mathbf{v}$	Net velocity vector
$u, v, w$	Components of $\mathbf{v}$ along body XYZ axes respectively
$y_{min}$	Simulation termination altitude
$w$	Wedge angle
$x, y, z$	Axes of inertial reference frame

X, Y, Z	Axes of body fixed reference frame
x"	Position of inertial x after second rotation 0
z'	New position of inertial z axis after rotation
$\alpha$	Angle of attack
$\beta$	Side slip angle
$\Delta t$	Numerical integration step size
$\phi'$	Angle from cross-velocity vector to Z fin
$\phi''$	Angle from cross-spin vector to Y fin
$\gamma, \theta, \phi$	Rotation about inertial y, z', x" axes
$\lambda$	Rotational parameter
$\eta$	Number of fins
$\rho$	Air density
$\omega^{bi}$	Rotation between body and inertial reference frames

Note for hand printed equations: X,Y,Z = X, Y, Z

$$X.Y.Z = x, y, z$$

## ABSTRACT

A six degree of freedom computer simulation was used to investigate the lateral progression of a free-fall ballistic trajectory due to spin rate, Magnus aerodynamic coefficients and initial projectile pitching motion. The increased spin rate extends the projectile impact point both downrange and cross range due to a slight increase in time of flight generated by a predominately positive angle of attack. The Magnus force, Magnus moment and side force coefficients, under normal release conditions, presents only a minor influence and can be omitted from the simulation without altering the trajectory appreciably. If the release altitude is sufficiently high, however, the small influence of these coefficients could propagate to a correctable magnitude. Projectile oscillations encountered at release can increase the lateral progression of the trajectory significantly, especially for high speed deliveries. Oscillations induced by an initial pitch rate of the projectile generates considerably more lateral deviation than an initial pitch displacement of equivalent maximum amplitude. This increased lateral displacement causes a corresponding decrease in range impact. Other observations concerning the performance of a projectile following a ballistic trajectory are included as support material in the last section of the study.

MAGNUS EFFECTS ON  
BALLISTIC TRAJECTORIES

I. Introduction

Purpose

This study uses computer simulations to investigate three factors that effect a free-fall ballistic trajectory. The first objective is to determine the relative influence of Magnus force, Magnus moment, and side force coefficients. The next area of interest is the effect of oscillatory motion induced by initial pitch rate motion compared to initial pitch displacement of the projectile. The third set of simulations determines how spin rate induced by the projectile fins alters the trajectory.

The development of the equations of motion used in the computer program is included in this study, followed by a discussion of the aerodynamic coefficients. The results of the simulations are presented in the last section.

Background

A ballistic projectile is designed to spin so that a predictable trajectory is generated. Without spin, aerodynamic lift created by non-symmetrical shape resulting from manufacturing imperfections would cause the projectile to fly away from the expected ballistic trajectory. Spin is also required for stability considerations. If the projectile has insufficient angular momentum, it will eventually begin precessing and, if the spin rate is in the neighborhood of the natural pitch frequency, it

may develop catastrophic yaw. Conversely, with excessive angular momentum, the projectile spin axis tends to become gyroscopically oriented with respect to inertial space and will not track properly throughout the trajectory. Conventional bombs are therefore designed so that a spin rate is achieved that will maintain satisfactory stability within either limit of spin rate (Ref 4:64 & 12:29). This spin, while desirable and necessary for a predictable trajectory, induces lateral errors which are attributable to Magnus lift and a gyroscopically induced lateral angle of attack. These effects are additive and can cause the bomb to progressively deviate laterally.

Assumptions

The set of equations that completely describe the trajectory of a spinning ballistic projectile are fully coupled, non-linear expressions that are developed in dynamics texts (such as Ref 4:99). The solutions to this set of equations requires extensive digital computer capability even with the following simplifying assumptions:

1. The earth curvature, variation in terrain, and earth rotation are neglected. For normal conventional weapon delivery airspeeds and altitudes, no significant error is introduced since the range and time of flight of the projectile is sufficiently small. This assumption eliminates the earth reference and allows the advantage of direct transformations between the body and inertial reference frames (See Fig 1). This greatly decreases the required computer time with no appreciable loss in accuracy.
2. The gravitational field is considered uniform over the entire trajectory.
3. The coriolis acceleration is neglected even though it can have

a small but discernable effect on the projectile impact point. For this investigation, the change in trajectory is of primary interest, not the precise trajectory itself. Coriolis acceleration is addressed in Appendix E but is not written into the computer program.

4. A standard atmosphere is assumed adequate for normal release altitudes. The ARDC 1959 Model Atmosphere was used and no winds were included in the simulation.

## II. Mathematical Theory

### Reference Frame Transformation Matrix

The orthogonal reference frame used in this development is the body fixed reference frame (XYZ) moving with respect to the inertial frame (xyz). The origin of the body frame is located at the center of gravity of the projectile.

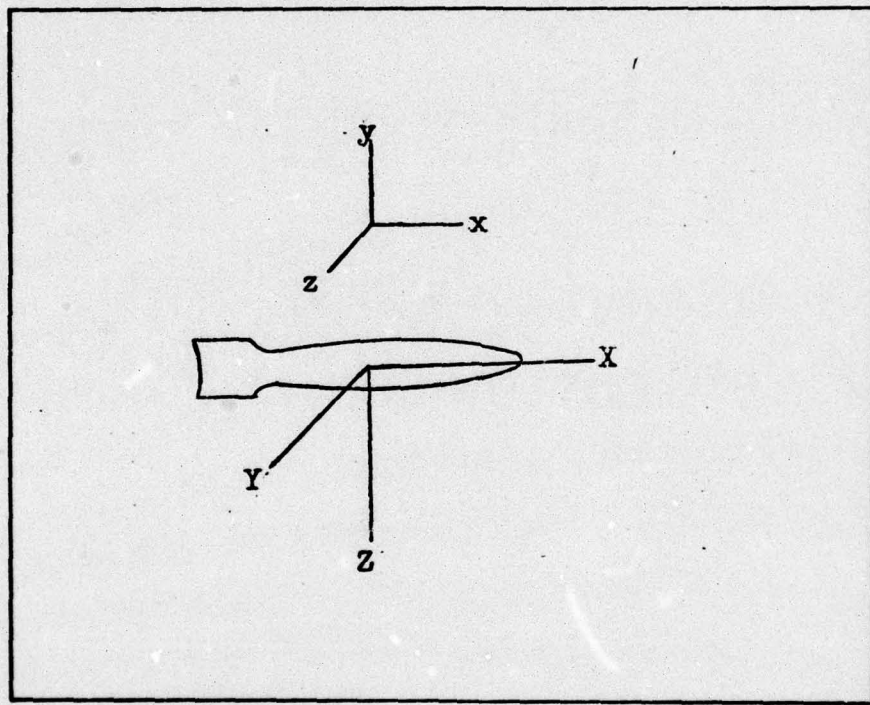


Fig. 1. Reference Frames

To facilitate the direction cosine matrix development, the body reference frame is rotated  $90^\circ$  in the negative direction about the X axis to align the YZ axes with the corresponding yz axes. The following sequence of Euler angles is then used to generate the direction cosine matrix (Ref 2:8): yaw rotation  $\psi$  about the y axis, pitch rotation  $\theta$  about the new z' axis, then roll rotation  $\phi$  about the new x'' axes.

The resulting matrix is:

$$\begin{bmatrix} 1 & 0 & 0 \\ 0 & C\phi & S\phi \\ 0 & -S\phi & C\phi \end{bmatrix} \begin{bmatrix} C\theta & S\theta & 0 \\ -S\theta & C\theta & 0 \\ 0 & 0 & 1 \end{bmatrix} \begin{bmatrix} C\psi & 0 & S\psi \\ 0 & 1 & 0 \\ -S\psi & 0 & C\psi \end{bmatrix} \quad (1)$$

which expands to a single Euler angle transformation so that the set of equations describing the velocity vector is (Ref 7:10):

$$\begin{bmatrix} \dot{x} \\ \dot{y} \\ \dot{z} \end{bmatrix} = \begin{bmatrix} C\psi C\theta & S\theta & C\theta S\psi \\ -S\theta S\psi - C\phi C\psi S\theta & C\phi C\theta & S\phi C\psi - C\phi S\psi S\theta \\ -C\phi S\psi + S\phi C\psi S\theta & -S\phi C\theta & C\phi C\psi + S\phi S\psi S\theta \end{bmatrix}^T \begin{bmatrix} u \\ v \\ w \end{bmatrix} \quad (2)$$

Where  $\dot{x}$ ,  $\dot{y}$ ,  $\dot{z}$  are the velocity components in the inertial reference frame and  $u$ ,  $v$ ,  $w$  are the velocities along the body frame (Fig 2).  $S$ ,  $C$  denotes sine and cosine respectively.

#### Equations of Motion

The relationship between vector derivatives in any two reference frames (where  $\bar{Z}$  denotes any vector) can be expressed as (Ref 6:109):

$$\frac{d}{dt} \bar{Z}^i = \frac{d}{dt} \bar{Z}^b + \bar{\omega}^b \times \bar{Z}^i \quad (3)$$

Then, for a velocity vector  $\bar{V}$

$$\frac{d}{dt} \bar{V}^i = \frac{d}{dt} \bar{V}^b + \bar{\omega}^b \times \bar{V}^i \quad (4)$$

Consequently,  $F = ma = mV$  can be expressed in the reference frame of interest as

$$\bar{F} = m \dot{\bar{V}} + m \bar{\omega} \times \bar{V} \quad (5)$$

The rotational parameters  $p$ ,  $q$ , and  $r$  are defined as the angular velocities about the  $X$ ,  $Y$ ,  $Z$  body axes respectively and  $u$ ,  $v$  and  $w$  are the linear velocity components along the  $X$ ,  $Y$ ,  $Z$  axes:

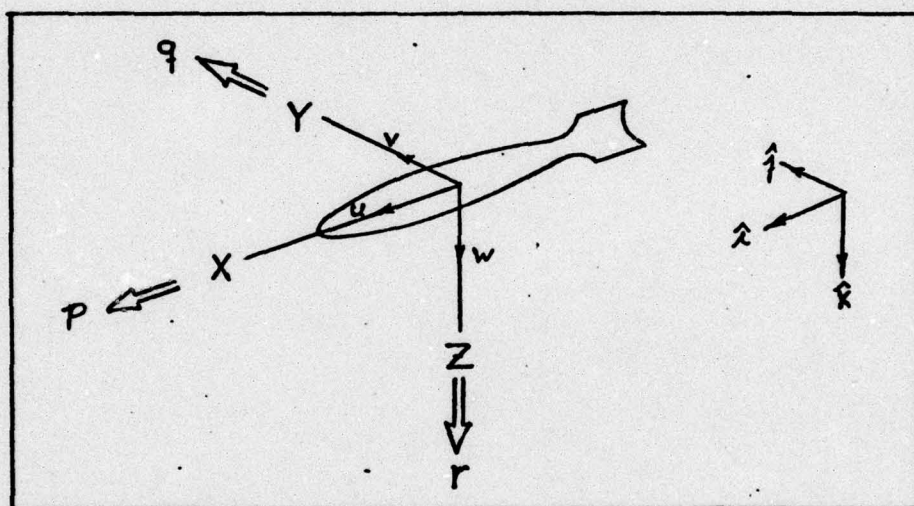


Fig. 2. Rotational and Linear Velocity Axes

The scalar components of equation 5 can be expressed in the body frame as (Ref 4:99):

$$\begin{aligned} F_x &= m(\dot{u} + qw - rv) \\ F_y &= m(\dot{v} + ru - pw) \\ F_z &= m(\dot{w} + pv - qu) \end{aligned} \quad (6)$$

or, equivalently,

$$m \begin{bmatrix} \dot{U} \\ \dot{V} \\ \dot{W} \end{bmatrix} = \begin{bmatrix} F_x \\ F_y \\ F_z \end{bmatrix} - m \begin{bmatrix} qw - rv \\ ru - pw \\ pv - qu \end{bmatrix} \quad (?)$$

where the components of  $\bar{F}$  are expressed as the combination of aerodynamic and weight forces.

$$\begin{bmatrix} F_x \\ F_y \\ F_z \end{bmatrix} = Q S \begin{bmatrix} C_x \\ C_y \\ C_z \end{bmatrix} - mg \begin{bmatrix} s\theta \\ c\phi c\theta \\ -s\phi c\theta \end{bmatrix} \quad (8)$$

where  $Q = \frac{1}{2} \rho v_a^2$  = dynamic pressure

$S$  = cross sectional area

$C_x, C_y, C_z$  = aerodynamic force coefficients

This set of equations (Ref 2:11) describe the three translational degrees of freedom of a projectile as it proceeds along its path. Three additional equations are needed to account for the spin, pitch and yaw motion that will be encountered.

The expression relating the derivative of the angular momentum vector between the body and inertial frame, from Eq 2, is

$$\dot{\bar{h}}^i = \dot{\bar{h}}^b + \bar{\omega}^b \times \bar{h}^i \quad (9)$$

where

$$\begin{bmatrix} h_x \\ h_y \\ h_z \end{bmatrix} = \begin{bmatrix} I_x p \\ I_y q \\ I_z r \end{bmatrix} \quad (10)$$

The rate of change of angular momentum expressed in the body frame, for constant mass projectiles, is

$$\begin{bmatrix} \dot{h}_x \\ \dot{h}_y \\ \dot{h}_z \end{bmatrix}_b = \begin{bmatrix} I_x \dot{P} \\ I_y \dot{q} \\ I_z \dot{r} \end{bmatrix} \quad (11)$$

The origin of the body frame of reference is located at the center of gravity of the projectile which eliminates the products of inertia since the body frame is located on principal axes and the moment of inertia about the y & z axes are equal. The scalar components of Eq 9 can therefore be written as

$$\begin{aligned} \dot{h}_x^i &= M_x = I_x \dot{P} + qr [I_z - I_y] \\ \dot{h}_y^i &= M_y = I_y \dot{q} + pr [I_x - I_z] \\ \dot{h}_z^i &= M_z = I_z \dot{r} + pq [I_y - I_x] \end{aligned} \quad (12)$$

Since  $I_y = I_z$  for a projectile with rotational mass symmetry, this set is equivalently presented as (Ref 2:11):

$$\begin{bmatrix} I_x \dot{P} \\ I_y \dot{q} \\ I_z \dot{r} \end{bmatrix}_b = \begin{bmatrix} M_x \\ M_y \\ M_z \end{bmatrix} - (I_y - I_x) P \begin{bmatrix} 0 \\ -r \\ q \end{bmatrix} \quad (13)$$

where the M vector is the moment produced by aerodynamic forces expressed as a function of the aerodynamic moment coefficients  $C_L$ ,  $C_M$ ,  $C_N$  (Ref 2:12):

$$\begin{bmatrix} M_x \\ M_y \\ M_z \end{bmatrix} = Q S d \begin{bmatrix} C_L \\ C_M \\ C_N \end{bmatrix} \quad (14)$$

where  $d$  is the diameter of the projectile.

Eqs 7 and 13 completely describe the motion of a six degree-of-freedom ballistic projectile and form the basis of the six degree-of-freedom computer program used in this investigation.

#### Differential Equations of Motion in Rotational Parameters

Euler angles provide an effective description of body orientation in space and the heading, pitch and roll angles are easily visualized. The transformation matrix of nine direction cosine elements, however, requires considerable computer time to process the numerous trigonometric functions. Also, singularities in the differential equations arise when the pitch angle of  $\pm 90^\circ$  is reached, as well as inducing unacceptable truncation error when integrating in the neighborhood of the singularity point. The use of Euler rotational parameters (sometimes referred to as quaternions) provide a computational device that avoids the singularity limitation of Euler angles. This system uses four parameters to fix the position of a body in space: three direction cosine angles to specify the orientation of the spin axis, and another rotational parameter to specify the amount of spin about that axis. Instead of working with nine direction cosine elements and six constraint equations from the Euler set, the problem is now reduced to expressions for the rate of change of the four quaternion parameters ( $\dot{\lambda}_1, \dot{\lambda}_2, \dot{\lambda}_3, \dot{\lambda}_0$ ) and a single constraint equation  $\lambda_1^2 + \lambda_2^2 + \lambda_3^2 + \lambda_0^2 = 1$ . The computer time required to solve this set is reduced but still remains ex-

tensive. The rotational parameter equivalent of the direction cosine matrix of equation 2 is (Ref 2:7):

$$\begin{bmatrix} 2(\lambda_0^2 + \lambda_1^2) - 1 & 2(\lambda_1\lambda_2 + \lambda_0\lambda_3) & 2(\lambda_1\lambda_3 - \lambda_0\lambda_2) \\ 2(\lambda_1\lambda_2 - \lambda_0\lambda_3) & 2(\lambda_0^2 + \lambda_2^2) - 1 & 2(\lambda_2\lambda_3 + \lambda_0\lambda_1) \\ 2(\lambda_1\lambda_3 + \lambda_0\lambda_2) & 2(\lambda_2\lambda_3 - \lambda_0\lambda_1) & 2(\lambda_0^2 + \lambda_3^2) - 1 \end{bmatrix} \quad (15)$$

where

$$\begin{aligned} \lambda_0 &= C\frac{\phi}{2} C\frac{\theta}{2} C\frac{\psi}{2} + S\frac{\phi}{2} S\frac{\theta}{2} S\frac{\psi}{2} \\ \lambda_1 &= C\frac{\phi}{2} S\frac{\theta}{2} S\frac{\psi}{2} + S\frac{\phi}{2} C\frac{\theta}{2} C\frac{\psi}{2} \\ \lambda_2 &= C\frac{\phi}{2} C\frac{\theta}{2} S\frac{\psi}{2} + S\frac{\phi}{2} S\frac{\theta}{2} C\frac{\psi}{2} \\ \lambda_3 &= C\frac{\phi}{2} S\frac{\theta}{2} C\frac{\psi}{2} + S\frac{\phi}{2} C\frac{\theta}{2} S\frac{\psi}{2} \end{aligned} \quad (16)$$

The rate of change of these parameters are given by (Ref 2:10):

$$\begin{bmatrix} \dot{\lambda}_0 \\ \dot{\lambda}_1 \\ \dot{\lambda}_2 \\ \dot{\lambda}_3 \end{bmatrix} = -\frac{1}{2} \begin{bmatrix} 0 & p & q & r \\ -p & 0 & -r & q \\ -q & r & 0 & -p \\ -r & -q & p & 0 \end{bmatrix} \begin{bmatrix} \lambda_0 \\ \lambda_1 \\ \lambda_2 \\ \lambda_3 \end{bmatrix} \quad (17)$$

The algebra required to develop equations 15 and 16 is quite extensive as shown in Appendix D. The derivation of equation 17 is found in Appendix B of reference 2, page 11.

The differential equations of motion are now in the programmed form and are summarized in Table I.

Table I

Differential Equations of Motion

The kinematic relationships are:

$$\begin{bmatrix} \dot{x} \\ \dot{y} \\ \dot{z} \end{bmatrix} = \begin{bmatrix} 2(\lambda_0^2 + \lambda_1^2) - 1 & 2(\lambda_1\lambda_2 + \lambda_0\lambda_3) & 2(\lambda_1\lambda_3 - \lambda_0\lambda_2) \\ 2(\lambda_1\lambda_2 - \lambda_0\lambda_3) & 2(\lambda_0^2 + \lambda_2^2) - 1 & 2(\lambda_2\lambda_3 + \lambda_0\lambda_1) \\ 2(\lambda_1\lambda_3 + \lambda_0\lambda_2) & 2(\lambda_2\lambda_3 - \lambda_0\lambda_1) & 2(\lambda_0^2 + \lambda_3^2) - 1 \end{bmatrix} \begin{bmatrix} u \\ v \\ w \end{bmatrix} \quad (18)$$

$$\begin{bmatrix} \dot{\lambda}_0 \\ \dot{\lambda}_1 \\ \dot{\lambda}_2 \\ \dot{\lambda}_3 \end{bmatrix} = -\frac{1}{2} \begin{bmatrix} 0 & p & q & r \\ -p & 0 & -r & q \\ -q & r & 0 & -p \\ -r & -q & p & 0 \end{bmatrix} \begin{bmatrix} \lambda_0 \\ \lambda_1 \\ \lambda_2 \\ \lambda_3 \end{bmatrix} \quad (19)$$

The dynamic relationships are:

$$m \begin{bmatrix} \dot{u} \\ \dot{v} \\ \dot{w} \end{bmatrix} = \begin{bmatrix} F_x \\ F_y \\ F_z \end{bmatrix} - m \begin{bmatrix} qw - rv \\ ru - pw \\ pv - qu \end{bmatrix} \quad (20)$$

$$\begin{bmatrix} I_x \dot{P} \\ I_y \dot{q} \\ I_z \dot{r} \end{bmatrix} = \begin{bmatrix} M_x \\ M_y \\ M_z \end{bmatrix} - (I_y - I_x) P \begin{bmatrix} 0 \\ -r \\ q \end{bmatrix} \quad (21)$$

where  $\bar{F}$  and  $\bar{M}$  are described in Eqs 8 and 14.

### III. Method of Problem Solution

#### The Computer Program

Solution of the set of coupled, non-linear differential equations listed in Table I requires extensive computer capability. The program used in this study was originally coded for the Naval Ordnance Research Computer and has been updated as more advanced generations of computers became operational. The Fortran IV program used for this study was developed by Charles W. Ingram and R.S. Eikenberry using Cohen & Werners' work (Ref 2) as a point of departure. It was written originally for stability analysis applications rather than precision trajectory prediction. The six degree of freedom computer program numerically integrates the set of kinematic and dynamic Euler equations of Table I in the body reference frame and outputs in the inertial reference frame. The accuracy of the program is limited primarily by the quality of the aerodynamic coefficients that are input. The complete program is listed in Appendix F.

Both the Runge-Kutta numerical integration step size (value of A-(20) Table B-2) and the output time increment can be adjusted by the user as a means of tailoring the computer time and cost against the accuracy required. If high projectile spin rates are encountered, coarse step sizes on the order of .01 second could result in erroneous outputs due to insufficient data points to properly resolve the integration problem. The time step should be small enough to provide at least ten integration steps during one revolution of the highest spin rate expected. A step size of .002 second is used for most simulations in this report. Since extensive core memory and computer time is required to pro-

cess this program, it is written for only a single trajectory per run. A core memory of 100,000 was adequate for all trajectories used in this study. (An integration step size of .001 second requires in excess of 200 seconds of computer time for a 10,000 ft drop.)

Discussion of the computer program input and output is included in Appendices B and C.

#### Projectile Model Description

The standard Mark 82 warhead with an experimental tail section was the projectile model used to determine the aerodynamic coefficients. The cylindrical aft section has four slotted fins, each fitted with a trailing edge wedge to provide the roll driving moment. The designation of the configuration is FFSW (fin, fixed, slotted, wedge). This particular projectile was selected because of the similarity to existing conventional weapons and, significantly, most of the aerodynamic coefficients were available (Ref 14).

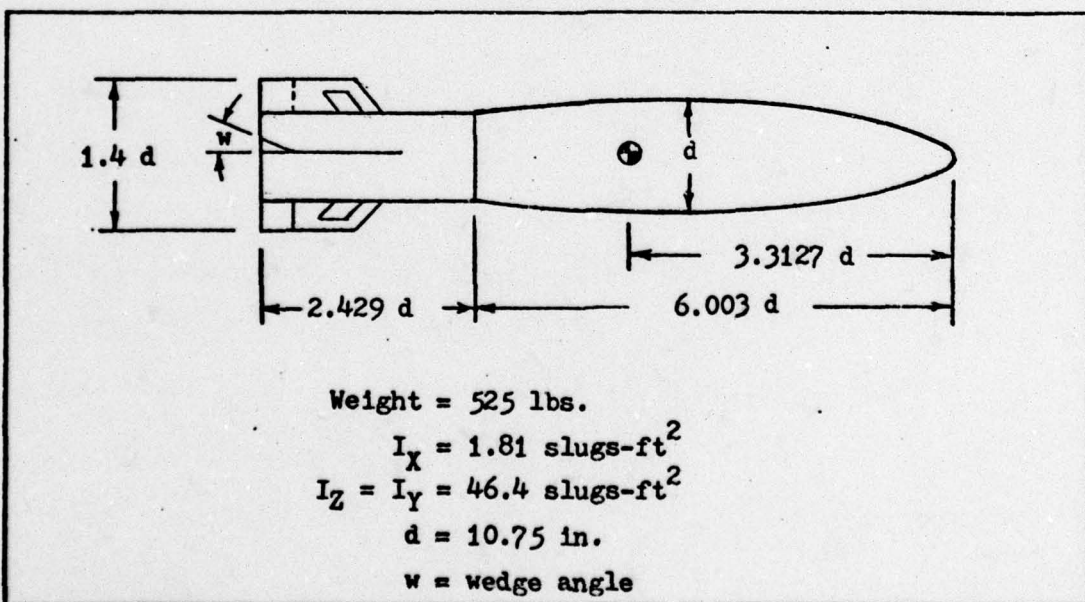


Fig. 3. Projectile Model

The cylindrical tail section provides both a higher drag coefficient and a housing for an inflatable high drag device that may be installed; the slotted fins increase the probability of a well-behaved roll rate throughout the trajectory (Ref 3:1).

A wedge angle of ten degrees is used for most of the simulations in this study. This wedge angle provides sufficient roll acceleration to overcome adverse dynamics encountered during release. The steady state spin rate produced is fast enough to investigate the influence of Magnus coefficients without inducing the type of instabilities that can occur when the spin rate exceeds approximately ten times the nutation frequency (Ref 8; Sec 3,5).

#### Aerodynamic Coefficients

Values of the aerodynamic coefficients used in equations 8 and 14 must be adequately determined by wind tunnel testing of the projectile model before satisfactory trajectory simulations are possible. The aerodynamic force and moment coefficients can, for most applications, be reduced to the expressions listed in Table II. These expressions include cross-velocity terms in both the force and moment coefficients, but cross spin terms are included only in moment coefficients about pitch and yaw axes. (See Fig 6 for definitions of cross-velocity and cross spin terms.) Table III describes the terms which make up the total aerodynamic force and moment coefficients. These mathematical expressions were determined in Cohen and Werners' work (Ref 2:15-19).

In order to illustrate the utility of the aerodynamic coefficient terms, the expression for induced roll moment is used as an example (See Table III):

$$C_{l_0} + C_{l_7} \sin \eta \phi' + C_{l_8} \cos \eta \phi' \quad (22)$$

where

$\phi'$  = Angle to cross velocity vector (See Fig 6)

$C_{l_0}$  = Initial curve shift (See Fig 5)

$C_{l_7}, C_{l_8}$  = Amplitude of curve

$\eta$  = Number of fins

The  $C_{l_0}$  term is the residual rolling moment that remains after the projectile has been aligned in the wind tunnel at the angle of attack of interest with no fin deflection; that is, an index of rolling moment due to body shape.

The next set of terms,  $C_{l_7} \sin \eta \phi' + C_{l_8} \cos \eta \phi'$ , is the mathematical format required to describe the data curve obtained from the wind tunnel measurements. This application can best be appreciated by the illustration of a spinning projectile at various stages of roll moving away at an angle of attack sufficient to cause a vortex to trail along the top of the missile as in Figure 4.

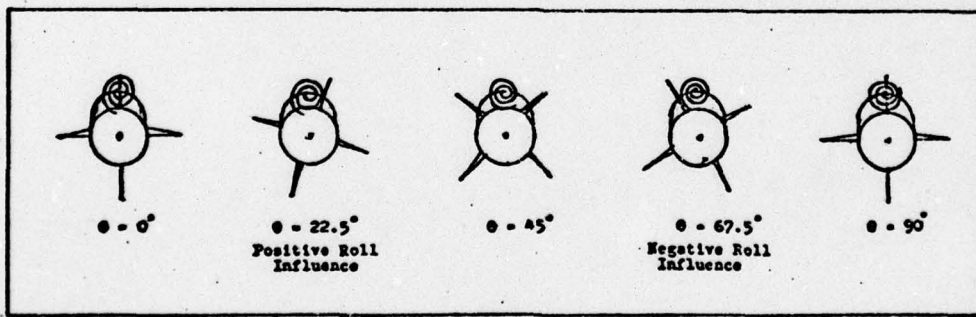


Fig. 4. Periodic Change in Aerodynamic Coefficient  $C_{l_0}$

At the beginning of the sequence, the trailing vortex is cut symmetrically by the fin, so no net roll influence is imposed by the dynamic pressure change on the fin due to the vortex. After 22.5 degrees of

roll, the vortex is in a position to exert a maximum rolling influence. At the  $45^\circ$  angle, a condition of symmetry is again encountered. For this type of oscillating characteristic,  $C_x$  could be graphed for the entire sequence as the solid curve of Fig 5. The graph obtained from the actual wind tunnel data for the coefficient of interest, however, is generally skewed from the theoretical curve as indicated by the dotted curve.

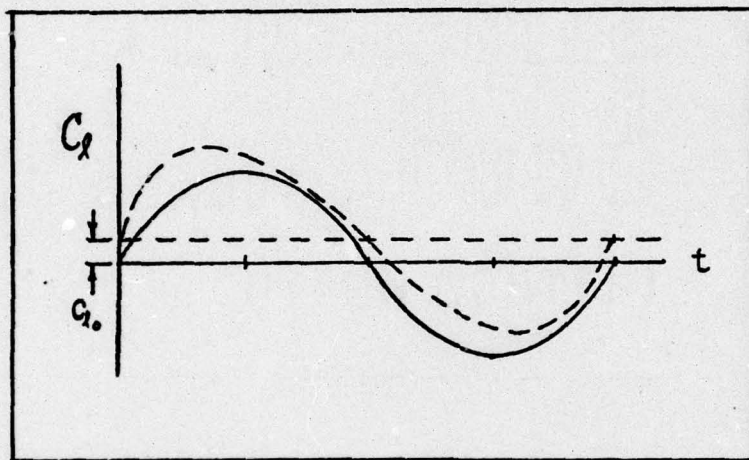


Fig. 5. Theoretical vs Experimental Data Curves

The three terms,  $C_{x_0} + C_{x_7} \sin\eta\phi' + C_{x_8} \cos\eta\phi'$ , are therefore used in whatever combination of magnitudes and sinusoidals that produce the best simulation of the actual wind tunnel data. The relative magnitude of  $C_{x_0}$  versus the amplitude of the sinusoidals often makes one or the other of the terms negligible.

The remaining trigonometric expressions in Table II not defined in Table III are attributable to transformations between reference frames.

Most of the aerodynamic coefficient arrays used in this computer program had been previously determined through a joint effort between the Naval Surface Weapons Center, Dahlgren Laboratory, and the Aero-

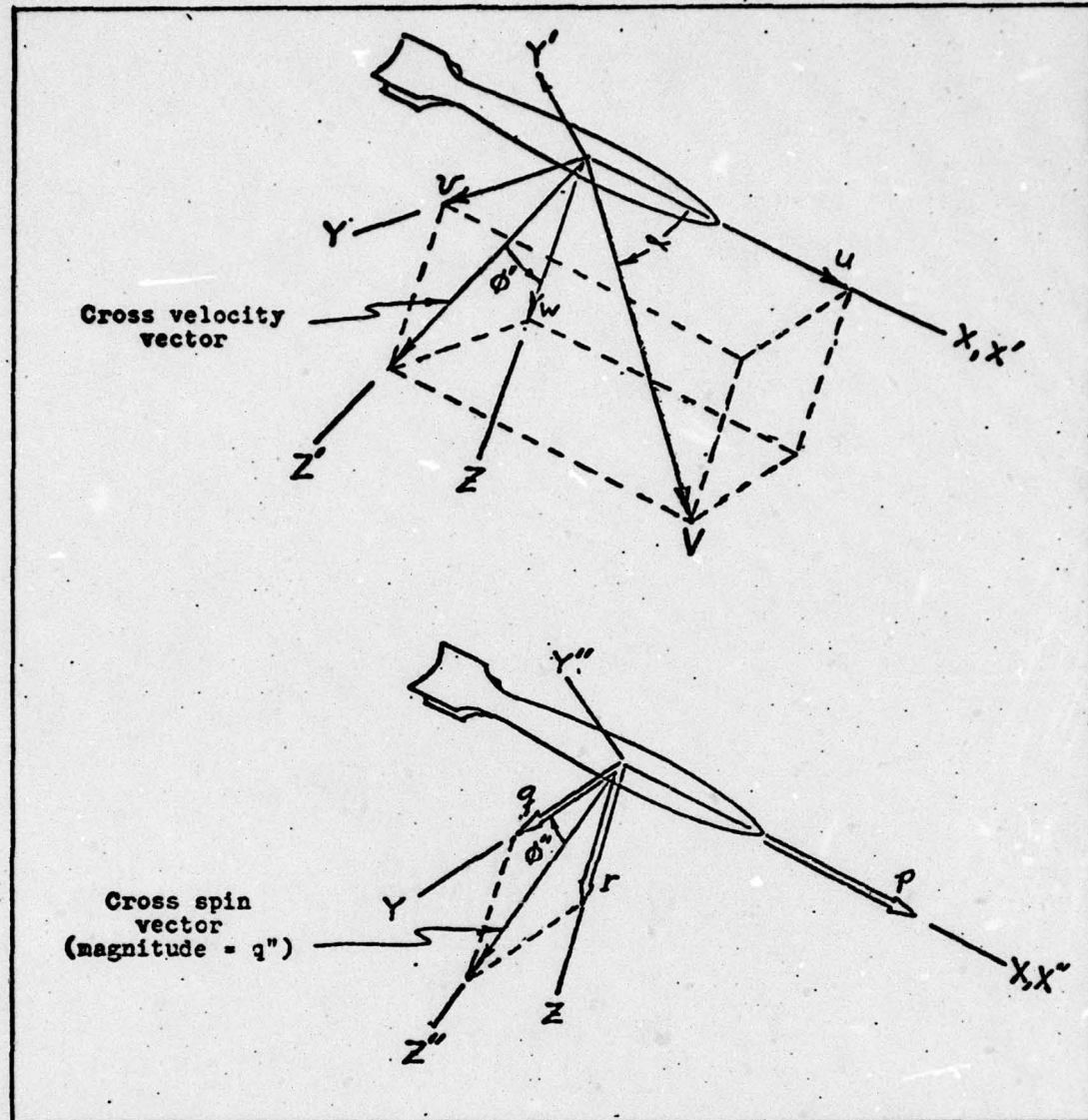


Fig. 6 . Definition of Cross-Spin/Velocity Terms.

where (Ref 2)

$$q'' = \sqrt{q^2 + r^2} , \text{ magnitude of cross-spin (rad/sec)}$$

$$\alpha = \text{arc tan } \sqrt{\frac{v^2 + w^2}{u}} , \text{ magnitude of yaw or angle of attack (deg)}$$

$$\phi'' = \text{arc tan } \frac{v}{w} \text{ (angle about X-axis from cross-velocity vector of the center of gravity of missile to Z sin) (deg)}$$

$$\phi'' = \text{arc tan } \frac{(-r)}{q} \text{ angle about the X-axis from cross-spin vector to Y sin) (deg)}$$

$$C_x = C_x$$

$$C_y = [C_{y_0} + C_{y_7} \sin \eta \phi' + C_{y_8} \cos \eta \phi' + \frac{Pd}{2V_a} C_{y_p}] \cos \phi' + [C_{z_0} + C_{z_7} \sin \eta \phi' + C_{z_8} \cos \eta \phi'] \sin \phi' + C_{y_4}(\epsilon)$$

$$C_z = [C_{y_0} + C_{y_7} \sin \eta \phi' + C_{y_8} \cos \eta \phi' + \frac{Pd}{2V_a} C_{y_p}] (-\sin \phi') + [C_{z_0} + C_{z_7} \sin \eta \phi' + C_{z_8} \cos \eta \phi'] \cos \phi' + C_z(\epsilon)$$

$$C_L = C_{x_0} + C_{x_7} \sin \eta \phi' + C_{x_8} \cos \eta \phi' + \frac{Pd}{2V_a} C_{x_p} \cos \phi' + \alpha (C_{L_0} \hat{\delta}_0 + C_{L_7} \hat{\delta}_7 \sin \phi' + C_{L_8} \hat{\delta}_8 \cos \phi')$$

$$C_M = [C_{m_0} + C_{m_7} \sin \eta \phi' + C_{m_8} \cos \eta \phi'] \cos \phi' + [C_{n_0} + C_{n_7} \sin \eta \phi' + C_{n_8} \cos \eta \phi' + \frac{Pd}{2V_a} C_{n_p}] \sin \phi' \\ + [C_{mq_0} + C_{mq_7} \sin \eta \phi'' + C_{mq_8} \cos \eta \phi''] \frac{q''d}{2V_a} \cos \phi'' + C_{m_4}(\epsilon)$$

$$C_N = [C_{m_0} + C_{m_7} \sin \eta \phi' + C_{m_8} \cos \eta \phi'] (-\sin \phi') + [C_{n_0} + C_{n_7} \sin \eta \phi' + C_{n_8} \cos \eta \phi' + \frac{Pd}{2V_a} C_{n_p}] \cos \phi' \\ + [C_{mq_0} + C_{mq_7} \sin \eta \phi'' + C_{mq_8} \cos \eta \phi''] \frac{q''d}{2V_a} (-\sin \phi'') + C_n(\epsilon)$$

TABLE II

Force And Moment Coefficients (Adapted from Ref 2)

TABLE III

Aerodynamic Coefficients  
(Adapted from Ref 2)

<u>Description of Coefficient</u>		<u>Array Symbol *</u>
$C_x$	Axial force	CX
$C_{y_0} + C_{y_7} \sin \eta \phi' + C_{y_8} \cos \eta \phi'$	Induced side force	CY?
$C_{y_p}$	Magnus force	CYP
$C_{z_0} + C_{z_7} \sin \eta \phi' + C_{z_8} \cos \eta \phi'$	Normal force	CZ
$C_y (\epsilon)$	Trim force along Y-axis	N/A
$C_z (\epsilon)$	Trim force along Z-axis	N/A
$C_{l_0} + C_{l_7} \sin \eta \phi' + C_{l_8} \cos \eta \phi'$	Induced roll moment	CLGA
$C_l (\delta w)$	roll moment due to fin cant	CLDW
$C_{l_p}$	Roll damping moment	CLP
$C_{m_0} + C_{m_7} \sin \eta \phi' + C_{m_8} \cos \eta \phi'$	Restoring moment	CM
$[C_{m_{q0}} + C_{m_{q7}} \sin \eta \phi'' + C_{m_{q8}} \cos \eta \phi''] \frac{d}{2 V_s}$	Damping moment	CMQ
$C_{n_0} + C_{n_7} \sin \eta \phi' + C_{n_8} \cos \eta \phi'$	Induced side moment	CNGA
$C_{n_p}$	Magnus moment	CNP
$C_m (\epsilon)$	Trim moment about y-axis	CMDE
$C_n (\epsilon)$	Trim moment about z-axis	N/A
$\& (C_{le\alpha_0} + C_{le\alpha_1} \sin \phi' + C_{le\alpha_2} \cos \phi')$	Roll moment due to eccentric tail	N/A

\* See Appendix G

space Research Laboratory, Wright-Patterson Air Force Base and were available for this project (See Appendix G). The Magnus force coefficient, however, was not available and had to be determined so that its effect on lateral error could be studied. The Magnus force coefficient is determined from the definition

$$C_{y_p} = \frac{\partial C_y}{\partial (pd/2V)} \quad (23)$$

where  $p$  = spin rate,  $d$  = projectile diameter,  $V$  = wind tunnel velocity.

This relation states that the slope of a line fit through a plot of  $C_y$  versus  $pd/2V$  should yield the nominal value of  $C_{y_p}$  for a specific angle of attack and Mach number. Tables A-I and A-II show the wind tunnel data taken at Mach 0.8 at an angle of attack of 1.87 degrees.  $C_y$  was plotted against  $pd/2V$  and then a "best fit" line was drawn through the data points (Fig 8). Greater weight was given to the lower values  $pd/2V$  so that the cluster of data points in the neighborhood of the steady state spin condition would not overly influence the slope. No attempt was made to force the line through the origin. As long as the axis intercept remains small, the error in the wind tunnel measuring instruments will dominate. The primary objective is to provide a best estimate of the most representative slope of the plot. The slope of the resulting line produced the nominal value of  $C_{y_p}$  that was entered as a single element in the CYP array corresponding to Mach = 0.8 and  $\alpha = 2$  (Ref Table IV). The remaining 71 elements of the  $8 \times 9$  matrix were determined in the same manner. Note that the Mach = 0.4 values are used to fill the Mach = 0 row. This is done because, at lower Mach numbers, the compressibility effects diminish and the coefficient remains nearly constant. Fig. 7 shows a typical force coefficient progression.

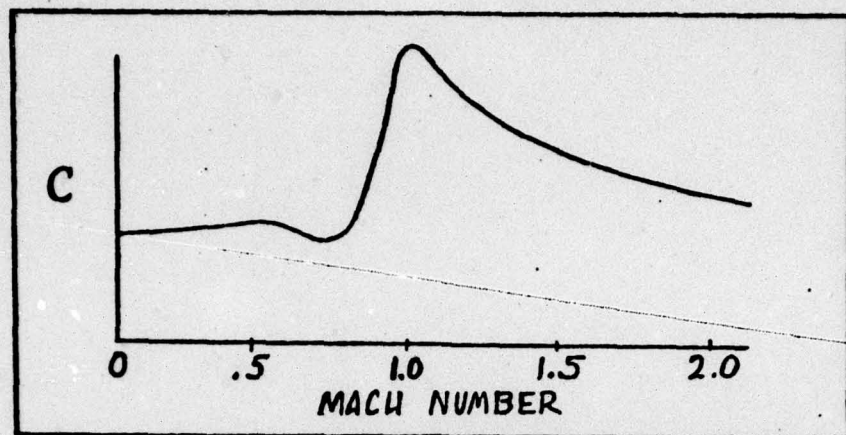


Fig. 7. Force Coefficient vs Mach Number

The  $\alpha = 50^\circ$  column contains unreliable data but is used only to provide a value for the program to interpolate against in the event  $\alpha \leq 25^\circ$  is exceeded. The computer program is written so that interpolation is accomplished for any intermediate value of angle of attack and Mach. The angles of attack used in this study were well below 25 degrees so this ill-defined edge of the array was not encountered.

#### Approach to the Investigation

The primary objective of this study is to investigate the relative contributions of the Magnus coefficients to lateral deflection of a spinning projectile following a ballistic trajectory. The general approach is to isolate the effect of the Magnus force coefficient  $C_{y_p}$ , the induced side coefficient  $C_{y_\gamma}$ , and the Magnus moment coefficient  $C_{n_p}$  on the trajectories initiated from identical release conditions. Each coefficient is studied individually, and in pairs; then compared to the performance of all three coefficients together. The initial conditions include a range of airspeed, altitudes and attitude perturbations.

The Magnus force coefficient,  $C_{y_p}$ , is of interest because it is

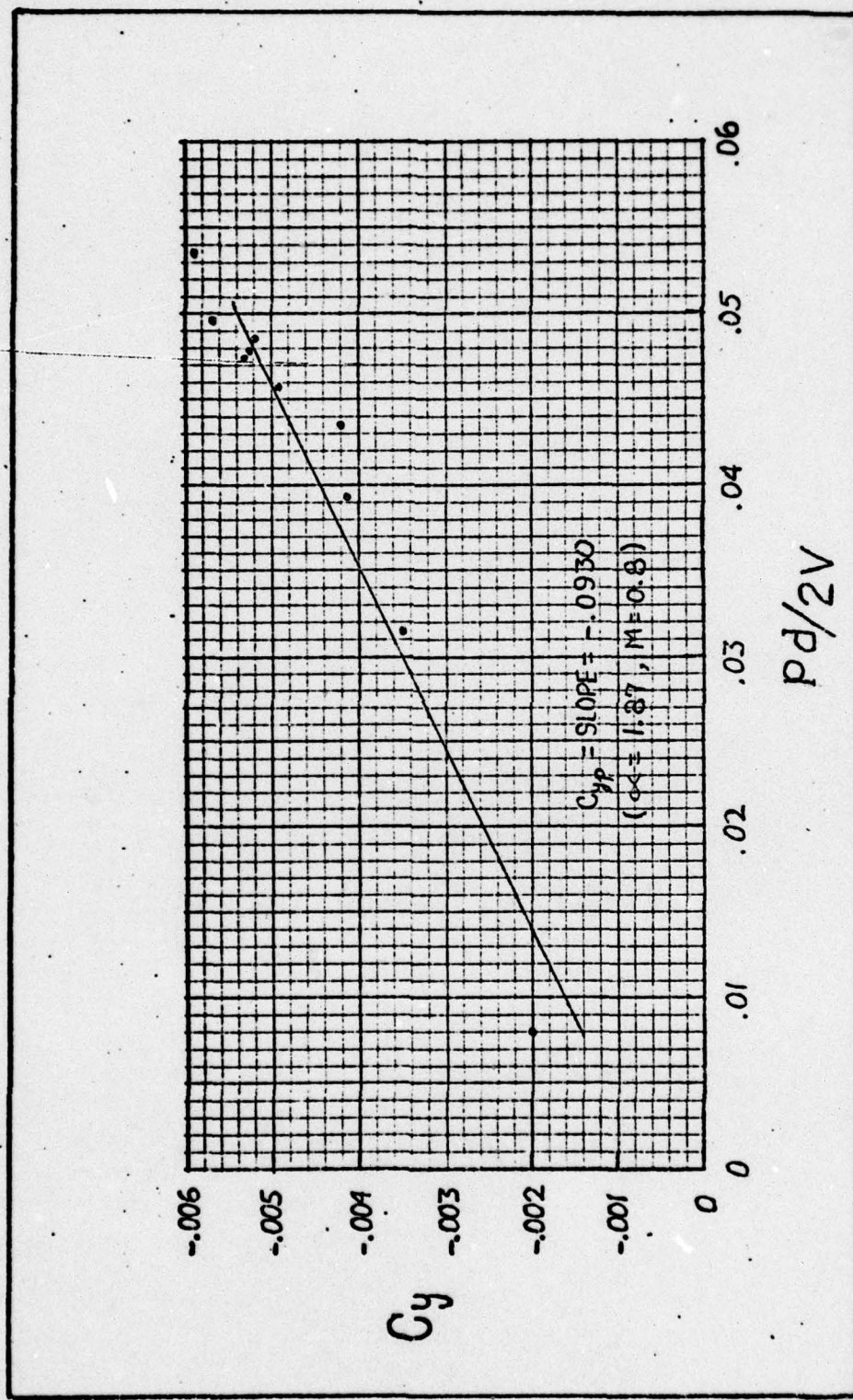


Fig. 8. Change in Magnus Force Coefficient

TABLE IV  
Magnus Force Aerodynamic Coefficient Array  
(Extracted from Appendix G)

CYP	C(9)	0.0000	2.0000	4.0000	6.0000	10.0000	15.0000	20.0000	25.0000	30.0000
MACH	0.0000	0.0000	-0.0300	-0.3350	-0.5350	-0.7750	-2.1630	-5.9180	-12.5000	-12.5000
MACH	.4000	0.0000	-0.0300	-0.1350	-0.5350	-0.7750	-2.1630	-5.9180	-12.5000	-12.5000
MACH	.8000	0.0000	-0.0300	-0.1750	-0.4100	-0.6600	-1.1650	-2.6900	-6.1500	-6.1500
MACH	.9000	0.0000	-0.1050	-0.3500	-0.6400	-1.1000	-2.6000	-5.0000	-5.0000	-5.0000
MACH	1.0000	0.0000	-0.0700	-0.1620	-0.2950	-0.3300	-0.7800	-2.3720	-3.4570	-3.4570
MACH	1.1000	0.0000	-0.0800	-0.1600	-0.3120	-0.2540	-0.6000	-2.4630	-3.4000	-3.4000
MACH	1.2000	0.0000	-0.0600	-0.1600	-0.3100	-0.2650	-0.6750	-1.7700	-2.3300	-2.3300
MACH	2.0000	0.0000	-0.0800	-0.1600	-0.3100	-0.2650	-0.6750	-1.7700	-2.3300	-2.3300

the source of Magnus lift that is generated by a spinning body subject to a relative wind component acting perpendicular to the body spin axis. This force will therefore be generated anytime the spinning projectile is falling with an angle of attack. The direction of the lateral Magnus lifting force is determined by the direction of spin and the cross-velocity component  $w$ . The spin rate,  $p$ , causes a velocity differential to be produced as shown in Fig. 9. A corresponding pressure differential is generated which produces lift in the lateral direction.

The side force coefficient,  $C_{y\gamma}$ , contributes to the deflection of a projectile by influencing side lift due to a lateral angle of attack.

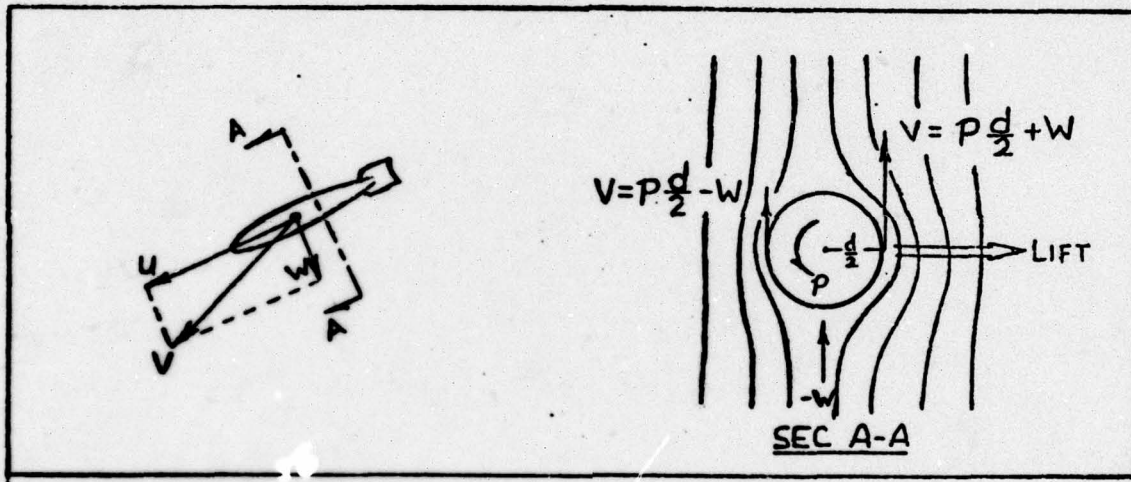


Fig. 9. Magnus Lift

The Magnus moment coefficient,  $C_{n_p}$ , can directly effect lateral progression of a projectile following a ballistic trajectory. Magnus moment is generated when the projectile, at a sufficiently high angle of attack, trails a wake vortex that blanks out the rolling lift of the fin passing through it. This causes a change in roll torque and a fin force imbalance that produces a yaw moment on the projectile (Fig 10). The value of the aerodynamic coefficient is a measure of the sensitivity of the projectile to this effect.

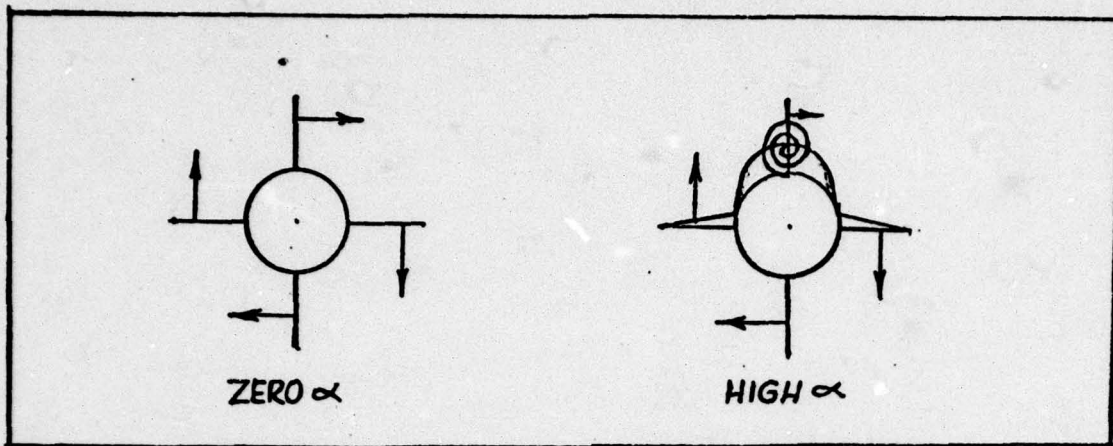


Fig. 10. Magnus Moment

The release velocities used as initial conditions are 600 ft/sec for a lower limit (approximately 350 knots) and 1000 ft/sec for the high speed delivery. The lower limit was selected as a representative velocity for a slow delivery. The 1000 ft/sec velocity remains in the subsonic region and provides adequate velocity spread for comparisons. A velocity of 1200 ft/sec was used, in some cases, to investigate the effect of a supersonic delivery (Mach 1.1 at 10,000 ft).

The 10,000 foot altitude was selected for most of the simulations. This altitude provides sufficient time of flight to identify any significant trajectory trends and does not require prohibitive computer time to process. An altitude of 20,000 feet was used when a lower air density trajectory was desired for comparison.

All releases are from a level flight path. The projectile is, however, perturbed initially under three conditions: zero perturbation, a nose-down rate motion, and a nose-down displacement. The zero perturbation condition simulates a projectile perfectly aligned with the velocity vector at release. The pitch rate motion of  $\dot{\alpha} = -.5$  radians/sec is used to investigate the effect of motion that could be induced

by the bomb ejection mechanism. The initial angle of attack of  $\alpha_0 = -7.75$  degrees, the third condition, is approximately the same maximum amplitude achieved by the preceding initial motion, but obtained in a different manner.

Spin rate of the projectile directly influences Magnus lift and, consequently, lateral progression of the trajectory. Wedge angles of 5, 10, and 15 degrees were used in the simulations to investigate the relative influence of the different wedges.

The parameters studied under various initial conditions are listed in an overview in Table V.

TABLE V  
Parameters Investigated

Parameters	Initial Conditions							
	10K	20K	600	1000	1200	0	-7.75	0
					$\alpha_0$	$q_0$	$v_0$	
All Coefficients	x	x	x	x	x	x	x	x
$c_{np}$	(Omitted)	x	x	x	x	x	x	x
$c_{yp}$	"	x	x	x	x	x	x	x
$c_{y\gamma}$	"	x	x	x	x	x	x	x
$c_{yp}, c_{np}$	"	x	x	x	x	x	x	x
$c_{yp}, c_{y\gamma}$	"	x	x	x	x	x	x	x
$c_{np}, c_{y\gamma}$	"	x	x	x	x	x	x	x
$c_{yp}, c_{np}, c_{y\gamma}$	"	x	x	x	x	x	x	x
$c_z$	"	x	x	x	x	x	x	x
$\rho$	x	x	x	x	x	x	x	x
$10^0$	x	x	x	x	x	x	x	x
$15^0$	x	x	x	x	x	x	x	x
$z$	x	x	x	x	x	x	x	x
$t$	x	x	x	x	x	x	x	x

#### IV. Results of the Simulations

##### Effect of Magnus Coefficients

The first simulations were run to determine the relative influence of the Magnus coefficients. Initial release conditions of level flight at an altitude of 10,000 feet and 600 feet per second, using all twelve available aerodynamic coefficient arrays produced the result shown in Fig. 11. The ground zero impact point for the trajectory using all coefficients was 57.73 feet to the left of the inertial x-y plane containing the release point. With three coefficients removed that influence lateral displacement ( $C_{np}$ ,  $C_{y7}$ ,  $C_{yp}$ ), the impact point was changed to 56.58 feet. This total spread of only 1.15 feet, generated over a relatively long trajectory, is lost in the accuracy limitations of the aerodynamic coefficients and the simplifying assumptions used in the equation of motion development. This small, Magnus induced lateral motion is initiated early and propagates slowly throughout the trajectory.

A second set of simulations were run at a velocity of 1200 ft/sec to determine if higher velocity would cause these coefficients to generate a more significant change in the trajectories. The net difference in the trajectories with and without the three coefficients remains on the order of only a few feet.

There are a number of possible explanations why the Magnus influence is so small. Magnus lift depends on both the relative velocity component acting on the projectile due to angle of attack and the spin rate of the projectile. For normal weapon deliveries, the angle of attack is relatively small on release and dampens toward zero early in the fall. During the time the angle of attack is at a maximum, shortly after release, high spin rate has not yet developed. After the projectile

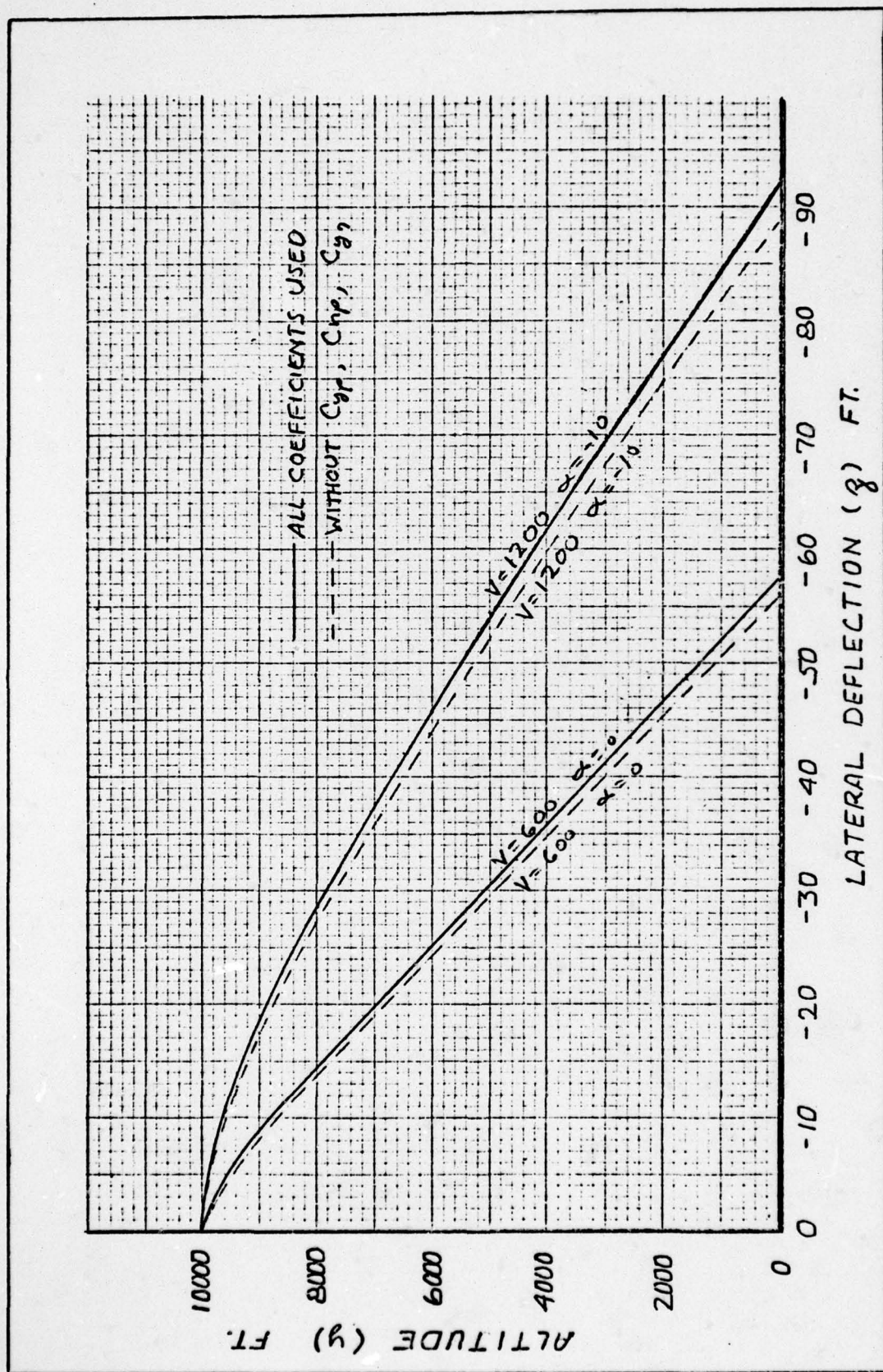


Fig. 11. Effect of Magnus &amp; Side Force Coefficients on Lateral Displacement

has fallen long enough to generate a high spin rate, the angle of attack is negligible. The Magnus side force due to body lift is negligible because the lateral angle of attack is small. The Magnus moment is also small since there is no significant wake generated at small angles of attack to produce a lift differential in the fins.

If oscillatory motion is encountered during release, the projectile angle of attack alternates from positive to negative. The Magnus lift will therefore alternate from positive to negative and average the net influence to zero.

#### Effect of Initial Pitch Motion

To simulate an initial release condition more realistic than perfect alignment of the projectile with the velocity vector, an initial angle of attack of -7.75 degrees was used as a perturbation. The same release initial conditions were used as before and simulations were run first using all coefficients, and then with  $C_{yp}$ ,  $C_{np}$ ,  $C_{y7}$  removed. There was essentially no difference in the resulting trajectories for  $\alpha_0 = -7.75$  degrees compared to  $\alpha_0 = 0$  as shown in Table VI).

An initial pitch rotation of the projectile at release, as might be induced by an ejector mechanism, was then implemented by entering a value of  $q_0 = -.5$  rad/sec. This initial rotation produced the same maximum amplitude of oscillation as the  $\alpha_0 = -7.75^\circ$  case, but a considerable difference in the resulting impact point of the projectile was generated. The increased lateral displacement caused a corresponding decrease in range which is consistent with the principle of conservation of energy. The oscillation induced by an initial angular displacement produced a trajectory that impacted at 14,165 feet downrange and 57.73 feet cross

TABLE VI (a)  
Effect of Magnus Coefficients

Velocity = 600 ft/sec

Altitude = 10,000 ft

Wedge angle = 10°

Level flight release

Aerodynamic Coefficient	Initial Pitch Motion			t Sec
	$q_o = 0$	$q_o = 0$	$q_o = -0.5$	
	$\alpha_o = 0^\circ$	$\alpha_o = -7.75^\circ$	$\alpha_o = 0^\circ$	
All coefficients	14165.16	-57.73	14179.60	-56.44
Less $C_{y_p}$	14165.48	-57.64		
Less $C_{n_p}$	14166.83	-56.54	14178.94	-55.86
Less $C_{y_p}$ & $C_{y_7}$	14178.31	-56.60		
Less $C_{y_p}$ & $C_{n_p}$	14167.15	-56.45		
Less $C_{y_p}$ & $C_{n_p}$	14165.98	-57.73		
Less $C_{y_7}$ & $C_{n_p}$	14167.34	-56.66		
Less $C_{y_p}$ , $C_{y_7}$ & $C_{n_p}$	14167.67	-56.58	14179.45	-55.82
Less $C_Z$ , $C_{y_p}$ , $C_{y_7}$ & $C_{n_p}$			14191.70	+ 2.53
Less $C_Z$			14191.06	+ 1.79

 $X = \text{Range (Ft)}$  $Z = \text{Lateral displacement (Ft)}$

TABLE VI (b)  
Effect of Magnus Coefficients

Velocity = 600 ft/sec  
Altitude = 10,000 ft  
Wedge angle = 10°  
Level flight release

Aerodynamic Coefficient	Initial Pitch Motion		
	$q_o = 0$ $\alpha_o = 0^\circ$	$q_o = 0$ $\alpha_o = -7.75^\circ$	$q_o = -.5$ $\alpha_o = 0^\circ$
All coefficients	889.06	62.9	889.37
Less $C_{y_p}$	889.06	62.9	889.36
Less $C_{y_7}$	889.05	62.9	62.9
Less $C_{n_p}$	889.37	62.9	
Less $C_{y_p}$ & $C_{y_7}$	889.05	62.9	
Less $C_{y_p}$ & $C_{n_p}$	889.10	62.9	
Less $C_{y_7}$ & $C_{n_p}$	889.10	62.9	
Less $C_{y_p}$ , $C_{y_7}$ & $C_{n_p}$	889.10	62.9	889.38
Less $C_z$ , $C_{y_p}$ , $C_{y_7}$ & $C_{n_p}$			889.76
Less $C_z$			889.76

Impact velocity  $V_f$  in ft/sec  
Impact spin rate  $P_f$  in rad/sec

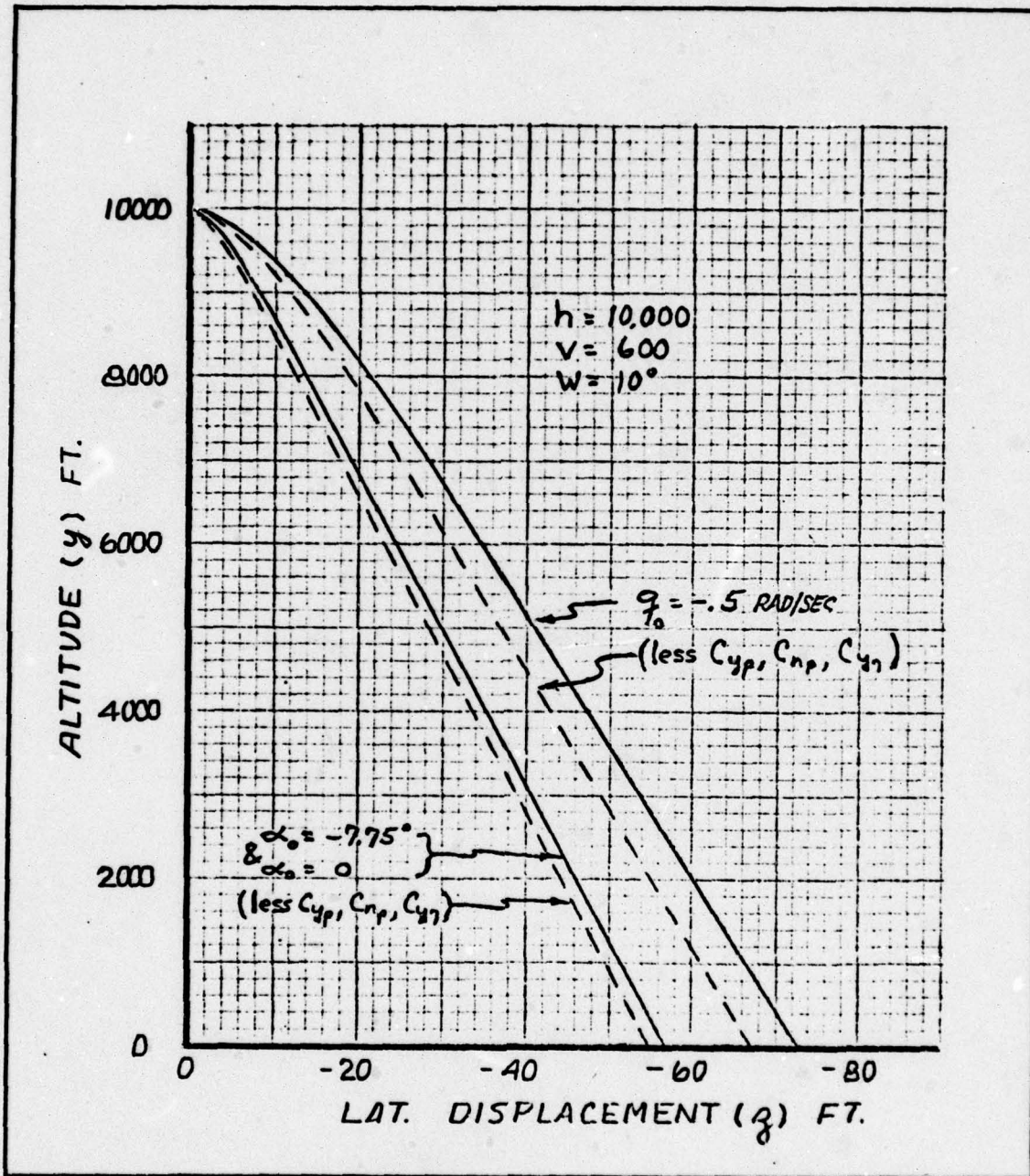


Fig. 12. Effect of Pitch Motion and Magnus Coefficients on Lateral Displacement

range to the left. The rate induced oscillation, with the same release conditions, impacted at 14,179 feet downrange and 73.02 feet cross range (See Table VI and Fig 12).

To investigate the cause of the difference in trajectory, the nose track, viewing the projectile from behind, was plotted for the two different inputs in Fig. 13. The beta versus alpha plot represents a close approximation of the nose track of the projectile early in the trajectory before the body reference frame and the projectile velocity vector rotate a significant amount with respect to the inertial frame. The motion of the projectile nose for the two conditions is quite different. Fig 13a represents single arm coning motion caused by nutation. No precession is evident and the damping is relatively constant. The nose track in Fig 13b shows less coning and displays two arm motion with both nutation and precession. This oscillation dampens faster in pitch than in yaw. The direction of nutation is opposite to the projectile spin rate while the precession is in the same direction. Figs 13c, d, e, f were plotted to identify any parameters that could cause the difference in trajectories. These plots show that the difference in spin rate build-up and velocity progression is very small. A slight phase shift in yaw oscillation is apparent, and the initial slopes of the  $\beta$  versus  $t$  plots are noticeably different. The last plot shows a significantly different behavior in the angle of attack oscillations between the two initial conditions.

The lateral displacement for both initial conditions is plotted against time in Fig. 14 to further define the projectile motion shortly after release. The linearized average slope of these plots produces a measure of the initial lateral average velocity. The slope for the

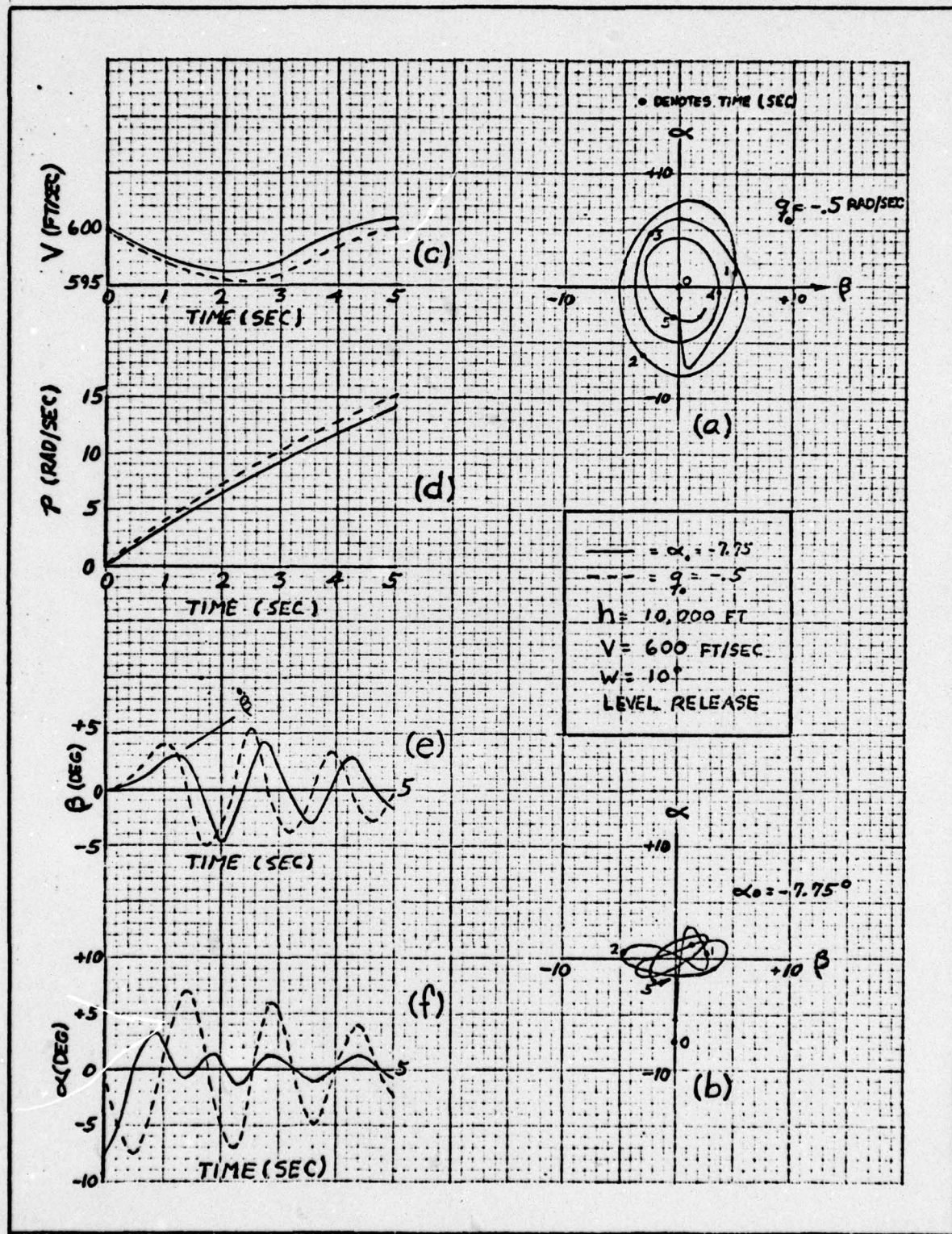


Fig. 13. Projectile Nose Track After Release

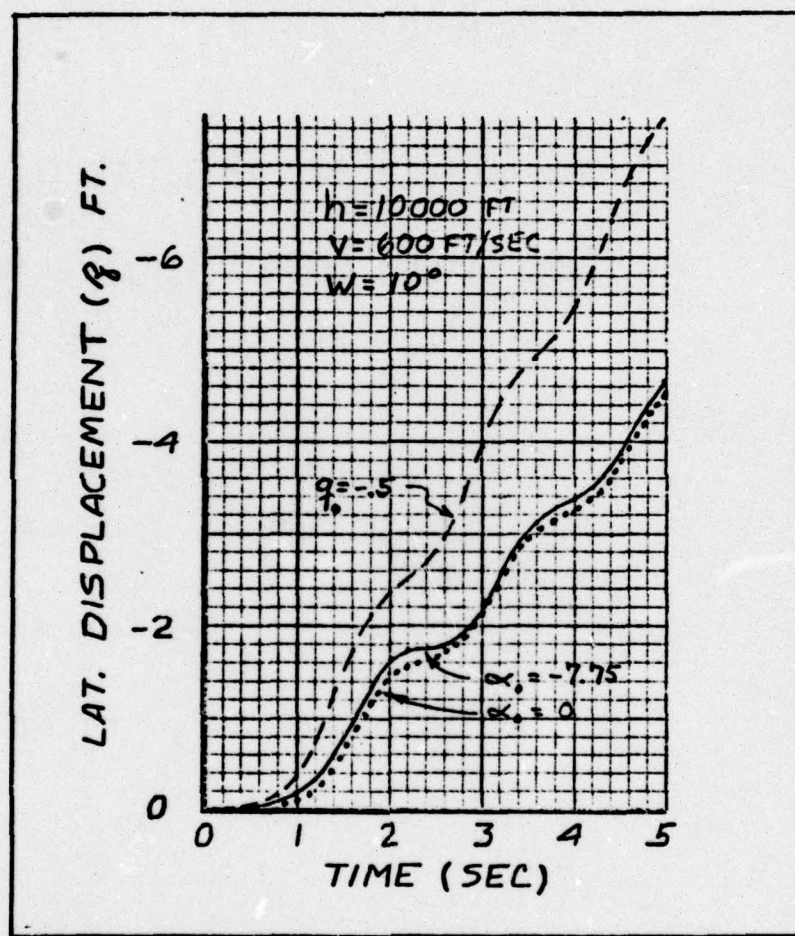


Fig. 14. Initial Rate of Lateral Displacement

$\alpha = -7.75^\circ$  initial condition is approximately 1 ft/sec; for  $q = -.5$  rad/sec, the slope is close to 1.5 ft/sec. These values of slope are significantly different and can be modeled as an initial lateral velocity of the projectile at release. The initial lateral velocity,  $v_0$ , can be input into the simulation to determine its effect. Fig. 15 shows the lateral progression of the trajectories resulting from an initial side velocity of -5, 0, +5 ft/sec. The remaining initial release conditions were the same for all three trajectories. As the plots show, the magnitude of  $v_0$  directly influences the overall trajectory. An equation for this lateral initial velocity is given by (Ref 1:53-68):

$$v_z = -\left(\frac{C_{Z_a} A}{M}\right) \left(\frac{T}{1 - \omega_T^2}\right) (2\beta + T\dot{\beta}) \quad (24)$$

where  $C_{Z_a}$  = the normal force coefficient (acting in plane containing the relative wind).

$A$  = frontal area of the projectile.

$q$  = dynamic pressure.

$M$  = mass

$T$  = time constant for oscillation damping.

$\omega$  = frequency of oscillation.

$\beta$  = yaw angle of attack.

$\dot{\beta}$  = yaw rate.

If the influence of the displacement term is considered small with respect to the rate term, the expression reduces to:

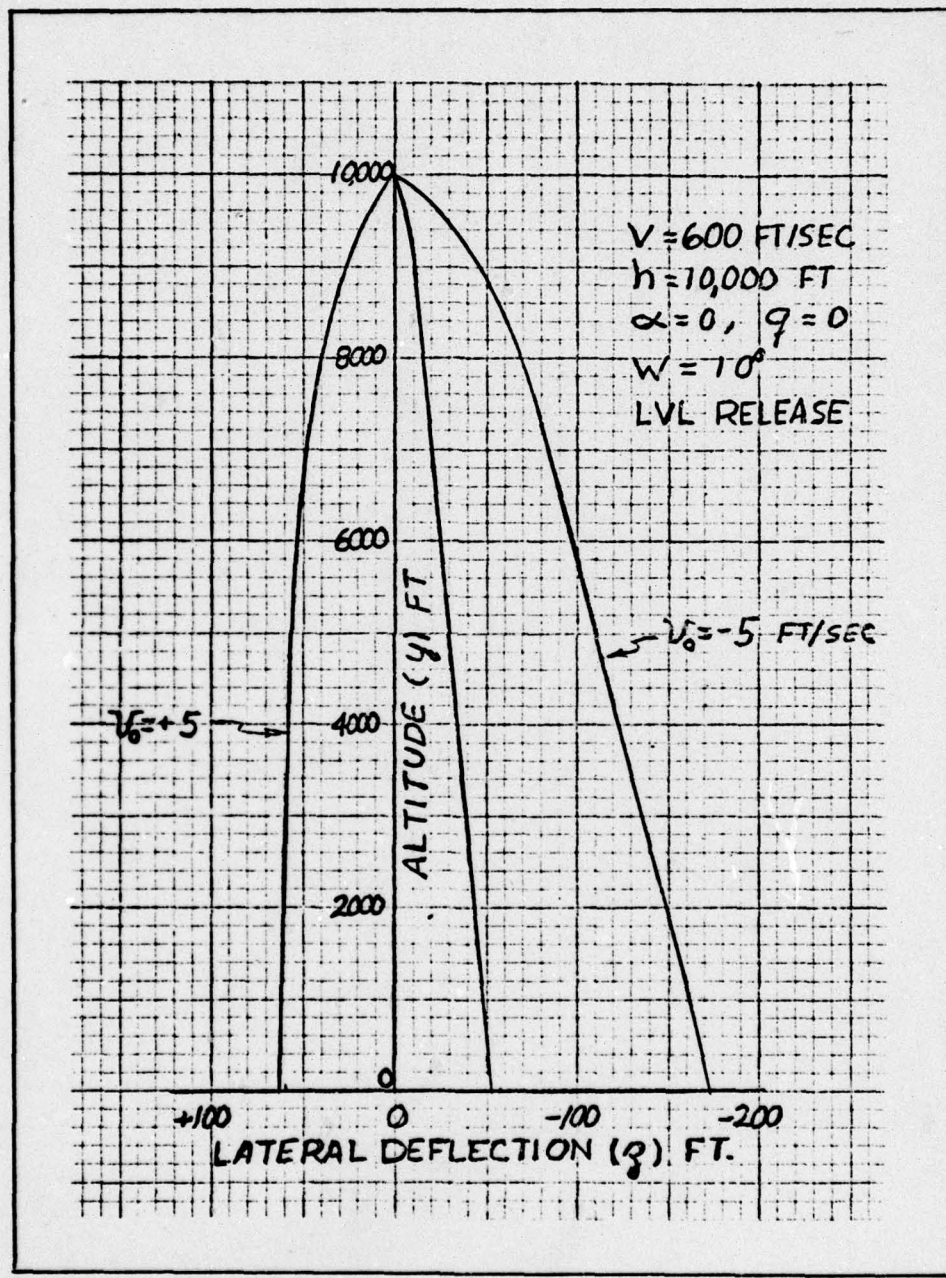


Fig. 15. Effect of Initial Side Velocity on Lateral Progression

$$v_z = - \frac{C_{Z\dot{\alpha}}}{C_{M\dot{\alpha}}} \frac{I}{M d} \quad (25)$$

where  $C_{M\dot{\alpha}}$  = moment coefficient (with respect to total angle of attack).

$I$  = transverse moment of inertia.

$d$  = max diameter of projectile.

and the following relation has been used:

$$\frac{T^2}{1 + \omega^2 T^2} = \frac{I}{C_{M\dot{\alpha}} \cdot q \cdot d} \quad (26)$$

Equation 25 shows that the lateral velocity induced by oscillation of the projectile is sensitive to the normal force coefficient  $C_Z$ , the moment coefficient  $C_M$ , and the yaw rate  $\dot{\beta}$ .

The magnitude of the side velocity predicted by this closed form approximation is given by (Ref 1:65)

$$v_z = \frac{\dot{\beta}}{\omega} (.362) \text{ ft/sec/degree} \quad (27)$$

where the constant, 0.362, is the result of equation 24 (displacement term neglected) using a velocity of 750 ft/sec, an altitude of 5000 ft, and coefficients of a projectile similar to that in this investigation (coefficients used in this derivation are determined with respect to the total angle of attack instead of  $pd/2V$ ). These same initial conditions were used in a six degree of freedom simulation and the lateral displacement and yaw oscillations were plotted in Fig. 16. From these plots, a representative yaw rate and frequency of oscillation were

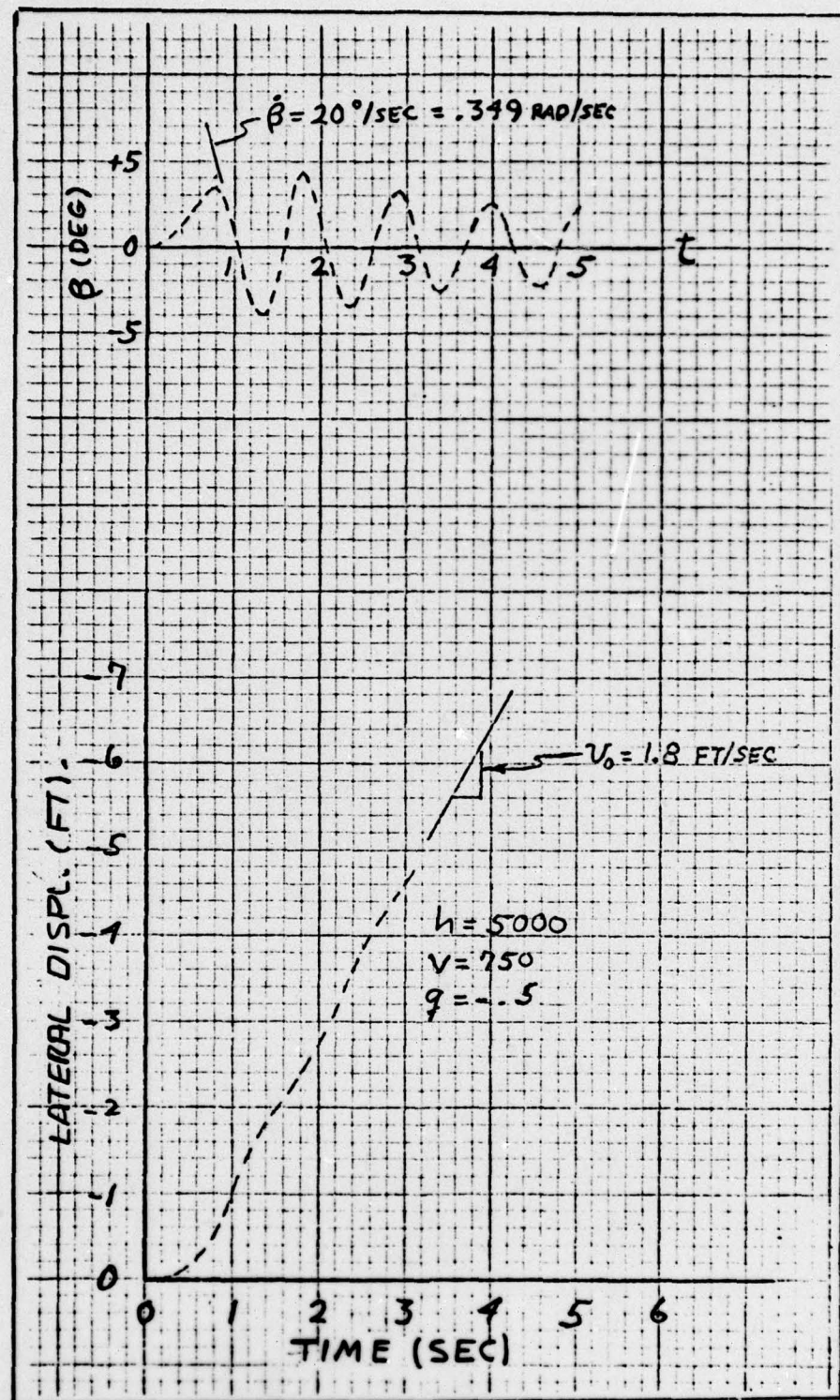


Fig. 16. Lateral Displacement and Yaw Oscillations

estimated as 0.349 radians/sec and 5.34 radians/sec respectively. The closed form approximation (Eqn 27) then produces a value of  $V_z = 1.36$  feet per second.

The plot of lateral displacement versus time indicates the initial lateral velocity, according to the simulation, is approximately 1.8 feet per second. This is on the order of 25% difference between the six degree of freedom simulation results and the closed form expression. This difference can be attributed to the more extensive simplifying assumptions used to make the closed form expression possible.

#### Effect of Spin Rate

The effect of spin rate induced by various wedge angles is investigated at different airspeeds and release perturbations (Table VII). The spin rate, induced by the wedge angle of fifteen degrees, produces the most nominally linear lateral deviation throughout the entire trajectory. This pattern holds for both velocities investigated (Fig 17).

Table VII also reveals that increasing the spin rate of the projectile causes the trajectory to impact longer and wider. This apparent contradiction to the principle of conservation of energy was initially thought to be an error caused by using an integration step size that was too large. A step size of .002 second, however, is adequate for the spin rates encountered.

Another possible explanation is that the projectile developed gyroscopic rigidity and was starting to fly at a net angle of attack rather than averaging to zero angle of attack in its oscillations. This concept is supported by the simulation readout which shows the angle of attack of the projectile with a five degree wedge angle oscillates on the

TABLE VII  
Effect of Spin Rate

Alt = 10,000 ft, level flt release, all coefficients included.

Wedge	V = 600				V = 600			
	$\alpha = 0$		$\alpha = -10$		$\alpha = 0$		$\alpha = -10$	
	X	Z	V <sub>f</sub>	P <sub>f</sub>	X	Z	V <sub>f</sub>	P <sub>f</sub>
5°	14159	-37.4	888.5	31.4	25.72	14165	-38.9	888.6
10°	14165	-57.7	889.1	62.9	25.72	14174	-59.1	889.2
15°	14185	-65.6	889.4	94.4	25.73	14199	-66.1	889.6
V = 1000								
Wedge	$\alpha = 0$		$\alpha = -10$		$\alpha = 0$		$\alpha = -10$	
	X	Z	V <sub>f</sub>	P <sub>f</sub>	X	Z	V <sub>f</sub>	P <sub>f</sub>
	22668	-30.7	1029.6	38.0	26.11	22669	-41.1	1029.3
5°	22716	-79.7	1030.3	76.1	26.13	22718	-79.6	1030.5
10°	22746	-87.2	1030.6	114.2	26.14	22738	-93.2	1030.7
15°								

X = Range (ft)

Z = Lat displacement (ft/sec)

V = Impact spin rate (rad/sec)

t<sub>f</sub> = Time to impact

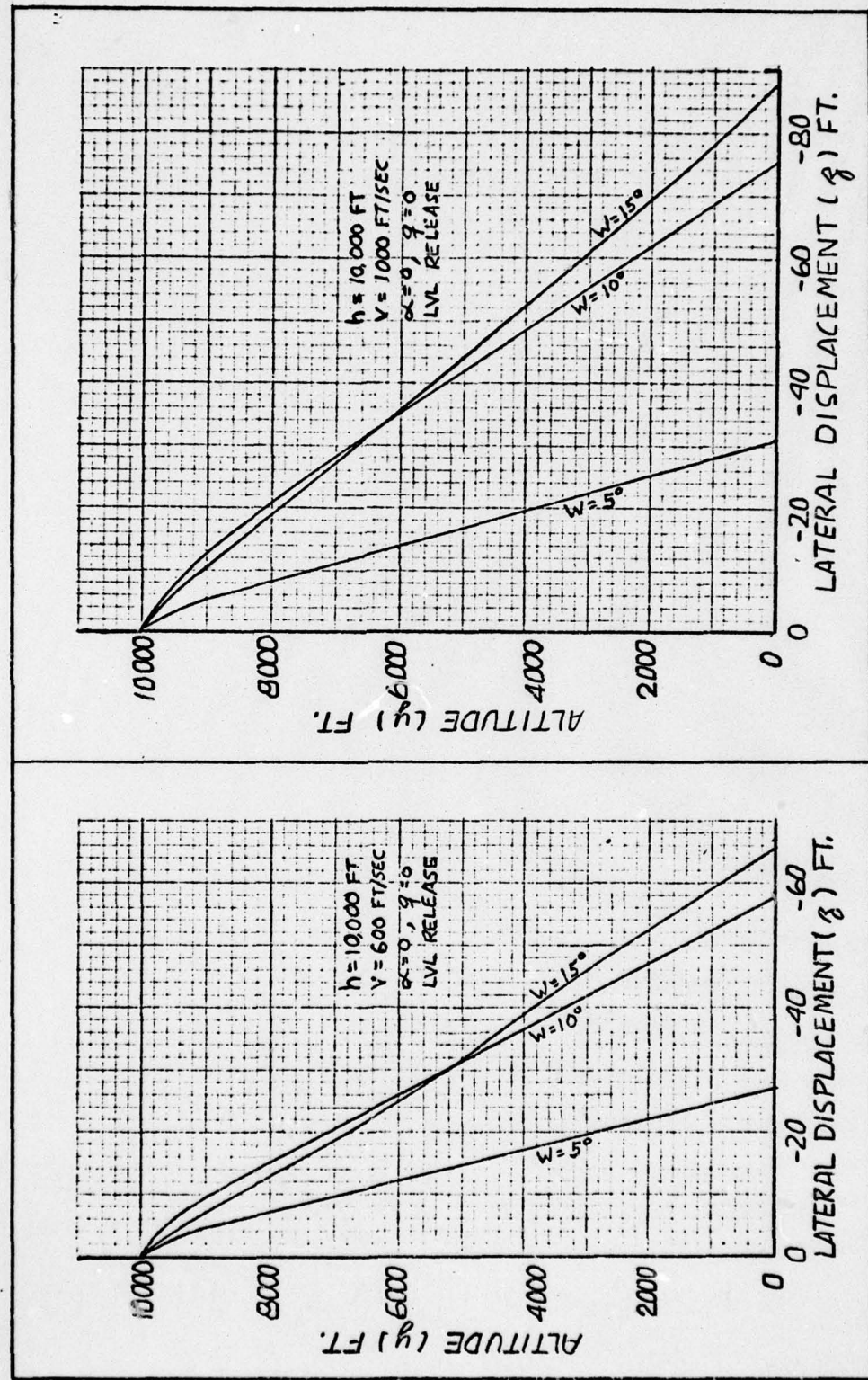


Fig. 17. Effect of Spin Rate on Lateral Displacement

order of  $\pm 0.1$  degree in the latter half of the trajectory. The fifteen degree wedge readout, however, shows only about half the magnitude of oscillation but the oscillations are predominantly positive in the last half of the trajectory. In fact, the angle of attack does not go negative at all during the final ten seconds of flight. Also, Table VII indicates the total time of flight of the projectile spinning at the faster rates is increased very slightly (on the order of 0.02 second). The downrange velocity just prior to impact is approximately 750 ft/sec which produces an opportunity for the projectile to impact 15 feet longer in the extra 0.02 second. This is compatible with the data shown in Table VII.

#### Other Observations

Fig. 18 shows the aerodynamic coefficients,  $C_{y7}$ ,  $C_{yp}$  &  $C_{np}$ , have no discernable effect on the projectile velocity. The velocity progression graphs remained the same regardless of whether or not these coefficients were included in the simulation.

The wedge angle did not change the velocity progression significantly. Simulations modeling spin rates as 5, 10, or  $15^\circ$  wedge angle indicates the velocity progression is not influenced by spin rate. This observation is subject to the projectile spin rate remaining low enough to preclude instability.

The higher dynamic pressure encountered during release at high air-speeds causes a significantly greater velocity change of the projectile after release. The magnitude of the difference in the release and steady state velocity of the projectile governs how the velocity will progress throughout the trajectory. The projectile shows significant velocity change throughout the trajectory when released from a low speed condition.

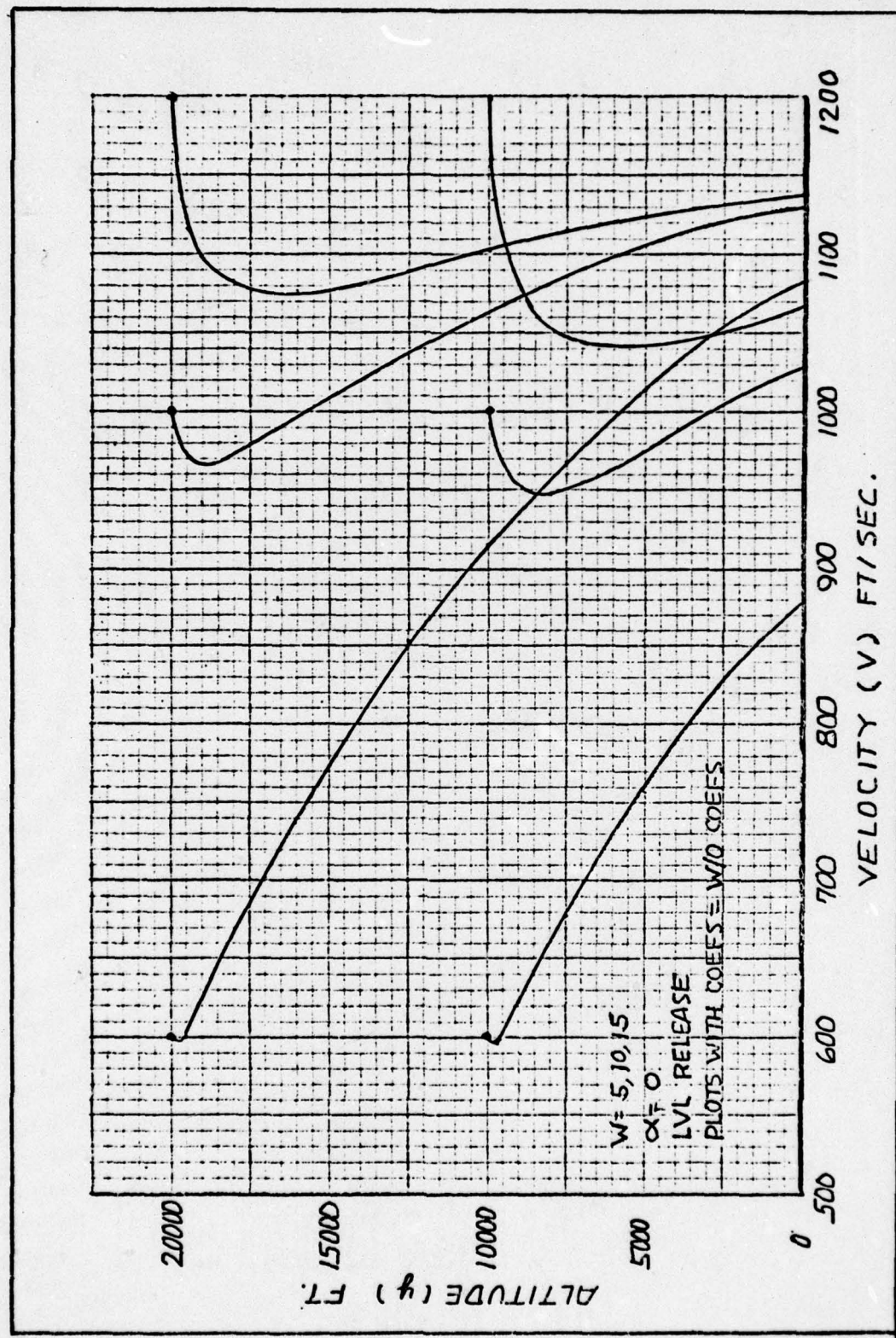


Fig. 18. Effect of Release Velocity and Altitude on Velocity Progression

The projectile shows much less acceleration when released from a high dynamic pressure condition.

Figure 19 investigates projectile acceleration from release to impact. The slope of the velocity vs time curve shows that maximum deceleration is proportional to the drag force encountered at release and, as a result, velocity loss is greater at high release velocities. The time required for transition from deceleration to acceleration also increases with higher release velocities. The same plots apply for each of the projectile fin wedge angles investigated. Also, there are no significant changes in the graphs for an initial angle of attack of  $\alpha_0 = 0$  versus  $\alpha_0 = -10$ .

Fig. 20 shows the lateral displacement progression of a projectile subjected to two different release perturbations ( $\alpha_0 = -10^\circ$  and  $a_0 = -5$  rad/sec) at two different release velocities. The slope of a pair of the curves is nearly identical at any given time but the magnitude of the lateral displacement attained in the same given time can be significantly different at the lower airspeed.

Fig. 21 shows that the rate of altitude loss does not change significantly with initial release airspeeds. For the 10,000 ft drop, time of flight through a standard atmosphere is increased on the order of one second compared to the time of flight through a vacuum.

The effect of release velocity and altitude is shown as a composite in Fig. 22. The set of trajectories initiated at 10,000 ft is essentially a duplication of Fig. 11 and is included with the 20,000 ft set to give an indication of the effect of air density on the lateral deflection.

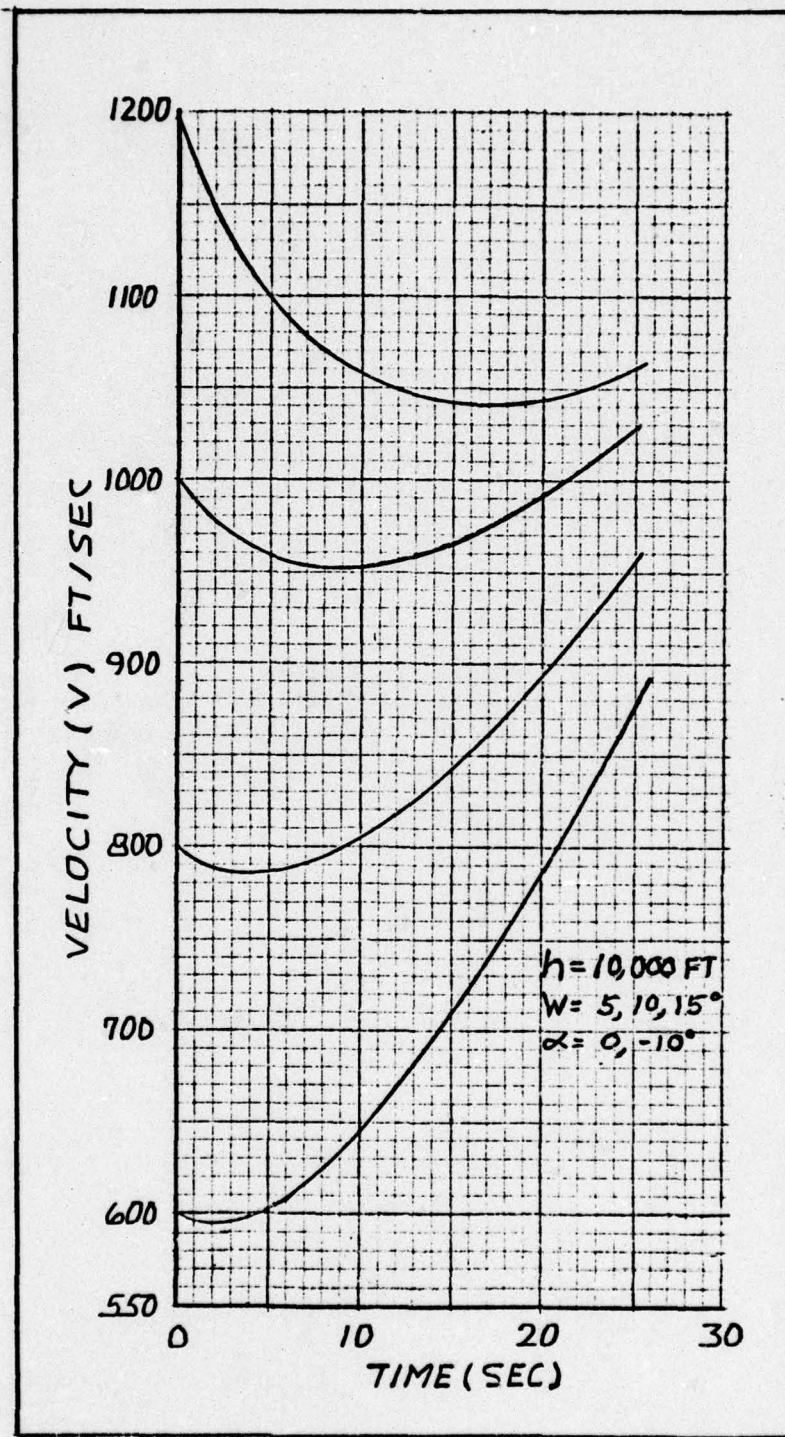


Fig. 19. Effect of Release Velocity on Total Projectile Acceleration

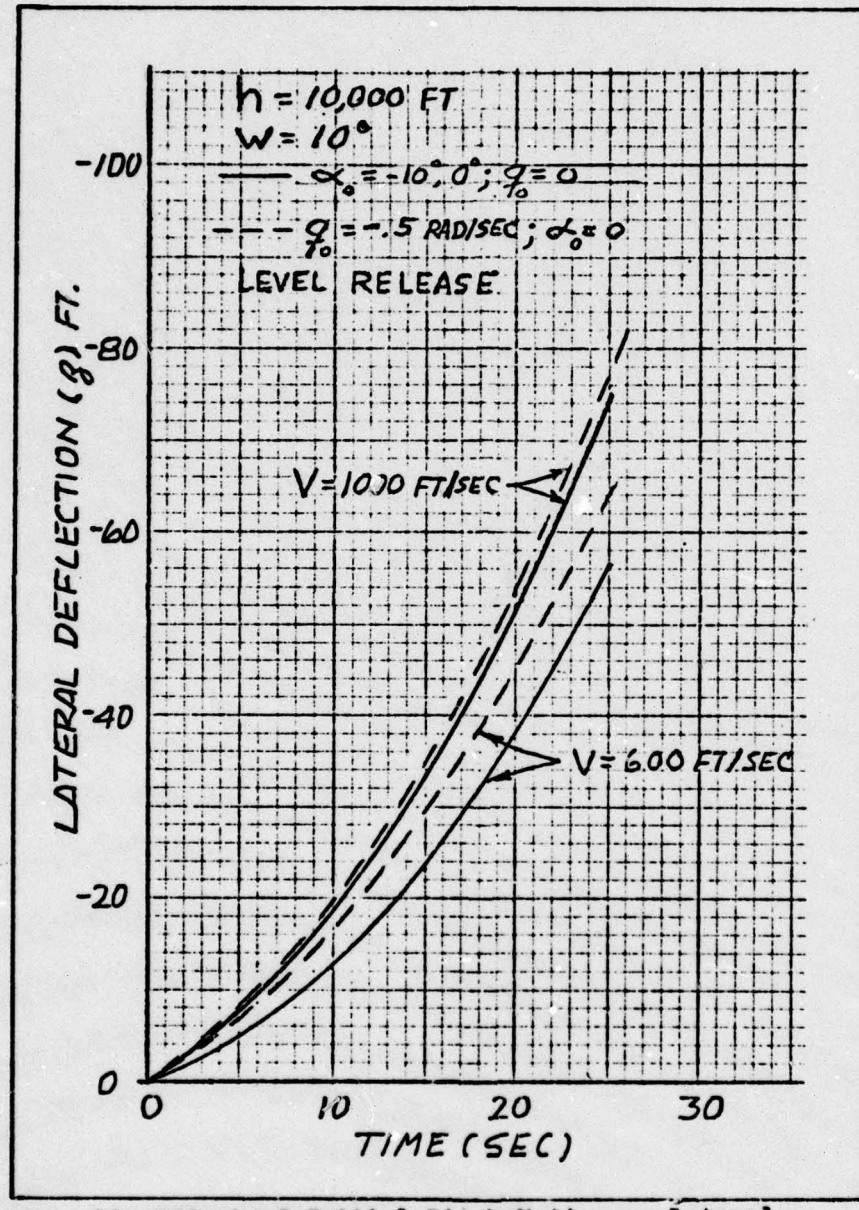


Fig. 20. Effect of Initial Pitch Motion on Lateral Deflection

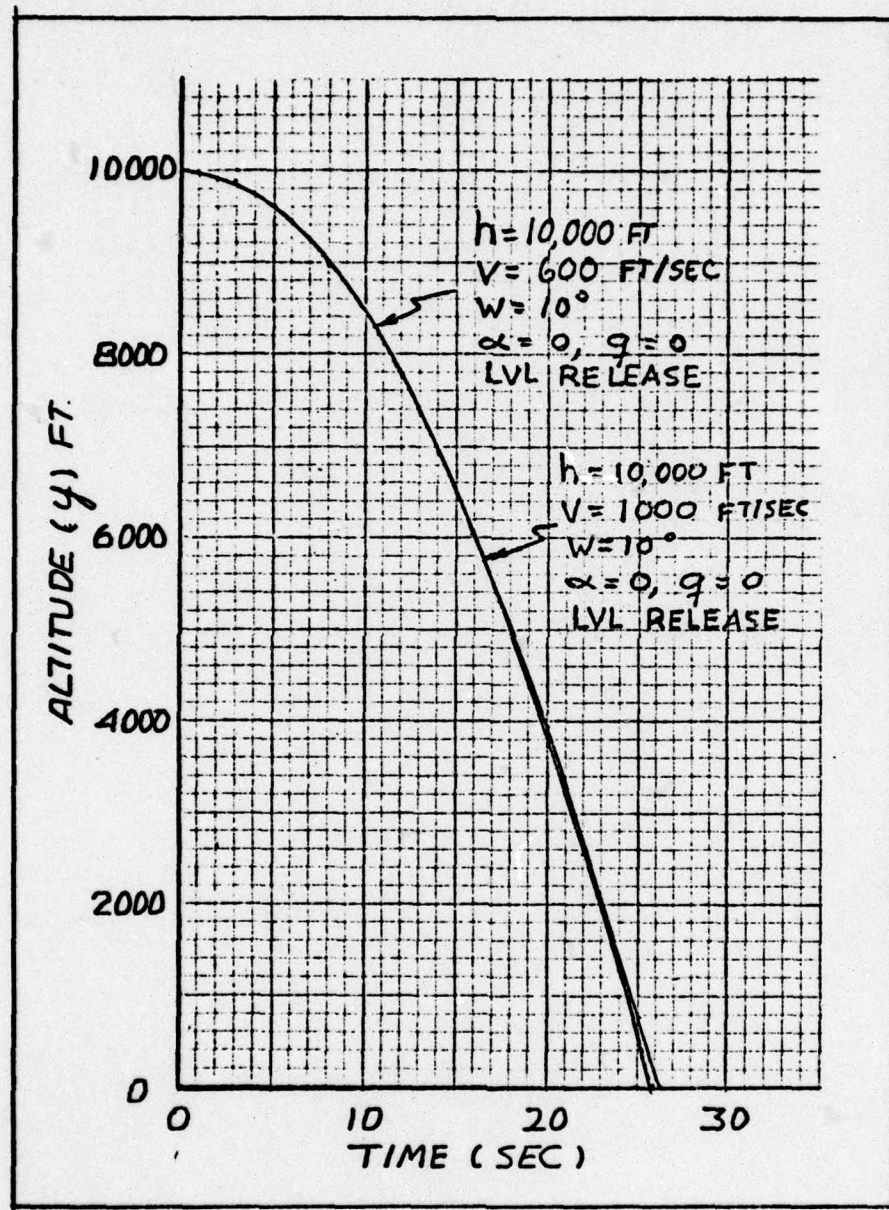


Fig. 21. Effect of Release Velocity on Altitude Progression

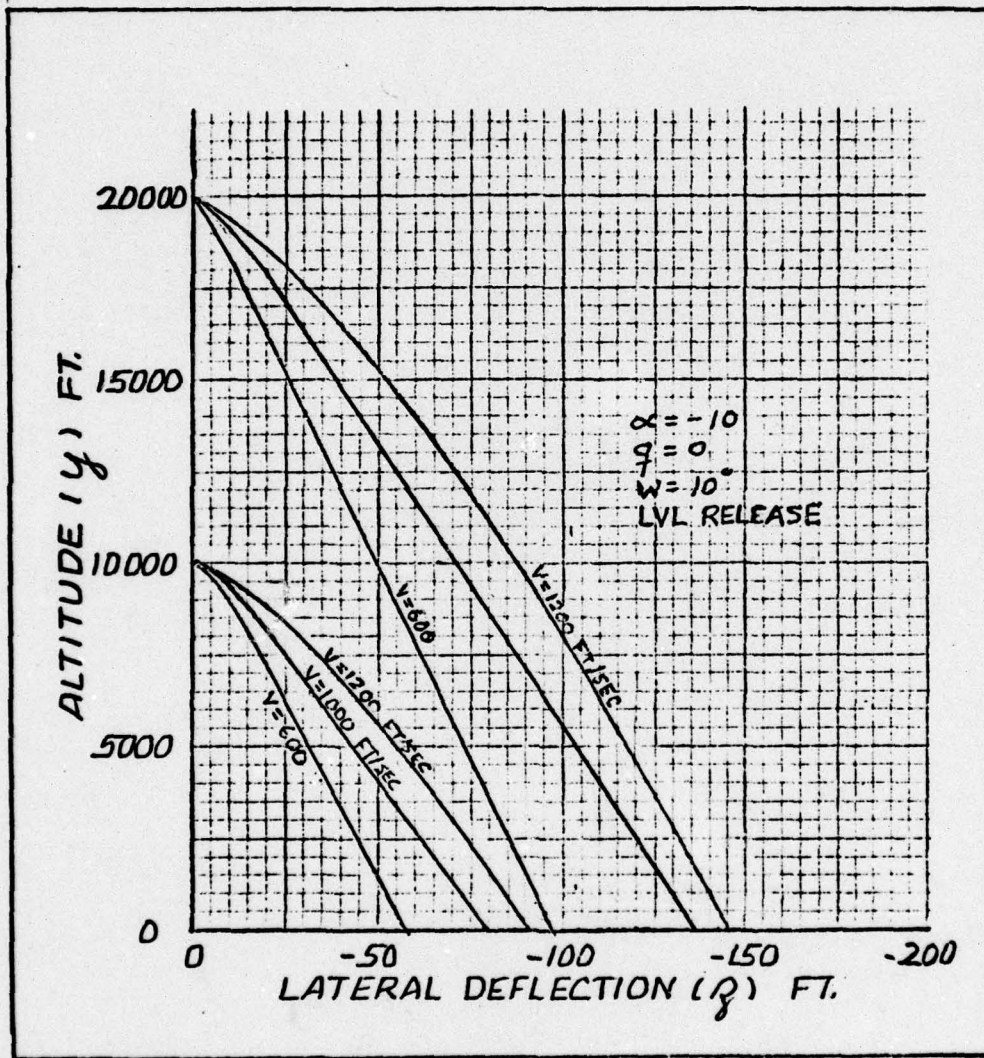


Fig. 22. Effect of Release Velocity and Altitude on Lateral Displacement

### V. Conclusions

The Magnus force, Magnus moment, and side force coefficients, for a projectile of the type modeled in the simulations, and for normal release conditions, exert only a very small influence on the impact point. The cross range displacement attributable to these coefficients, for a trajectory initiated at 10,000 feet, are on the order of only a few feet. The influence on the downrange component of the trajectory is also very small. These coefficients could be influential under conditions of high angle of attack and high spin rates which, for normal releases, are not present simultaneously. When the projectile oscillation and the corresponding angle of attack is maximum following release, the spin rate has not yet developed. As the projectile progresses along the trajectory, the spin rate builds up but the oscillations dampen to a very small value. Also, the oscillations alternate about the velocity vector of the center of gravity of the projectile so the Magnus force direction, being dependent on the direction of the angle of attack, also alternates and tends to average to zero effect.

The lateral displacement of the trajectory is, in general, increased with increasing spin rate. Insufficient spin rate can be a stability factor as can excessive spin rate. Low values of angular momentum can allow the projectile to develop catastrophic yaw. High spin rates induce gyroscopic resistance to change in projectile orientation, allowing a positive angle of attack to build up as the trajectory progresses. A net lift is then developed which increases the time of flight of the projectile and, consequently, the cross range and downrange impact point.

A projectile released at zero angle of attack with no initial per-

turbations produces the least lateral displacement of the trajectory. If the projectile is released with an initial negative angle of attack, the lateral progression is increased only slightly. If the projectile is released with a rate rotational motion, as could be induced by the ejector mechanism or an initial positive angle of attack, the lateral progression is significantly increased. This increase is directly proportional to the amplitude of the projectile oscillations. The difference in lateral progression between the rate induced and displacement induced oscillation is less at higher airspeeds. Also, as oscillations increase the cross range impact point of the trajectory, there is, in general, a corresponding decrease in the downrange impact point. These results suggest the following conclusions:

1. Magnus force, as such, exerts no significant influence on the trajectory of a projectile such as the Mk-82 bomb. For most release airspeeds and altitudes, compensation for this specific effect in a weapons delivery system would not be cost effective.
2. The projectile should be designed to spin as slow as possible consistent with stability considerations.
3. Release mechanisms should be designed so no significant moment is applied. If assisted separation of the projectile from the delivery aircraft is desired, a slight negative angle of attack should be used instead of a moment.

Bibliography

1. Ausman, J.S. Theoretical Analysis and Experimental Measurements of Separation Disturbances in Weapon Delivery Systems. Aircraft/Stores Compatability Symposium Proceedings, JTCC/MD WP No. 12:53-85 (September, 1975).
2. Cohen, C.J. and D. Werner. A Formulation of the Equations of Motion of a Four-Finned Missile. Defense Documentation Center Reference AD112006, September 1956.
3. Daniels, P. Minimization of Lock-In Roll Moment on Missiles via Slots. Defense Documentation Center Reference AD010130, January 1975.
4. Etkin, B. Dynamics of Flight. New York: John Wiley and Sons, Inc., 1959.
5. Ingram, C.W. A Computer Program for Integrating the Six Degree of Freedom Equations of Motion of a Symmetrical Missile. Unpublished notes, Aerospace Department, University of Notre Dame.
6. Likins, P.W. Elements of Engineering Mechanics. New York: McGraw-Hill Book Company, 1973.
7. Meirovitch, L. Methods of Analytical Dynamics. New York: McGraw-Hill Book Company, 1970.
8. Miklos, W. Analysis of the Stability and Flight Performance of the Candidate Replacement for the MK-82 Snakeye Bomb. Air Force Flight Dynamics Laboratory Report Number AFFDL-TR-77-108, June 1976.
9. Murphy, C.H. Free Flight Motion of Symmetric Missiles. Defense Documentation Center Reference AD442757, July 1963.
10. Naveh, B.Z.N. Untitled, unpublished notes, Aerospace Department, University of Notre Dame, 1974.
11. Nicolaides, J.D. Missile Flight and Astrodynamics. Defense Documentation Center Reference AD287400.
12. Vaughn, H.R. A Detailed Development of the Tricycle Theory. Sandia Laboratory Report SC-M-67-2933, February 1968.
13. Whittaker, E.T. A Treatise on the Analytical Dynamics of Particles and Rigid Bodies. Dover Publications, 1944.
14. Air Force Armament Laboratory Report. AFATL MK 82/84 Air Inflatable Retarder (Magnus Phase) in the Aerodynamic Wind Tunnel (4T) Off-Line Data, parts 6 through 153. P41C-86A, TC387 Arnold Air Force Station, Tennessee. (July 1975).

Appendix A

Typical Wind Tunnel Data

The aerodynamic coefficients for a specific projectile model are normally obtained from wind tunnel tabulated data. Table A-I shows the spin-up data of a projectile model at a specific Mach and angle of attack. The data measurements were made as the projectile was progressively accelerated from a zero roll rate to the steady state spin rate ( $P_{ss}$ ). Table A-II shows the spin-down data taken as the projectile was progressively decelerated from a high spin rate down to  $P_{ss}$ . Both of these figures were obtained from reference 11, part 31.

TABLE A-1  
Spin-up Data

TEST	PART	POINT	TIME	DATE	DATA SET	DAY	DATA MODE
TC-367	31	33200	07-15-75	1	343	92	TRANSONIC AT
M1	PP1	01	R4106-P1	R4106-P1	PCB-2	PE	TAA-1-TB-2-TM-W-TAA-2-TAA-N-SAURE
0.0005	1197.1	352.1	784.9	2.26W	1197.1	791.7	1010.0 92.8 0.00 4.97 5.02 4.97 4.98
MC	TPN	ALFI	PMII	TUWC	PMC	SCX100	SCHEM MH DN ER CODE WIND-OFF
0.7918	1.1852	2.00	0.0	39.9	0.0-62.197	8	0.800 0.010 0 27/-3
CONFIGURATION	MALH NO	P0	[0]	P=INF	I=INF	V=INF	RE/INX10-6 REDX10-6 RELX10-6 CVP CLMP
FFSd1	0.8005	6.3	552.5	5.451	409.7	2.445	866.606 0.189 7.573 -0.10974 0.02636 ..
SAMPLE	ALFA-H	CN	CLW	CY	CLW	XCY/D	TAVG
1	1.87	0.145	-0.160	-0.00266	0.00458	-1.108	-2.224
2	1.87	0.145	-0.162	-0.00261	0.00438	-1.118	-2.447
3	1.87	0.147	-0.167	-0.00415	0.00818	-1.137	-2.592
4	1.87	0.147	-0.165	-0.00351	0.00775	-1.127	-2.207
5	1.87	0.145	-0.163	-0.00260	0.00932	-1.126	-2.460
6	1.87	0.145	-0.166	-0.00359	0.00949	-1.142	-2.645
7	1.87	0.145	-0.166	-0.00418	0.01006	-1.142	-2.404
8	1.87	0.146	-0.168	-0.00419	0.01030	-1.152	-2.152
9	1.87	0.146	-0.168	-0.00476	0.01124	-1.152	-2.363
10	1.87	0.147	-0.171	-0.00420	0.01150	-1.161	-2.740
11	1.87	0.148	-0.171	-0.00448	0.01157	-1.159	-2.373
12	1.87	0.147	-0.172	-0.00515	0.01163	-1.161	-2.459
13	1.87	0.147	-0.172	-0.00499	0.01230	-1.167	-2.466
14	1.87	0.146	-0.170	-0.00499	0.01262	-1.163	-2.534
15	1.87	0.146	-0.171	-0.00519	0.01223	-1.169	-2.354
16	1.87	0.146	-0.170	-0.00533	0.01219	-1.164	-2.244
17	1.87	0.146	-0.171	-0.00531	0.01288	-1.169	-2.427
18	1.87	0.146	-0.171	-0.00514	0.01262	-1.169	-2.435
19	1.87	0.146	-0.171	-0.00526	0.01220	-1.169	-2.319
20	1.87	0.146	-0.170	-0.00547	0.01222	-1.164	-2.233
21	1.87	0.146	-0.171	-0.00531	0.01295	-1.169	-2.442
22	1.87	0.147	-0.172	-0.00511	0.01300	-1.173	-2.517
23	1.87	0.146	-0.171	-0.00543	0.01330	-1.162	-2.449

TABLE A-II  
Spin-down Data

TEST TC-JAN/ 31	PART #	POINT #	TIME 35330	DATE 07-15-75	DATA SET 1	DAY 143	DATA MODE 92	AEDC PROPULSION WIND TUNNEL TRANSONIC 47
M1	SP1	01	4X10-6	2TA-1	PCA-1	PCB-2	PE	TTA-1-TTB-2-TMA-TAU-S-TAU-S-TAU-S
0.7987	1198.0	351.4	786.9	2.268	1198.0	1197.5	793.7	794.4 1008.7 92.8 92.6 0.00 4.97 5.02 4.97 4.98
MC	TPH	ALFI	PHII	IUPC	PHC	SCX100	SCED MH	DM ER CODE WIND-OFF
0.7900	1.1877	2.00	0.0	40.1	0.0-62.197	8	0.800 0.010	0 27/-3

CONFIGURATION	MACH NO	P0	T0	P-1INF	T-1INF	U-1INF	V-1INF	RE/INX10-6	RE/INX10-6	RELX10-6	CYP	CLNP
FP/SJ1	0.7987	6.3	552.5	5.465	490.0	2.440	867.054	0.189	0.890	7.570	-0.10974	0.2636

SAMPLE	ALFA-M	CN	CLM	CY	CLN	XCP/D	XCY/D	TAVG	P(C)	HFM	P	PD/2V
1	1.87	0.137	-0.148	-0.0711	0.01368	-1.081	-1.953	1.7126	412.5	3963.	415.0	0.0947
2	1.87	0.154	-0.154	-0.00927	-0.02201	-1.307	-2.373	2.7418	3612.	378.3	378.3	0.0863
3	1.87	0.153	-0.153	-0.0065	0.02047	-1.348	-2.366	3.7711	348.3	3326.	348.3	0.0795
4	1.87	0.152	-0.151	-0.00861	0.02013	-1.658	-2.286	4.8003	324.5	3098.	324.4	0.0740
5	1.87	0.151	-0.151	-0.00802	0.01918	-1.269	-2.390	5.8296	304.9	2910.	304.7	0.0695
6	1.87	0.150	-0.150	-0.00714	0.01711	-1.330	-2.395	6.9589	288.8	2756.	288.6	0.0659
7	1.87	0.151	-0.151	-0.00689	0.01661	-1.237	-2.383	7.9881	275.6	2630.	275.4	0.0629
8	1.87	0.151	-0.151	-0.00677	0.01745	-1.270	-2.401	8.9173	264.8	2527.	264.6	0.0604
9	1.87	0.151	-0.152	-0.00678	0.01594	-1.210	-2.352	9.9466	255.8	2442.	255.7	0.0584
10	1.87	0.149	-0.149	-0.00693	0.01566	-1.203	-2.261	10.9759	248.5	2317.	248.5	0.0567
11	1.87	0.148	-0.148	-0.00696	0.01505	-1.195	-2.482	12.0051	242.5	2317.	242.6	0.0556
12	1.87	0.147	-0.147	-0.00617	0.01401	-1.194	-2.272	13.034	237.5	2269.	237.6	0.0542
13	1.87	0.147	-0.147	-0.00598	0.01547	-1.191	-2.272	14.0636	233.5	2230.	233.5	0.0533
14	1.87	0.147	-0.147	-0.00598	0.01357	-1.165	-2.219	15.0929	230.1	2197.	230.1	0.0525
15	1.87	0.147	-0.147	-0.00575	0.01432	-1.181	-2.490	16.1221	227.4	2171.	227.3	0.0519
16	1.87	0.147	-0.147	-0.00606	0.01522	-1.179	-2.510	17.1514	225.1	2148.	225.0	0.0514
17	1.87	0.147	-0.147	-0.00621	0.01401	-1.174	-2.096	18.1806	223.3	2120.	223.0	0.0509
18	1.87	0.147	-0.147	-0.00551	0.01325	-1.175	-2.402	19.210	2114.	2214.	2214.	0.0505
19	1.87	0.147	-0.147	-0.00555	0.01416	-1.161	-2.551	20.2392	220.5	2102.	220.1	0.0502
20	1.87	0.147	-0.147	-0.00576	0.01416	-1.179	-2.461	21.2685	219.5	2090.	218.9	0.0500
21	1.87	0.147	-0.147	-0.00579	0.01307	-1.174	-2.356	22.2978	218.6	2083.	216.1	0.0498
22	1.87	0.147	-0.147	-0.00570	0.01396	-1.175	-2.450	23.3271	217.9	2076.	217.4	0.0496
23	1.87	0.147	-0.147	-0.00525	0.01311	-1.175	-2.499	24.3563	217.4	2072.	216.9	0.0495

CYD	CLNO	CLD	CLP	PSS	(PSS)U/2V	CL-DEL	PSSF	LTYPE	LPTARE
-0.00116	0.01256	0.0551	-1.0465	230.49	0.05261	0.0367	214.73	0.0	-0.0003
FINAL CY COEFFICIENTS									
-3.3368E-02	1.5233E-02	0	-2.6386E-01	1.3946E-02					
FINAL CLN COEFFICIENTS									
-1.2107E-01	-5.5611E-01	0	9.2358E-01	-4.8057E-02					

## Appendix B

Computer Program Data InputsCoefficient Arrays

A single 000005 card precedes all of the coefficient matrix input decks. This card designates the total number of aerodynamic coefficient arrays used in the program and must match the actual number of arrays that have been input. The last digit of the array designator integer must be in column 12. For example, if ten coefficients are used, the lead card is:

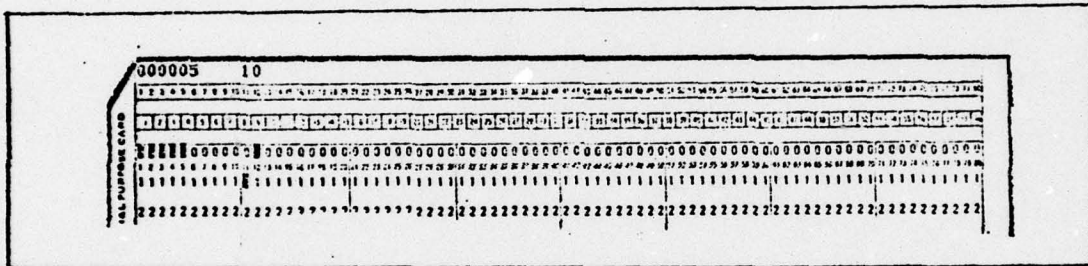


Fig. B-1a. Computer Input Card

Each individual coefficient array is then preceded by a card that specifies the desired coefficient symbol, the location of the array within the input deck in accordance with Table B-I, and the number of angle of attack columns and Mach number rows that will make up the array. A 20x20 matrix is the maximum size of the input array.

The first four spaces on the card shown in Fig. B-1b are available for the desired coefficient symbol. The last digit of the remaining three integers must lie on space 7, 9, and 11.

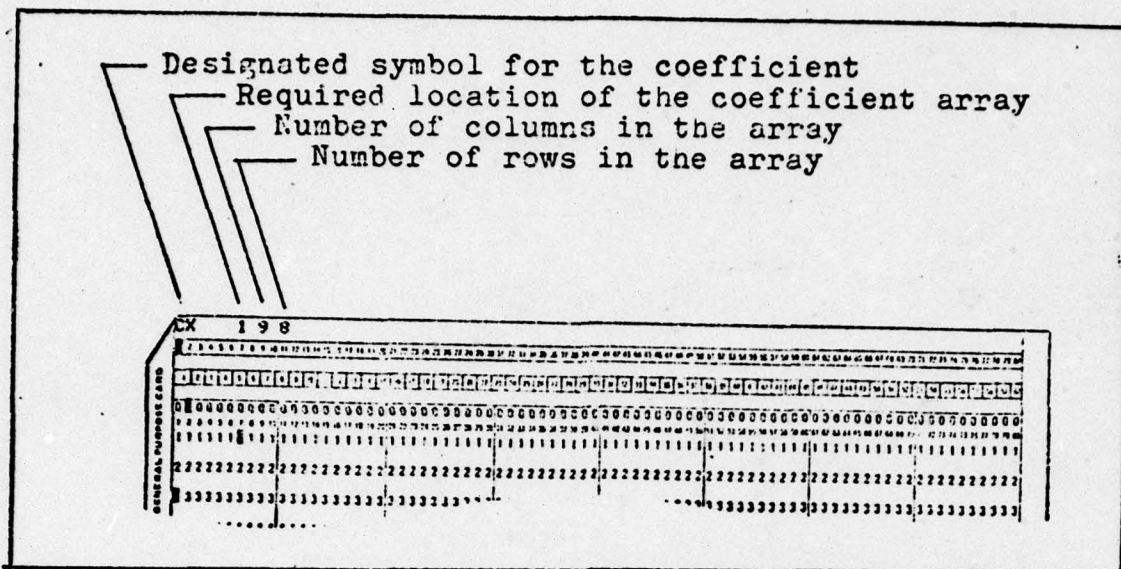


Fig. B-1b. Computer Input Card

The specific values of the input array are entered by rows.

For example, the nine angle of attack elements that make up the heading row of the  $C_x$  array (Appendix G) is entered as:

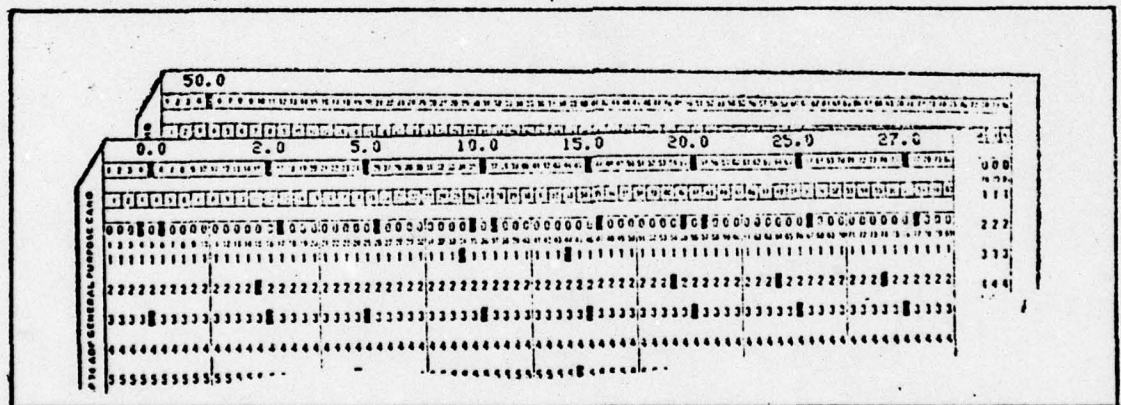


Fig. B-1c. Computer Input Card

and, in successive rows, values of the array elements are entered; such as the zero angle of attack row:

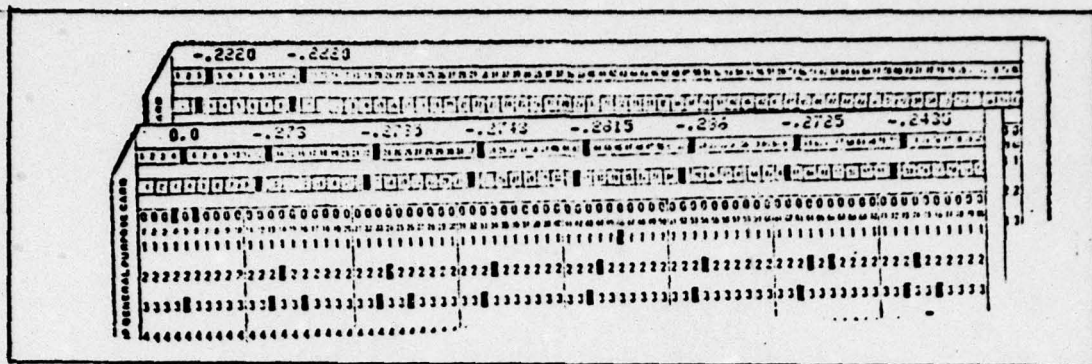


Fig. B-1d. Computer Input Card

The specific values of each element may be punched anywhere within successive ten-block segments of the card.

The remaining values of each element in the coefficient array are similarly entered until the matrix is complete (See Appendix G).

Each individual aerodynamic coefficient array used in the program is input in a similar manner. The sequence of these completed arrays must be in the order indicated in Table B-I. Only the desired aerodynamic coefficients need be input; zero entries are not required. The program will accept a maximum of thirty coefficient arrays.

#### Initial Conditions

The initial condition input deck is preceded with the desired title card. This title will appear as the heading of the computer output.

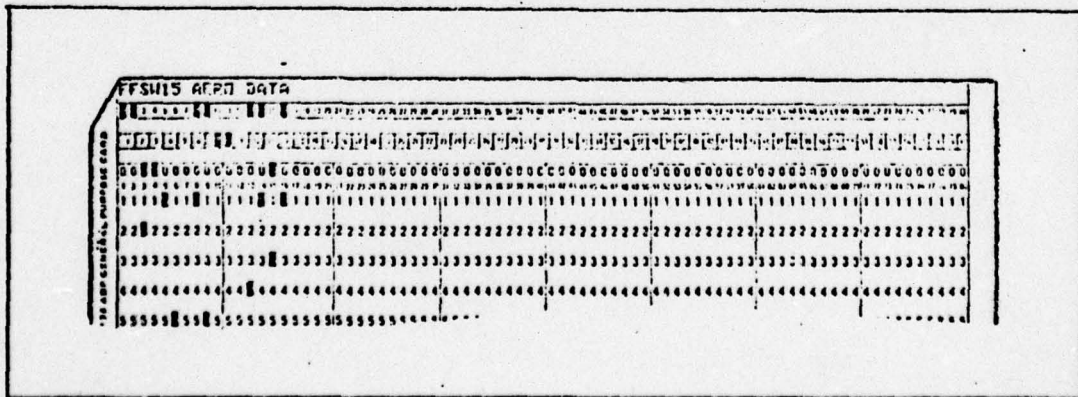


Fig. B-1e. Computer Input Card

The next card (Fig B-1f) identifies which of the option parameters available in the program are to be used. These parameters are (Ref 5:23):

**NORC:** Gravity designator

NORC=1 denotes constant gravity used.

NORC=0 denotes variable gravity will be input.

**IPRN:** Output time increment control

IPRN  $\times \Delta t$  = output increment that will be printed.  $\Delta t$  is the A(20) value (Table B-2II).

NALL  $\equiv$  1 for this program.

**IPUN:** Punch option for angle of attack ( $\alpha$ ) and sideslip ( $\beta$ ) data

IPUN=1 implements the option.

IPUN=0 option is not used.

**NBODY:** Reference frame output designator

NBODY=1 output prints and/or punches  $\alpha$  &  $\beta$  in body axes.

NBODY=0 output prints and/or punches  $\alpha$  &  $\beta$  aeroballistic axes.

**ISCALE:** Coefficient scaling option.

ISCALE=1 implements option

ISCALE=0 option is not used

**ITRST:** Thrust option

ITRST=1 implements thrust equation into program (See Ref 5: 11, 12)

ITRST=0 for unpowered projectile

The last digit of these integers must fall on every tenth space.

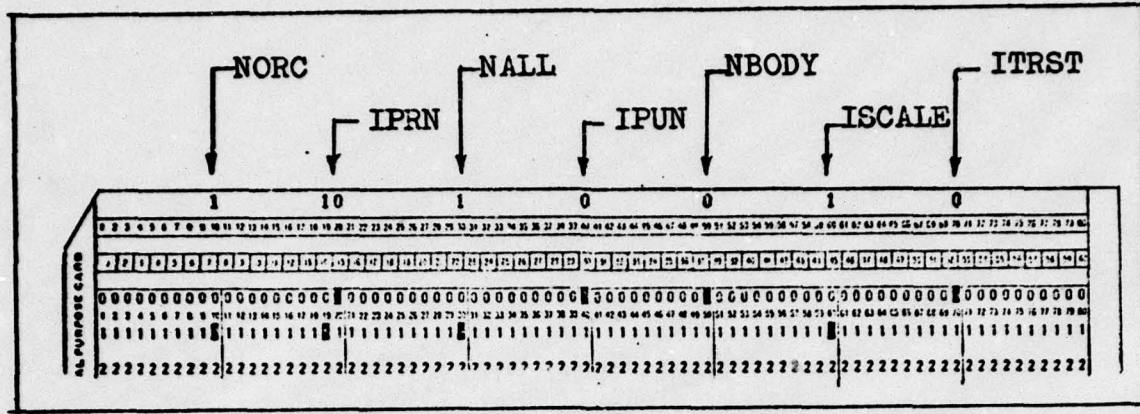


**Fig. B-1f. Computer Input Card**

The next three cards specify the desired initial conditions and projectile mass parameters in the sequence outlined by Table B-2II. All values are entered anywhere within successive ten-space segments.

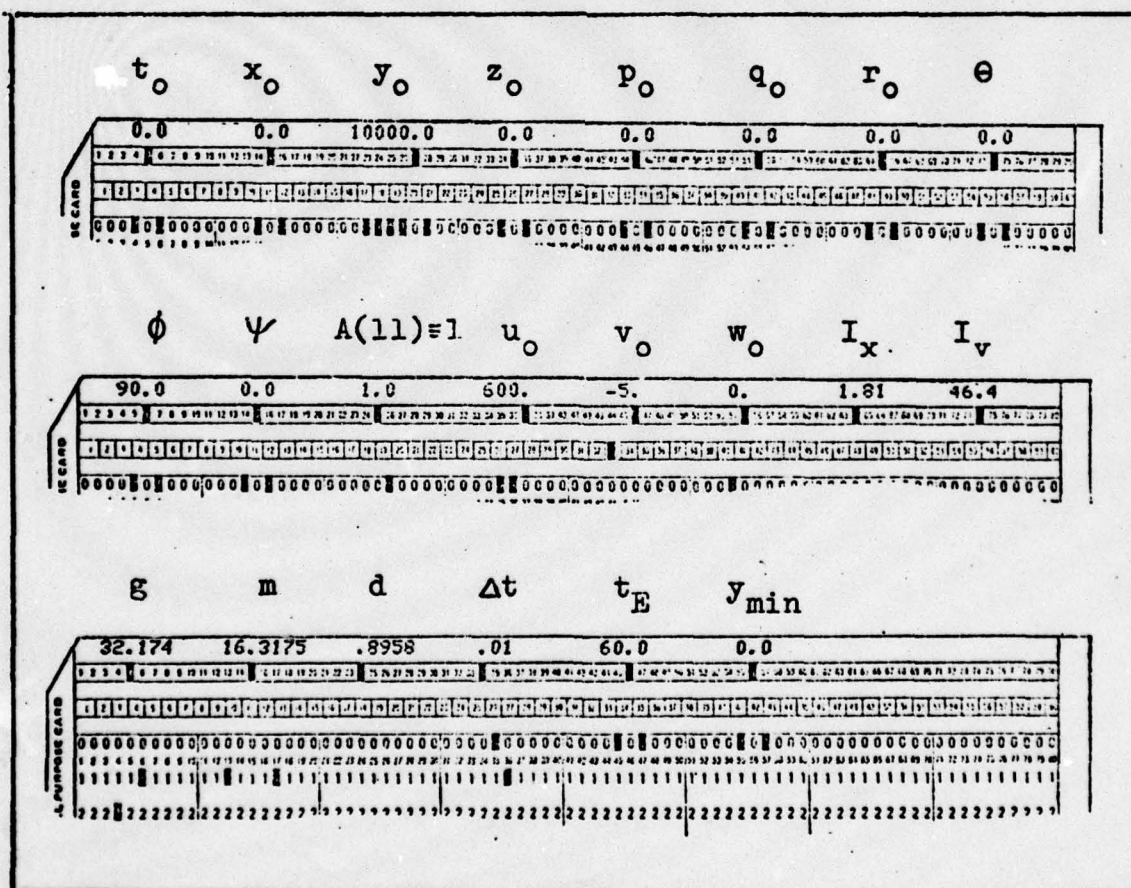


**Fig. B-1g.** Computer Input Cards

The units of the initial conditions are:

$t_0, \Delta t, t_E$	Sec
$x_0, y_0, z_0, d, y_{\min}$	Ft
$p_0, q_0, r_0$	Rad/Sec
$\theta, \phi, \psi$	Degrees
$u_0, v_0, w_0$	Ft/Sec
$I_x, I_y$	Lb-Ft-Sec <sup>2</sup>
$g$	Ft/Sec <sup>2</sup>
$m$	Slugs

The initial values of  $\theta$  and  $\alpha$  (which is input implicitly) as well as  $u_0$  &  $w_0$  are determined according to the following scheme:

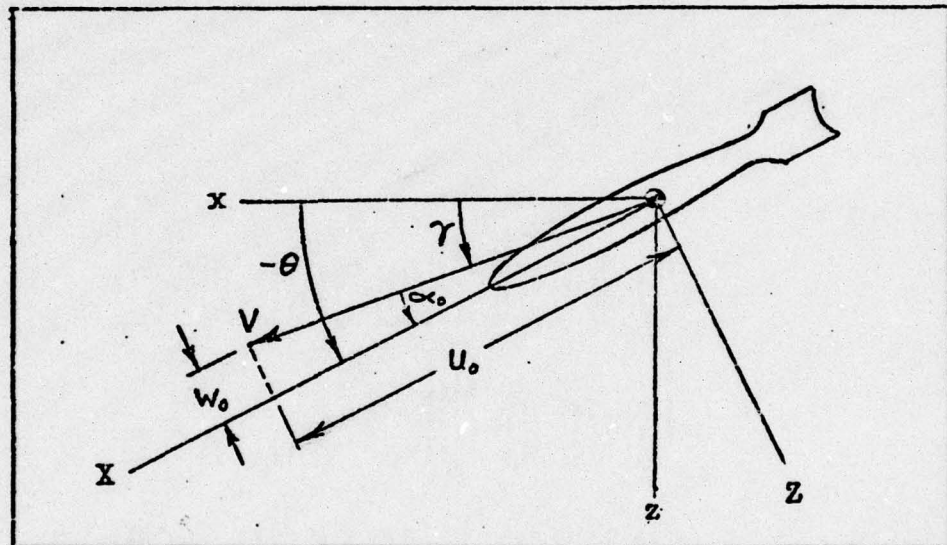


Fig. B-2. Flight Path/Perturbation Angle Input

where

$V$  = velocity vector of the center of gravity of the projectile.

$\theta$  = total angle between the body fixed and inertial frame.

$\gamma$  = flight path angle = angle between the inertial frame and velocity vector  $V$ .

$\alpha_0$  = initial perturbation angle from the initial flight path angle.

$w_0 = V \sin \alpha_0$  = projection of the velocity vector on the body Z axis.

$u_0 = V \cos \alpha_0$  = projection of the velocity vector on the body X axis.

For a projectile in a  $30^{\circ}$  initial dive angle at 800 ft/sec subjected to a  $5^{\circ}$  initial perturbation upon release, with no out-of-plane components, the following values would be input:

$$\theta = -35.0, \phi = 90.0, \psi = 0.0$$

$$u_0 = 800 \cos 10^{\circ} = 787.846$$

$$v_0 = 0.0$$

$$w_0 = -800 \sin 10^{\circ} = -138.918$$

Note:  $\theta \equiv 90^{\circ}$  to align the inertial frame with the body fixed frame (See Fig 1).

#### Scale Factors

The remaining four cards are for scale factors (applicable only if ISCALE was previously designated as 1). The scale factor changes the corresponding coefficient of Table B-I by the multiple of the scaling factor.

The only scaling factor used in this study was  $C_f (\delta w)$ .  $C_f (\delta w)$  is the coefficient for roll due to fin wedge angle. To scale the 15 degree wedge angle values of the coefficient array to, say, 10 degrees; the value .6666 is the appropriate scaling factor to enter in the ninth block of the scaling cards (Fig B-3).

The integer 1.0 is the required entry when no scaling of the corresponding coefficient array is desired.

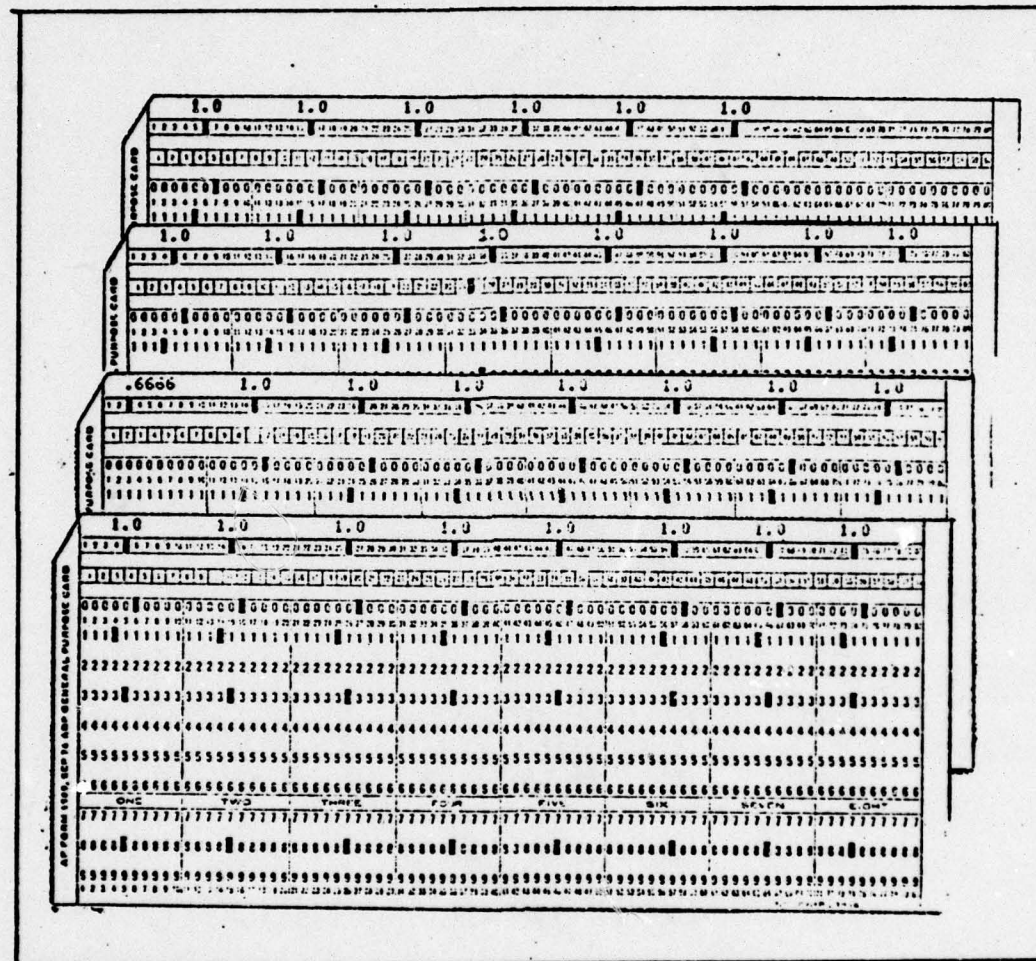


Fig. B-3. Scale Factor Inputs C(1) thru C(30)

TABLE B-I

Aerodynamic Coefficient Array  
(Adapted from Ref 5)

$C(I, J, K)$  Aerodynamic coefficient array

where: I Mach number array  
J Angle of attack array  
K Location of aerodynamic coefficient

$C(I, J, 1)$	$C_x$	$C(I, J, 2)$	$C_{y_0}$
$C(I, J, 3)$	$C_{y_7}$	$C(I, J, 4)$	$C_{y_8}$
$C(I, J, 5)$	$C_{y_p}$	$C(I, J, 6)$	$C_{z_0}$
$C(I, J, 7)$	$C_{z_7}$	$C(I, J, 8)$	$C_{z_8}$
$C(I, J, 9)$	$C_l (\delta w)$	$C(I, J, 10)$	$C_{l_7}$
$C(I, J, 11)$	$C_{l_8}$	$C(I, J, 12)$	$C_{l_p}$
$C(I, J, 13)$	$C_{m_0}$	$C(I, J, 14)$	$C_{m_7}$
$C(I, J, 15)$	$C_{m_8}$	$C(I, J, 16)$	$C_{n_0}$
$C(I, J, 17)$	$C_{n_7}$	$C(I, J, 18)$	$C_{n_8}$
$C(I, J, 19)$	$C_{n_p}$	$C(I, J, 20)$	$C_{m_\epsilon}$
$C(I, J, 21)$	$C_{n_\epsilon}$	$C(I, J, 22)$	$C_{y_\epsilon}$
$C(I, J, 23)$	$C_{z_\epsilon}$	$C(I, J, 24)$	$C_{l_\epsilon \alpha p}$
$C(I, J, 25)$	$C_{l_\epsilon \alpha_1}$	$C(I, J, 26)$	$C_{l_\epsilon \alpha_2}$
$C(I, J, 27)$	$C_{m_{q0}}$	$C(I, J, 28)$	$C_{m_{q7}}$
$C(I, J, 29)$	$C_{m_{q8}}$	$C(I, J, 30)$	$C_{l_0}$

TABLE B-II

Computer Input Array  
 (Adapted from Ref 5)

A(1)	$t_0$	A(12)	$v_0$
A(2)	$x_0$	A(13)	$v_0$
A(3)	$y_0$	A(14)	$w_0$
A(4)	$z_0$	A(15)	$L_x$
A(5)	$p_0$	A(16)	$L_y$
A(6)	$q_0$	A(17)	$g$
A(7)	$r_0$	A(18)	$m$
A(8)	$\theta$	A(19)	$d$
A(9)	$\phi$	A(20)	$\Delta t$
A(10)	$\psi$	A(21)	$t_E$
A(11)	1.0	A(22)	$y_{min}$

Appendix C

Computer Output Example

The computer output parameters are shown in Table C-I.

TIME is measured from release.

RANGE, ALT, Z correspond to x, y, z of the inertial reference frame.

V = total velocity of the projectile with respect to the air mass.

p = spin rate.

$\bar{\text{ALPHA}} = \sqrt{\alpha^2 + \beta^2}$  (where --- denotes vector).

M = mach number.

PHI = roll angle.

ALPHA = angle of attack.

BETA = yaw angle.

The next set of parameters are useful for stability analysis applications. The outputs are based on linearized equations for the tricyclic response of a projectile to an initial disturbance (Ref 12, 8 or 11):

L-N =  $\lambda_n$  = damping factor for nutation mode.

L-P =  $\lambda_p$  = damping factor for precession mode.

W-N =  $\omega_n$  = nutation frequency.

W-P =  $\omega_p$  = precession frequency.

S = s = stability factor.

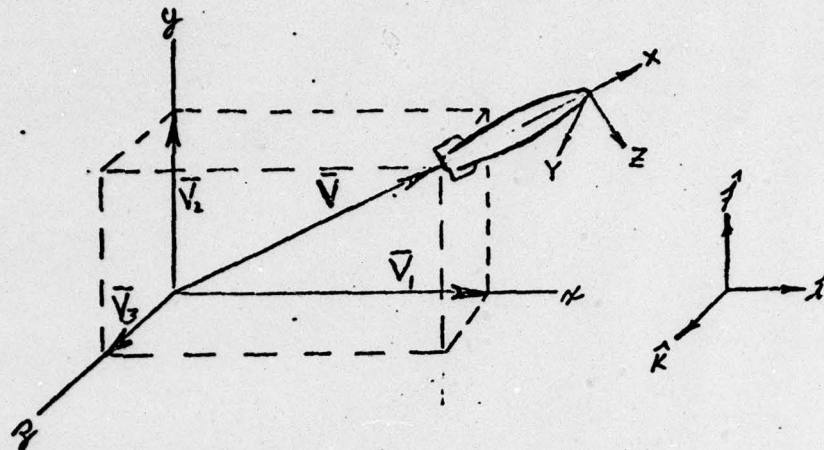
TAU =  $\tau$  = dynamic weight factor.

K-T =  $K_t$  = trim arm.

TABLE C-I  
Sample Computer Readout

FFSWIS AERO DATA				PAGE 1			
TIME SEC	RANGE FEET	ALT FEET	Z FEET	V FT/SEC	P RA/SFC	M RA/SFC DF3	W RA/SFC
0.1000	0.00	10000.00	0.00	60.02	0.0	-4.8	.96 90.00
0.1003	57.99	9999.84	.50	59.95	.4	-4.6	.55 73.51
1.1003	110.63	9199.36	.99	59.37	.7	-3.4	.56 104.46
1.1007	170.85	9199.35	1.43	59.07	1.0	-5.0	.56 167.97
1.1009	200.73	9197.42	1.97	59.79	1.4	-1.25	.56 190.57
1.1009	200.73	9197.46	2.46	59.52	1.7	-2.01	.56 201.95
1.1009	200.73	9197.46	2.95	59.27	2.1	-2.71	.56 211.11
1.1009	200.73	9197.46	3.42	59.03	2.4	-3.23	.56 219.72
1.1009	200.73	9194.51	3.90	57.80	2.8	-3.49	.55 227.79
1.1009	200.73	9194.51	4.36	57.59	3.1	-4.47	.55 238.47
1.1009	200.73	9193.49	4.82	57.40	3.4	-5.12	.55 239.08
1.1009	200.73	9193.49	5.25	57.23	3.7	-5.25	.55 236.52
1.1009	200.73	9193.49	5.67	67.94	4.0	-5.37	.55 236.52
1.1009	200.73	9193.49	6.17	67.47	4.56	-5.47	.55 227.03
1.1009	200.73	9191.49	6.05	59.95	4.0	-3.47	.55 230.49
1.1009	200.73	9191.49	6.41	51.83	4.56	-4.19	.55 239.96
1.1009	200.73	9187.54	6.41	51.83	4.9	-4.88	.55 253.10
1.1009	200.73	9185.61	6.74	53.67	5.1	-5.31	.55 267.52
1.1009	200.73	9185.61	7.05	53.60	5.4	-5.34	.55 280.09
1.1009	200.73	9185.61	7.36	51.64	5.4	-5.34	.55 280.09
1.1009	200.73	9185.61	7.67	51.34	5.7	-4.99	.55 297.52
1.1009	200.73	9185.61	8.00	51.34	6.1	-4.55	.55 295.73
1.1009	200.73	9185.61	8.37	51.20	6.4	-5.07	.55 308.44
1.1009	200.73	9185.61	8.78	51.27	6.8	-5.95	.55 328.71
1.1009	200.73	9185.61	9.22	51.25	7.2	-6.53	.55 328.71
1.1009	200.73	9185.61	9.69	51.23	7.4	-6.53	.55 328.71
1.1009	200.73	9185.61	10.17	51.21	7.7	-6.74	.55 352.77
1.1009	200.73	9185.61	10.65	51.21	8.0	-6.05	.55 379.19
1.1009	200.73	9185.61	11.10	51.28	8.4	-6.98	.55 53.71
1.1009	200.73	9185.61	11.51	51.37	9.5	-6.19	.55 63.75
1.1009	200.73	9185.61	11.99	51.46	9.9	-6.14	.55 92.97
1.1009	200.73	9185.61	12.23	51.61	9.1	-4.52	.55 127.73
1.1009	200.73	9185.61	12.55	51.64	9.4	-4.91	.55 159.95
1.1009	200.73	9185.61	12.87	51.79	9.7	-4.97	.55 212.90
1.1009	200.73	9185.61	13.19	51.75	10.0	-4.66	.55 255.05
1.1009	200.73	9185.61	13.52	51.73	10.3	-4.23	.55 291.17
1.1009	200.73	9185.61	13.86	51.64	10.5	-3.65	.55 317.67
1.1009	200.73	9185.61	14.24	51.55	10.9	-3.26	.55 343.24

## APPENDIX D

ROTATIONAL PARAMETER TRANSFORMATION (REF 10)

$x y z \equiv$  INERTIAL FRAME

$I J K \equiv$  INERTIAL UNIT VECTORS

$X Y Z \equiv$  BODY FIXED FRAME

THE UNIT VECTOR  $\bar{V}$  IS MADE UP OF THE THREE COMPONENTS  $\bar{V}_1, \bar{V}_2, \bar{V}_3$  SO THAT

$$\bar{V} = \bar{V}_1 \hat{x} + \bar{V}_2 \hat{y} + \bar{V}_3 \hat{z} \quad (1D)$$

NOW DEFINE  $\bar{V}_1 = \lambda_1 / \sin \alpha/2$

$$\bar{V}_2 = \lambda_2 / \sin \alpha/2 \quad (2D)$$

$$\bar{V}_3 = \lambda_3 / \sin \alpha/2$$

WHERE  $\lambda_1, \lambda_2, \lambda_3$  AND  $\alpha$  ARE UNKNOWN PARAMETERS.

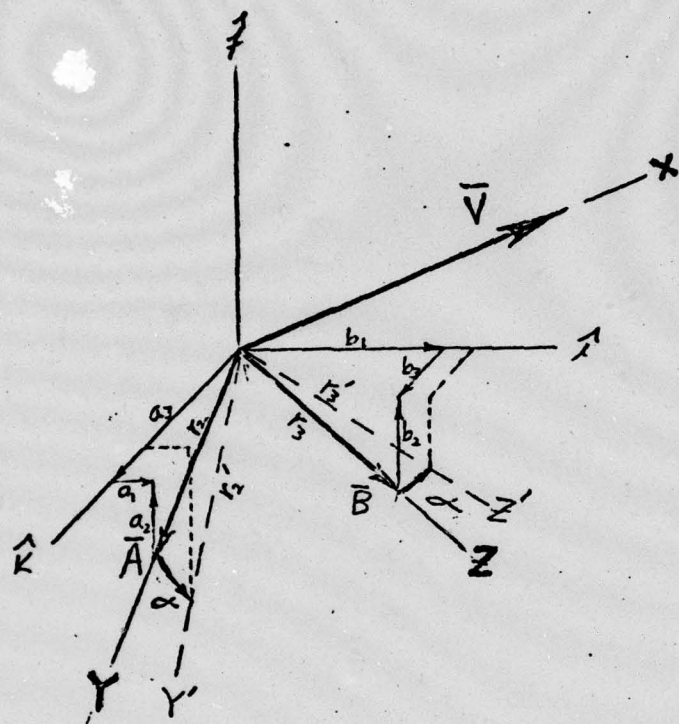
USING THE RELATION FOR DIRECTION COSINES THAT THE SUM OF THE SQUARES OF THE COMPONENTS OF A UNIT VECTOR MUST EQUAL ONE GIVES

$$\lambda_1^2 + \lambda_2^2 + \lambda_3^2 = \sin^2 \alpha/2 \quad (3D)$$

NOW DEFINE ANOTHER PARAMETER  $\lambda_0^2 = \cos^2 \alpha/2$ . SO THE EXPRESSION CAN BE WRITTEN AS

$$\lambda_1^2 + \lambda_2^2 + \lambda_3^2 + \lambda_0^2 = 1 \quad (4D)$$

THE BODY FIXED FRAME CAN BE RESOLVED INTO INERTIAL COMPONENTS AS FOLLOWS:



LET  $\bar{A}$  BE A UNIT VECTOR ALONG OY AND  $\bar{B}$  ALONG OZ SO THAT

$$\begin{aligned}\bar{A} &= a_1 \hat{x} + a_2 \hat{y} + a_3 \hat{z} \\ \bar{B} &= b_1 \hat{x} + b_2 \hat{y} + b_3 \hat{z}\end{aligned}\quad (51)$$

WHERE  $a_1, a_2, a_3, b_1, b_2, b_3$  ARE INERTIAL FRAME COMPONENTS. ALSO LET  $\alpha$  BE THE AMOUNT OF ROTATION OF THE PROJECTILE ABOUT THE OX AXIS WHERE  $r$  IS A VECTOR FIXED ON THE BODY BEFORE ROTATION AND  $r'$  IS THE POSITION AFTER ROTATION. THE DIRECTION COSINE MATRIX FOR

THIS ROTATION IS

$$\begin{bmatrix} r'_1 \\ r'_2 \\ r'_3 \end{bmatrix} = \begin{bmatrix} 1 & 0 & 0 \\ 0 & C\alpha & -S\alpha \\ 0 & S\alpha & C\alpha \end{bmatrix} \begin{bmatrix} r_1 \\ r_2 \\ r_3 \end{bmatrix} \quad (6)_D$$

OR

$$\begin{aligned} r'_1 &= r_2 C\alpha - r_3 S\alpha \\ r'_3 &= r_2 S\alpha + r_3 C\alpha \end{aligned} \quad (7)_D$$

WHERE  $r_1, r_2, r_3$  ARE COMPONENTS OF  $\vec{r}$ ;

$C \equiv \cos, S \equiv \sin;$

NEGATIVE ROTATION ABOUT X WAS USED  
SO EQN 12 SIMPLIFIES.

EXPRESSING  $\vec{r}$ 'S COMPONENTS IN THE INERTIAL FRAME:

$$\begin{aligned} r_1 \vec{v} &= \frac{\lambda_1}{\sin \alpha/2} \hat{x} + \frac{\lambda_2}{\sin \alpha/2} \hat{y} + \frac{\lambda_3}{\sin \alpha/2} \hat{z} \\ r_2 \vec{A} &= a_1 \hat{x} + a_2 \hat{y} + a_3 \hat{z} \\ r_3 \vec{B} &= b_1 \hat{x} + b_2 \hat{y} + b_3 \hat{z} \end{aligned} \quad (8)_D$$

COMBINING EQN 7 & 8 IN TERMS OF THE BODY FRAME:

$$\begin{aligned} \vec{r}' \vec{v} &= \frac{\lambda_1}{\sin \alpha/2} \hat{x} + \frac{\lambda_2}{\sin \alpha/2} \hat{y} + \frac{\lambda_3}{\sin \alpha/2} \hat{z} \\ \vec{r}' \vec{A} &= (a_1 \cos \alpha - b_1 \sin \alpha) \hat{x} + (a_2 \cos \alpha - b_2 \sin \alpha) \hat{y} + (a_3 \cos \alpha - b_3 \sin \alpha) \hat{z} \\ \vec{r}' \vec{B} &= (a_1 \sin \alpha - b_1 \cos \alpha) \hat{x} + (a_2 \sin \alpha - b_2 \cos \alpha) \hat{y} + (a_3 \sin \alpha - b_3 \cos \alpha) \hat{z} \end{aligned} \quad (9)_D$$

DENOTING THE TRANSFORMATION MATRIX BY [C], THE EXPRESSION THAT TRANSFORMS THE COMPONENTS OF THE MOVING BODY AXES SYSTEM TO INERTIAL REFERENCE IS:

$$\begin{bmatrix} C_{11} & C_{12} & C_{13} \\ C_{21} & C_{22} & C_{23} \\ C_{31} & C_{32} & C_{33} \end{bmatrix} \begin{bmatrix} \frac{\lambda_1}{\sin \omega/2} & a_1 & b_1 \\ \frac{\lambda_2}{\sin \omega/2} & a_2 & b_2 \\ \frac{\lambda_3}{\sin \omega/2} & a_3 & b_3 \end{bmatrix} = \begin{bmatrix} \frac{\lambda_1}{\sin \omega/2}, a_1 c\alpha - b_1 s\alpha, a_1 s\alpha + b_1 c\alpha \\ \frac{\lambda_2}{\sin \omega/2}, a_2 c\alpha - b_2 s\alpha, a_2 s\alpha + b_2 c\alpha \\ \frac{\lambda_3}{\sin \omega/2}, a_3 c\alpha - b_3 s\alpha, a_3 s\alpha + b_3 c\alpha \end{bmatrix}$$

EQN (10)D

POST MULTIPLYING BY THE INVERSE (TRANSPOSE FOR THE ORTHOGONAL SYSTEM):

$$\begin{bmatrix} C_{11} & C_{12} & C_{13} \\ C_{21} & C_{22} & C_{23} \\ C_{31} & C_{32} & C_{33} \end{bmatrix} = \begin{bmatrix} \frac{\lambda_1}{\sin \omega/2}, a_1 c\alpha - b_1 s\alpha, a_1 s\alpha + b_1 c\alpha \\ \frac{\lambda_2}{\sin \omega/2}, a_2 c\alpha - b_2 s\alpha, a_2 s\alpha + b_2 c\alpha \\ \frac{\lambda_3}{\sin \omega/2}, a_3 c\alpha - b_3 s\alpha, a_3 s\alpha + b_3 c\alpha \end{bmatrix} \begin{bmatrix} \frac{\lambda_1}{\sin \omega/2}, \frac{\lambda_2}{\sin \omega/2}, \frac{\lambda_3}{\sin \omega/2} \\ a_1 & a_2 & a_3 \\ b_1 & b_2 & b_3 \end{bmatrix}$$

EQN(11)D

MULTIPLYING IT OUT:

$$\begin{bmatrix} C_{11} & C_{12} & C_{13} \\ C_{21} & C_{22} & C_{23} \\ C_{31} & C_{32} & C_{33} \end{bmatrix} = \begin{bmatrix} \frac{\lambda_1^2}{\sin^2 \omega/2} + (a_1^2 + b_1^2) c\alpha^2, \frac{\lambda_1 \lambda_2}{\sin^2 \omega/2} + (a_1 b_2 - a_2 b_1) s\alpha c\alpha + (a_1 a_2 + b_1 b_2) c\alpha s\alpha, \\ \frac{\lambda_1 \lambda_3}{\sin^2 \omega/2} + (a_1 b_3 - b_1 a_3) s\alpha c\alpha + (b_1 b_3 + a_3 a_1) c\alpha^2, \\ \frac{\lambda_2 \lambda_3}{\sin^2 \omega/2} + (b_2 a_1 - b_1 a_2) s\alpha c\alpha + (a_2 a_3 + b_2 b_3) c\alpha^2 \end{bmatrix}$$

$$\begin{bmatrix} \frac{\lambda_1 \lambda_3}{\sin^2 \omega/2} + (a_1 a_3 + b_1 b_3) c\alpha + (b_1 a_3 - a_1 b_3) s\alpha, \\ \frac{\lambda_2 \lambda_3}{\sin^2 \omega/2} + (a_3 a_2 + b_3 b_2) c\alpha + (b_2 a_3 - b_3 a_2) s\alpha, \frac{\lambda_2^2}{\sin^2 \omega/2} + (a_2^2 + b_2^2) c\alpha^2 \end{bmatrix}$$

EQN(12)D

THE FOLLOWING RELATIONSHIPS BETWEEN DIRECTION COSINES  
APPLY TO AN ORTHOGONAL, RIGHT-HAND SYSTEM :

$$a_1^2 + a_2^2 + a_3^2 = 1 \quad (13)_D$$

$$b_1^2 + b_2^2 + b_3^2 = 1 \quad (14)_D$$

$$a_1 \lambda_1 + a_2 \lambda_2 + a_3 \lambda_3 = 0 \quad (15)_D$$

$$b_1 \lambda_1 + b_2 \lambda_2 + b_3 \lambda_3 = 0 \quad (16)_D$$

$$a_1 b_1 + a_2 b_2 + a_3 b_3 = 0 \quad (17)_D$$

$$b_1 = \frac{1}{\sqrt{\lambda_2}} (\lambda_2 a_3 - \lambda_3 a_2) \quad (18)_D$$

$$b_2 = \frac{1}{\sqrt{\lambda_2}} (\lambda_3 a_1 - \lambda_1 a_3) \quad (19)_D$$

$$b_3 = \frac{1}{\sqrt{\lambda_2}} (\lambda_1 a_2 - \lambda_2 a_1) \quad (20)_D$$

$$\begin{vmatrix} \frac{\lambda_1}{\sqrt{\lambda_2}} & \frac{\lambda_2}{\sqrt{\lambda_2}} & \frac{\lambda_3}{\sqrt{\lambda_2}} \\ a_1 & a_2 & a_3 \\ b_1 & b_2 & b_3 \end{vmatrix} = 1 \quad (21)_D$$

EQUATIONS (15) AND (16) CAN BE WRITTEN AS:

$$a_2 = -\frac{1}{\lambda_2} (a_1 \lambda_1 + a_3 \lambda_3) \quad (22)_D$$

$$b_2 = -\frac{1}{\lambda_2} (b_1 \lambda_1 + b_3 \lambda_3) \quad (23)_D$$

SUBSTITUTING (22) & (23) INTO (17)

$$a_1 b_1 + \frac{1}{\lambda_2^2} (a_1 \lambda_1 + a_3 \lambda_3)(b_1 \lambda_1 + b_3 \lambda_3) + a_3 b_3 = 0 \quad (24)_D$$

$$a_1 b_1 (\lambda_1^2 + \lambda_3^2) + a_3 b_3 (\lambda_2^2 + \lambda_3^2) + (a_3 b_1 + b_3 a_1) \lambda_1 \lambda_3 = 0$$

SUBSTITUTING (22) INTO (13) AND (23) INTO (14)

$$a_1^2(\lambda_1^2 + \lambda_2^2) + a_3^2(\lambda_2^2 + \lambda_3^2) = \lambda_2^2 - 2\lambda_1\lambda_2 a_1 a_3 \quad (25)_D$$

$$b_1^2(\lambda_1^2 + \lambda_2^2) + b_3^2(\lambda_2^2 + \lambda_3^2) = \lambda_2^2 - 2\lambda_1\lambda_2 b_1 b_3 \quad (26)_D$$

EQUATIONS (22), (23) INTO (21)

$$-\frac{\lambda_1 b_3}{\lambda_2} (a_1 \lambda_1 + a_3 \lambda_3) + \lambda_2 b_1 a_3 - \frac{\lambda_3 a_1}{\lambda_2} (b_1 \lambda_1 + b_3 \lambda_3)$$

$$+ \frac{\lambda_2 b_1}{\lambda_2} (a_1 \lambda_1 + a_3 \lambda_3) - \lambda_2 a_1 b_3 + \frac{\lambda_1 a_3}{\lambda_2} (b_1 \lambda_1 + b_3 \lambda_3) = S \approx \frac{S}{2}$$

AFTER CANCELLATIONS AND REGROUPING

$$-b_3 a_1 [\lambda_1^2 + \lambda_2^2 + \lambda_3^2] + b_1 a_3 [\lambda_1^2 + \lambda_2^2 + \lambda_3^2] = \lambda_2 S \approx \frac{S}{2}$$

AND SINCE  $\lambda_1^2 + \lambda_2^2 + \lambda_3^2 = 1$ 

$$b_3 = \frac{1}{a_1} [b_1 a_3 - \lambda_2 S \approx \frac{S}{2}] \quad (27)_D$$

EQUATION (27) INTO (24)

$$a_1 b_1 (\lambda_1^2 + \lambda_2^2) + \frac{a_2}{a_1} (\lambda_1^2 + \lambda_3^2) b_1 a_3 - \frac{\lambda_2}{S \approx \frac{S}{2}} + \lambda_1 \lambda_2 [2a_3 b_1 - \frac{\lambda_2}{S \approx \frac{S}{2}}] = 0$$

$$a_1^2 b_1 (\lambda_1^2 + \lambda_2^2) + b_1 a_3^2 (\lambda_2^2 + \lambda_3^2) + a_3 [2\lambda_1 \lambda_3 a_1 b_1 - \frac{\lambda_2}{S \approx \frac{S}{2}} (\lambda_2^2 + \lambda_3^2)] = \frac{a_1}{S \approx \frac{S}{2}} \lambda_1 \lambda_2 \lambda_3 \quad (28)_D$$

EQUATION (27) INTO (26)

$$b_1^2 (\lambda_1^2 + \lambda_2^2) + \frac{1}{a_1^2} [b_1 a_3 - \frac{\lambda_2}{S \approx \frac{S}{2}}]^2 (\lambda_2^2 + \lambda_3^2) = \lambda_2^2 - 2 \frac{b_1}{a_1} (b_1 a_3 - \frac{\lambda_2}{S \approx \frac{S}{2}}) \lambda_1 \lambda_3$$

$$a_1^2 b_1^2 (\lambda_1^2 + \lambda_2^2) + a_3^2 b_1^2 (\lambda_2^2 + \lambda_3^2) + a_3 b_1 [2\lambda_1 \lambda_3 a_1 b_1 - \frac{\lambda_2}{S \approx \frac{S}{2}} (\lambda_2^2 + \lambda_3^2)] = \\ \lambda_2^2 a_1^2 + 2b_1 a_1 \frac{\lambda_1 \lambda_2 \lambda_3}{S \approx \frac{S}{2}} - \frac{\lambda_2^2}{S^2 \approx \frac{S^2}{2}} (\lambda_2^2 + \lambda_3^2) + a_3 b_1 \frac{\lambda_2}{S \approx \frac{S}{2}} (\lambda_2^2 + \lambda_3^2) \quad (29)_D$$

LEFT SIDE OF (28)  $\times b_1$  = LEFT SIDE OF (29) THEREFORE

$$-\frac{\alpha_1 b_1}{S^2 \omega_2} \lambda_1 \lambda_2 \lambda_3 = \lambda_2^2 a_1^2 + 2 b_1 \alpha_1 \frac{\lambda_1 \lambda_2 \lambda_3}{S^2 \omega_2} + \alpha_1 b_1 \frac{\lambda_2}{S^2 \omega_2} (\lambda_1^2 + \lambda_2^2) - \frac{\lambda_1^2}{S^2 \omega_2} (\lambda_2^2 + \lambda_3^2)$$

MULTIPLYING THRU BY  $\frac{S^2 \omega_2}{b_1}$

$$\alpha_1 = \left\{ \left[ \frac{\lambda_2}{S^2 \omega_2} (\lambda_1^2 + \lambda_2^2) - S^2 \omega_2 \lambda_2 a_1^2 \right] \frac{1}{b_1} - \alpha_1 \lambda_1 \lambda_3 \right\} \frac{1}{\lambda_2^2 + \lambda_3^2} \quad (30)_D$$

EQUATION (18) AND (24)

$$b_1 = \frac{1}{S^2 \omega_2} \left[ \lambda_2 \alpha_1 + \lambda_3 \frac{\lambda_1 \alpha_1 + \lambda_3 \alpha_3}{\lambda_2} \right] = \frac{\lambda_1 \lambda_3}{S^2 \omega_2 \lambda_2} \alpha_1 + \left( \frac{\lambda_2}{S^2 \omega_2} + \frac{\lambda_3^2}{S^2 \omega_2 \lambda_2} \right) \alpha_3 \quad (31)_D$$

EQUATION (30) INTO (33)

$$\begin{aligned} b_1 &= \frac{\lambda_1 \lambda_3}{S^2 \omega_2 \lambda_2} \alpha_1 + \left( \frac{\lambda_2}{S^2 \omega_2} + \frac{\lambda_3^2}{S^2 \omega_2 \lambda_2} \right) \left( \frac{1}{\lambda_2^2 + \lambda_3^2} \right) \left\{ \left[ \frac{\lambda_2}{S^2 \omega_2} (\lambda_1^2 + \lambda_3^2) - \alpha_1^2 \lambda_2 S^2 \omega_2 \right] \frac{1}{b_1} - \alpha_1 \lambda_1 \lambda_3 \right\} \\ &= \frac{\lambda_1 \lambda_3}{S^2 \omega_2 \lambda_2} \alpha_1 + \left( \frac{\lambda_2^2 + \lambda_3^2}{S^2 \omega_2 \lambda_2} \right) \left( \frac{1}{\lambda_2^2 + \lambda_3^2} \right) \left\{ \left[ \frac{\lambda_2}{S^2 \omega_2} (\lambda_1^2 + \lambda_3^2) - (\alpha_1^2 \lambda_2 S^2 \omega_2) \right] \frac{1}{b_1} - \lambda_1 \lambda_3 \alpha_1 \right\} \\ &= \frac{\lambda_1 \lambda_3}{S^2 \omega_2 \lambda_2} \alpha_1 + \frac{1}{S^2 \omega_2 \lambda_2} \left\{ \left[ \frac{\lambda_2}{S^2 \omega_2} (\lambda_1^2 + \lambda_3^2) - (\alpha_1^2 \lambda_2 S^2 \omega_2) \right] \frac{1}{b_1} - \lambda_1 \lambda_3 \alpha_1 \right\} \\ b_1 &= \frac{1}{S^2 \omega_2 \lambda_2} \left[ \frac{\lambda_2}{S^2 \omega_2} (\lambda_1^2 + \lambda_3^2) - \alpha_1^2 \lambda_2 S^2 \omega_2 \right] \frac{1}{b_1} \\ b_1^2 + a_1^2 &= \frac{1}{S^2 \omega_2} (\lambda_2^2 + \lambda_3^2) \end{aligned} \quad (32)_D$$

EQUATION (32) IS USED TO EVALUATE  $C_{11}$  IN (12)

$$C_{11} = \frac{\lambda_1^2}{S^2 \omega_2} + (a_1^2 + b_1^2) \cos \alpha$$

FROM THE DEFINITIONS  $\lambda_0^2 = \cos^2 \omega_2$  AND  $\cos 2\alpha = 2\cos^2 \alpha - 1$

$$\begin{aligned} C_{11} &= \frac{1}{S^2 \omega_2} \left[ \lambda_1^2 + (\lambda_2^2 + \lambda_3^2)(2\lambda_0^2 - 1) \right] \\ &= \frac{1}{S^2 \omega_2} \left[ \lambda_1^2 + (1 - \lambda_0^2 - \lambda_1^2)(2\lambda_0^2 - 1) \right] \\ &= \frac{1}{S^2 \omega_2} \left[ \lambda_1^2 + 2\lambda_0^2 - 1 - 2\lambda_0^2 + \lambda_0^2 - 2\lambda_1^2 \lambda_0^2 + \lambda_1^2 \right] \\ &= \frac{1}{S^2 \omega_2} \left[ 2(\lambda_1^2 + \lambda_0^2) - 2(\lambda_0^2 + \lambda_1^2) \lambda_0^2 + \lambda_0^2 - 1 \right] \end{aligned}$$

$$= \frac{1}{s^2 \omega_2} [2(\lambda_1^2 + \lambda_0^2)(1 - \lambda_0^2) - (1 - \lambda_0^2)]$$

$$= \frac{(1 - \lambda_0^2)}{s^2 \omega_2} [2(\lambda_1^2 + \lambda_0^2) - 1]$$

$$\text{USING } s^2 \omega_2 = 1 - c^2 \omega_2 = 1 - \lambda_0^2$$

$$C_{11} = \underline{2(\lambda_1^2 + \lambda_0^2) - 1} \quad (33)_D$$

SIMILARLY

$$C_{22} = \frac{\lambda_2^2}{s^2 \omega_2} + (a_2^2 + b_2^2) \cos \omega_2 = \underline{2(\lambda_2^2 + \lambda_0^2) - 1} \quad (34)_D$$

$$C_{33} = \frac{\lambda_3^2}{s^2 \omega_2} + (a_3^2 + b_3^2) \cos \omega_2 = \underline{2(\lambda_3^2 + \lambda_0^2) - 1} \quad (35)_D$$

FROM EQUATION (27)

$$b_1 a_3 - b_3 a_1 = \frac{\lambda_2}{s \omega_2} \quad (36)_D$$

BY ANALOGY AND WITH (21)

$$b_2 a_1 - b_1 a_2 = \frac{\lambda_3}{s \omega_2} \quad (37)_D$$

$$b_3 a_2 - b_2 a_3 = \frac{\lambda_1}{s \omega_2} \quad (38)_D$$

EVALUATE  $a_1 a_3 + b_1 b_3$  BY USING (27)

$$\begin{aligned} a_1 a_3 + b_1 b_3 &= a_1 a_3 + b_1 \frac{1}{a_1} (b_1 a_3 - \frac{\lambda_2}{s \omega_2}) \\ &= \frac{a_3}{a_1} (a_1^2 + b_1^2) - \frac{b_1}{a_1} \frac{\lambda_2}{s \omega_2} \end{aligned}$$

SUB EQUATION (32):

$$= \frac{a_3}{a_1} \frac{\lambda_2^2 + \lambda_3^2}{s^2 \omega_2} - \frac{b_1}{a_1} \frac{\lambda_2}{s \omega_2}$$

SUB EQUATION (30):

$$\begin{aligned}
 &= \frac{1}{S^2 \alpha/2} a_1 \left\{ \frac{1}{b_1} \left[ \frac{\lambda_2}{S^2 \alpha/2} (\lambda_2^2 + \lambda_3^2) - S^2 \alpha/2 \lambda_2 a_1^2 \right] - a_1 \lambda_1 \lambda_3 \right\} - \frac{b_1 \lambda_2}{a_1 S^2 \alpha/2} \\
 &= \frac{\lambda_2}{S^2 \alpha/2 a_1 b_1} (\lambda_2^2 + \lambda_3^2) - \frac{\lambda_2 a_1^2}{S^2 \alpha/2 b_1 a_1} - \frac{\lambda_1 \lambda_3}{S^2 \alpha/2} - \frac{b_1^2}{a_1} \frac{\lambda_2}{b_1 S^2 \alpha/2} \\
 &= \frac{\lambda_2}{S^2 \alpha/2 a_1 b_1} (\lambda_2^2 + \lambda_3^2) - \frac{\lambda_2}{S^2 \alpha/2 a_1 b_1} (a_1^2 + b_1^2) - \frac{\lambda_1 \lambda_3}{S^2 \alpha/2}
 \end{aligned}$$

SUB EQUATION (32)

$$a_1 a_3 + b_1 b_2 = - \frac{\lambda_1 \lambda_3}{S^2 \alpha/2} \quad (39)_D$$

SIMILARLY

$$a_1 a_2 + b_1 b_3 = - \frac{\lambda_1 \lambda_2}{S^2 \alpha/2} \quad (40)_D$$

$$a_2 a_3 + b_2 b_3 = - \frac{\lambda_2 \lambda_3}{S^2 \alpha/2} \quad (41)_D$$

EVALUATING  $C_{12}$  FROM EQN(12) WITH (40) AND (37)

$$\begin{aligned}
 C_{12} &= \frac{\lambda_1 \lambda_2}{S^2 \alpha/2} + (a_1 a_2 + b_1 b_3) \cos \alpha + (a_1 b_2 - a_2 b_1) \sin \alpha \\
 &= \frac{\lambda_1 \lambda_2}{S^2 \alpha/2} - \frac{\lambda_1 \lambda_2}{S^2 \alpha/2} (2 \lambda_0^2 - 1) + \frac{\lambda_3}{S^2 \alpha/2} 2 S^2 \alpha/2 \lambda_0
 \end{aligned}$$

WHERE  $\cos 2(\alpha/2) = 2(\cos^2 \alpha/2) - 1$   
 $\sin 2(\alpha/2) = 2(\sin \alpha/2)(\cos \alpha/2)$

$$= \lambda_1 \lambda_2 \left[ \frac{2(1 - \lambda_0^2)}{S^2 \alpha/2} \right] + 2 \lambda_0 \lambda_3$$

$$\underline{C_{12} = 2[\lambda_1 \lambda_2 + \lambda_0 \lambda_3]} \quad (42)_D$$

IN THE SAME MANNER, USING EQUATIONS

(32) (37) (38) (39) (40) (41), THE

REMAINING COMPONENTS ARE

$$C_{21} = 2[\lambda_1 \lambda_2 - \lambda_0 \lambda_3] \quad (43)_D$$

$$C_{13} = 2[\lambda_1 \lambda_3 - \lambda_0 \lambda_2] \quad (44)_D$$

$$C_{31} = 2[\lambda_1 \lambda_3 - \lambda_0 \lambda_2] \quad (45)_D$$

$$C_{23} = 2[\lambda_2 \lambda_3 - \lambda_0 \lambda_1] \quad (46)_D$$

$$C_{32} = 2[\lambda_2 \lambda_3 - \lambda_0 \lambda_1] \quad (47)_D$$

SO THAT THE DIRECTION COSINE MATRIX  
BETWEEN THE INERTIAL AND BODY FIXED  
REFERENCE FRAMES AFTER ROTATION  $\alpha$  IS

$$\begin{bmatrix} C_{11} & C_{12} & C_{13} \\ C_{21} & C_{22} & C_{23} \\ C_{31} & C_{32} & C_{33} \end{bmatrix} = \begin{bmatrix} 2(\lambda_1^2 + \lambda_0^2) - 1 & 2(\lambda_1 \lambda_2 + \lambda_0 \lambda_3) & 2(\lambda_1 \lambda_3 - \lambda_0 \lambda_2) \\ 2(\lambda_1 \lambda_2 - \lambda_0 \lambda_3) & 2(\lambda_2^2 + \lambda_0^2) - 1 & 2(\lambda_2 \lambda_3 + \lambda_0 \lambda_1) \\ 2(\lambda_1 \lambda_3 + \lambda_0 \lambda_2) & 2(\lambda_2 \lambda_3 - \lambda_0 \lambda_1) & 2(\lambda_3^2 + \lambda_0^2) - 1 \end{bmatrix}$$

EQN (48)<sub>D</sub>

WHICH IS EQUIVALENT TO THE EULER ANGLE FORM  
OF THE DIRECTION COSINE MATRIX

$$\begin{bmatrix} C\theta C\psi & S\theta & S\psi C\theta \\ -S\psi S\phi - C\psi S\theta C\phi & C\theta C\phi & C\psi S\phi - S\psi S\theta C\phi \\ S\psi C\phi + C\psi S\theta S\phi & -C\theta S\phi & C\psi C\phi + S\psi S\theta S\phi \end{bmatrix}$$

EQN (19)<sub>D</sub>

## COMPARING COEFFICIENTS

$$C_{11} = 2(\lambda_0^2 + \lambda_1^2) - 1 = C\psi C\theta \quad (50)_D$$

$$C_{22} = 2(\lambda_0^2 + \lambda_2^2) - 1 = C\phi C\theta \quad (51)_D$$

$$C_{33} = 2(\lambda_0^2 + \lambda_3^2) - 1 = C\psi C\phi + S\psi S\theta S\phi \quad (52)_D$$

FROM EQN (4)

$$\lambda_0^2 = 1 - (\lambda_1^2 + \lambda_2^2 + \lambda_3^2) \quad (53)_D$$

EQUATION (53) INTO (50)(51)(52)

$$1 - 2(\lambda_2^2 + \lambda_3^2) = C\psi C\theta \quad (54)_D$$

$$1 - 2(\lambda_1^2 + \lambda_3^2) = C\phi C\theta \quad (55)_D$$

$$1 - 2(\lambda_2^2 + \lambda_1^2) = C\psi C\phi + S\psi S\theta S\phi \quad (56)_D$$

EQN (56) - (55)

$$-2(\lambda_2^2 + \lambda_3^2) = C\psi C\phi + S\psi S\theta S\phi - C\phi C\theta \quad (57)_D$$

EQN (54) + (57)

$$1 - 4\lambda_2^2 = C\psi(C\theta + C\phi) + S\psi S\theta S\phi - C\phi C\theta$$

$$4\lambda_2^2 = 1 - C\psi(C\theta + C\phi) + C\phi C\theta - S\psi S\theta S\phi \quad (58)_D$$

USING THE IDENTITY  $C\theta + C\phi = 2C\left(\frac{\theta+\phi}{2}\right)C\left(\frac{\theta-\phi}{2}\right)$ 

$$4\lambda_2^2 = 1 - 2C\psi\left[C\left(\frac{\theta+\phi}{2}\right)C\left(\frac{\theta-\phi}{2}\right)\right] + C\phi C\theta - S\psi S\theta S\phi$$

USING THE IDENTITY  $C2\psi = C^2\psi - S^2\psi$ 

$$4\lambda_2^2 = 1 - 2\left(C^2\frac{\psi}{2} - S^2\frac{\psi}{2}\right)\left(C^2\frac{\theta}{2}C^2\frac{\phi}{2} - S^2\frac{\theta}{2}S^2\frac{\phi}{2}\right) + C\phi C\theta - S\psi S\theta S\phi$$

$$4\lambda_2^2 = 1 + 2\left[C^2\frac{\psi}{2}S^2\frac{\theta}{2}S^2\frac{\phi}{2} + S^2\frac{\psi}{2}C^2\frac{\theta}{2}C^2\frac{\phi}{2}\right] + C\phi C\theta - S\psi S\theta S\phi + \\ - 2\left[C^2\frac{\psi}{2}C^2\frac{\theta}{2}C^2\frac{\phi}{2} + S^2\frac{\psi}{2}S^2\frac{\theta}{2}S^2\frac{\phi}{2}\right]$$

USING IDENTITIES  $C2\theta = 2C^2\theta - 1$  &  $C2\theta = 1 - 2S^2\theta$

$$4\lambda_1^2 = 2 \left[ C_{\frac{\psi}{2}}^2 S_{\frac{\theta}{2}}^2 S_{\frac{\phi}{2}}^2 + S_{\frac{\psi}{2}}^2 C_{\frac{\theta}{2}}^2 C_{\frac{\phi}{2}}^2 \right] + 1 + \\ - \frac{3}{8} \left[ (C\psi + 1)(C\theta + 1)(C\phi + 1) + (1 - C\psi)(1 - C\theta)(1 - C\phi) \right] + \\ + C\phi C\theta - S\psi S\theta S\phi$$

$$4\lambda_2^2 = 2 \left[ C_{\frac{\psi}{2}}^2 S_{\frac{\theta}{2}}^2 S_{\frac{\phi}{2}}^2 + S_{\frac{\psi}{2}}^2 C_{\frac{\theta}{2}}^2 C_{\frac{\phi}{2}}^2 \right] + 1 + \\ - \frac{1}{2} \left[ C\psi C\theta + C\psi C\phi + C\theta C\phi + 1 \right] + \\ + C\phi C\theta - S\psi S\theta S\phi$$

$$4\lambda_3^2 = 2 \left[ C_{\frac{\psi}{2}}^2 S_{\frac{\theta}{2}}^2 S_{\frac{\phi}{2}}^2 + S_{\frac{\psi}{2}}^2 C_{\frac{\theta}{2}}^2 C_{\frac{\phi}{2}}^2 \right] + \\ + \frac{1}{2} \left[ 1 - C\psi(C\theta + C\phi) + C\phi C\theta - S\psi S\theta S\phi \right] \\ - \frac{S\psi S\theta S\phi}{2}$$

$$4\lambda_2^2 = 2 \left[ C_{\frac{\psi}{2}}^2 S_{\frac{\theta}{2}}^2 S_{\frac{\phi}{2}}^2 + S_{\frac{\psi}{2}}^2 C_{\frac{\theta}{2}}^2 C_{\frac{\phi}{2}}^2 \right] + 2\lambda_2 - \frac{1}{2} S\psi S\theta S\phi$$

USING THE IDENTITY  $S2\theta = 2S\theta C\theta$

$$\lambda_2^2 = C_{\frac{\psi}{2}}^2 S_{\frac{\theta}{2}}^2 S_{\frac{\phi}{2}}^2 + S_{\frac{\psi}{2}}^2 C_{\frac{\theta}{2}}^2 C_{\frac{\phi}{2}}^2 - 2C_{\frac{\psi}{2}} S_{\frac{\psi}{2}} C_{\frac{\theta}{2}} S_{\frac{\theta}{2}} C_{\frac{\phi}{2}} S_{\frac{\phi}{2}}$$

WHICH FACTORS INTO

$$\lambda_2^2 = \left( C_{\frac{\psi}{2}} S_{\frac{\theta}{2}} S_{\frac{\phi}{2}} - S_{\frac{\psi}{2}} C_{\frac{\theta}{2}} C_{\frac{\phi}{2}} \right)^2$$

$$\underline{\underline{\lambda_2^2 = C_{\frac{\psi}{2}} S_{\frac{\theta}{2}} S_{\frac{\phi}{2}} - S_{\frac{\psi}{2}} C_{\frac{\theta}{2}} C_{\frac{\phi}{2}}}} \quad (59)_D$$

BY ANALOGY

$$\underline{\underline{\lambda_1^2 = - C_{\frac{\phi}{2}} S_{\frac{\theta}{2}} S_{\frac{\psi}{2}} + S_{\frac{\phi}{2}} C_{\frac{\theta}{2}} C_{\frac{\psi}{2}}}} \quad (60)_D$$

EQN (57) - (59)

$$4\lambda_3^2 - 1 = C\Psi C\phi + S\Psi S\theta S\phi - C\phi C\theta - C\Psi C\theta$$

$$4\lambda_3^2 = 1 - C\theta(C\Psi + C\phi) + C\phi C\Psi + S\Psi S\theta S\phi$$

THE SOLN TO THIS EQN IS SIMILAR TO EQN 58:

$$\underline{\lambda_3 = C \frac{\theta}{2} S \frac{\Psi}{2} S \frac{\phi}{2} + S \frac{\theta}{2} C \frac{\Psi}{2} C \frac{\phi}{2}} \quad (61)_D$$

EQN (59) INTO (53)

$$\lambda_0^2 = 1 - [\lambda_1^2 + \frac{1}{2}(1 - C\Psi C\theta)] = \frac{1}{2}(1 + C\Psi C\theta) - \lambda_1^2$$

$$\lambda_0^2 = \frac{1}{2} + \frac{1}{2} C\Psi C\theta - C^2 \frac{\phi}{2} S^2 \frac{\theta}{2} S^2 \frac{\Psi}{2} - S \frac{\phi}{2} C \frac{\Psi}{2} C \frac{\theta}{2} + 2 C \frac{\phi}{2} S \frac{\phi}{2} C \frac{\Psi}{2} S \frac{\Psi}{2} C \frac{\theta}{2} S \frac{\theta}{2}$$

$$\lambda_0^2 = \frac{1}{2}(1 + C\Psi C\theta) - (1 - S^2 \frac{\phi}{2}) S^2 \frac{\phi}{2} S^2 \frac{\Psi}{2} - S^2 \frac{\phi}{2} C^2 \frac{\Psi}{2} C^2 \frac{\theta}{2} + 2 C \frac{\phi}{2} S \frac{\phi}{2} C \frac{\Psi}{2} S \frac{\Psi}{2} C \frac{\theta}{2} S \frac{\theta}{2}$$

$$\lambda_0^2 = \frac{1}{2}[1 + (2C^2 \frac{\Psi}{2} - 1)(2C^2 \frac{\theta}{2} - 1)] + S^2 \frac{\phi}{2} S^2 \frac{\theta}{2} S^2 \frac{\Psi}{2} + S^2 \frac{\theta}{2} S^2 \frac{\Psi}{2} - S^2 \frac{\phi}{2} C^2 \frac{\Psi}{2} C^2 \frac{\theta}{2} + 2 C \frac{\phi}{2} S \frac{\phi}{2} C \frac{\Psi}{2} S \frac{\Psi}{2} C \frac{\theta}{2} S \frac{\theta}{2}$$

$$\lambda_0^2 = 1 + C^2 \frac{\Psi}{2} C^2 \frac{\theta}{2} (1 - S^2 \frac{\phi}{2}) + S^2 \frac{\phi}{2} S^2 \frac{\theta}{2} S^2 \frac{\Psi}{2} + C^2 \frac{\Psi}{2} C^2 \frac{\theta}{2} + - C^2 \frac{\Psi}{2} - C^2 \frac{\theta}{2} - S^2 \frac{\theta}{2} S^2 \frac{\Psi}{2} + 2 C \frac{\phi}{2} S \frac{\phi}{2} C \frac{\Psi}{2} S \frac{\Psi}{2} C \frac{\theta}{2} S \frac{\theta}{2}$$

NOTE THAT

$$1 + C^2 \frac{\Psi}{2} C^2 \frac{\theta}{2} - C^2 \frac{\Psi}{2} - C^2 \frac{\theta}{2} - S^2 \frac{\theta}{2} S^2 \frac{\Psi}{2} =$$

$$1 + C^2 \frac{\theta}{2} (1 - S^2 \frac{\Psi}{2}) - C^2 \frac{\Psi}{2} - S^2 \frac{\theta}{2} S^2 \frac{\Psi}{2} =$$

$$1 - S^2 \frac{\Psi}{2} - C^2 \frac{\Psi}{2} = 0$$

THEREFORE

$$\lambda_0^2 = C^2 \frac{\Psi}{2} C^2 \frac{\theta}{2} C^2 \frac{\phi}{2} + S^2 \frac{\phi}{2} S^2 \frac{\theta}{2} S^2 \frac{\Psi}{2} + 2 C \frac{\phi}{2} S \frac{\phi}{2} C \frac{\Psi}{2} S \frac{\Psi}{2} C \frac{\theta}{2} S \frac{\theta}{2}$$

$$\underline{\lambda_0 = C \frac{\Psi}{2} C \frac{\phi}{2} C \frac{\theta}{2} + S \frac{\Psi}{2} S \frac{\phi}{2} S \frac{\theta}{2}} \quad (62)_D$$

THE SET OF ROTATIONAL PARAMETERS ARE

$$\lambda_0 = C\frac{\psi}{2} C\frac{\phi}{2} C\frac{\theta}{2} + S\frac{\psi}{2} S\frac{\phi}{2} S\frac{\theta}{2}$$

$$\lambda_1 = -C\frac{\phi}{2} S\frac{\theta}{2} S\frac{\psi}{2} + S\frac{\phi}{2} C\frac{\theta}{2} C\frac{\psi}{2}$$

$$\lambda_2 = C\frac{\psi}{2} S\frac{\theta}{2} S\frac{\phi}{2} - S\frac{\psi}{2} C\frac{\theta}{2} C\frac{\phi}{2}$$

$$\lambda_3 = C\frac{\theta}{2} S\frac{\psi}{2} S\frac{\phi}{2} + S\frac{\theta}{2} C\frac{\psi}{2} C\frac{\phi}{2}$$

## Appendix E

Coriolis

From the kinematical expression for motion in terms of moving reference frames (Ref 7:111):

$$\ddot{\mathbf{r}}^i = \ddot{\mathbf{r}}^e + 2\omega^{ei} \times \dot{\mathbf{r}}^e + \dot{\boldsymbol{\omega}} \times \mathbf{r}^e + \boldsymbol{\omega}^{ei} \times (\boldsymbol{\omega}^{ei} \times \mathbf{r}^e) \quad (1)E$$

where the superscripts denote the applicable frame of reference.

The term  $2\omega^{ei} \times \dot{\mathbf{r}}$  is the coriolis acceleration and, for the application of a projectile moving with a velocity ( $\mathbf{v}$ ) over the earth rotating at rate ( $\Omega$ ), the coriolis expression becomes

$$2\Omega \times \mathbf{v} \quad (2)E$$

Define the body frame (XYZ) moving globally with respect to a north-east-down reference frame (NED):

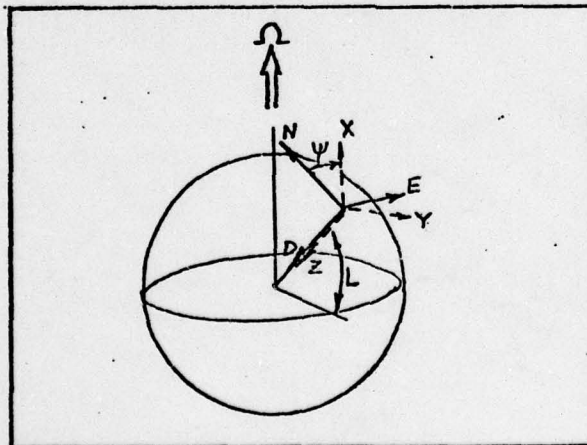


Fig. E-1. Local Level Reference Frame

where  $\psi$  is the heading with respect to north and  $L$  denotes latitude.

The transformation between the body frame and north frame is

$$C_n^b = \begin{bmatrix} \cos \psi & \sin \psi & 0 \\ -\sin \psi & \cos \psi & 0 \\ 0 & 0 & 1 \end{bmatrix} \quad (3)E$$

The earth rate component as seen by the body frame is then

$$\begin{aligned} \Omega^b &= C_n^b \Omega^n = \begin{bmatrix} \cos \psi & \sin \psi & 0 \\ -\sin \psi & \cos \psi & 0 \\ 0 & 0 & 1 \end{bmatrix} \begin{bmatrix} \Omega \cos L \\ 0 \\ -\Omega \sin L \end{bmatrix} \\ &= \begin{bmatrix} \Omega \cos L \cos \psi \\ -\Omega \cos L \sin \psi \\ -\Omega \sin L \end{bmatrix} \end{aligned} \quad (4)E$$

so that the coriolis expression becomes

$$2\Omega \times V = 2 \begin{bmatrix} \hat{i} & \hat{j} & \hat{k} \\ \Omega CL C\psi & -\Omega CL S\psi & -\Omega SL \\ V_N & V_E & V_D \end{bmatrix} \quad (5)E$$

where  $V_N$ ,  $V_E$ ,  $V_D$  are the N, E, D velocity components. The scalar components of coriolis acceleration then, are

$$\begin{aligned} (2\Omega \times V)_x &= -2V_D \Omega CL S\psi + 2V_E \Omega SL \\ (2\Omega \times V)_y &= -2V_D \Omega CL C\psi - 2V_E \Omega SL \\ (2\Omega \times V)_z &= 2V_E \Omega CL C\psi + 2V_N \Omega CL S\psi \end{aligned} \quad (6)E$$

AD-A048 966 AIR FORCE INST OF TECH WRIGHT-PATTERSON AFB OHIO SCH--ETC F/G 19/4  
MAGNUS EFFECTS ON BALLISTIC TRAJECTORIES.(U)  
DEC 77 J D SCHNEIDER

UNCLASSIFIED

AFIT/GA/AA-77D-8

NL

2F2

ADA048 966



END

DATE  
FILMED

2-78

DDC

Appendix F

Six Degree of Freedom Computer Program

PROGRAM SIXDOF 74/74 OPT=1 FTN 4.5+414 09/12/77 17.09.00

```
1      PROGRAM SIXDOF (INPUT,OUTPUT,TAPES=INPUT)
      EXTERNAL ARDCHA
      CALL CFRO
      CALL INIT6
      5     CALL SIXDEG (ARDCHA)
      STOP
      END
```

BEST AVAILABLE COPY

SUBROUTINE AROCHA 74/76 OPT=1 FTH 4.5+414 09/12/77 17.09.

```

1      SUBROUTINE AROCHA(M)
C  WORK E 250   R. S. EIKENFELD, AERO-SPACE ENGR.
C                      UNIVERSITY OF NOTRE DAME, NOTRE DAME, IND.      MBL01256
C                      MBL01257
C
5      C AROCH 1959 MODEL ATMOSPHERE SUBROUTINE      MBL01258
C
C COMMON /AROBLK/ T,P,V,K,VS      MBL01259
C DIMENSION A(3),B(3),C(3),D(3)      MBL01260
C DIMENSION H9(12),H1(11),H2(11),H3(11),TB(11),PB(11),RN(11)      MBL01261
C
10     C
        DATA H9/0.,11000.,25000.,47000.,53000.,73000.,90000.,105000.,16000
        DATA 80.,170000.,200000.,270000./      MBL01262
        DATA H1/-225563E-4,0.,-138456E-4,0.,-153202E-4,0.,-241459E-4,
        DATA $885239E-4,-7543.1E-5,.75716E-5,.222129E-5/      MBL01263
        DATA H2/-525612E1,0.,-113837E2,0.,-759218E1,0.,-854120E1,
        DATA $8.170324E1,.341643E1,.687295E1,.976137E1/      MBL01264
        DATA H3/0.,.1576349E-3,0.,.127959E-3,0.,.206234E-3,0.,0.,0.,0./
        DATA TB/.518684E3,.389088E3,.399944E3,.503793E3,.503793E3,
        DATA $8.298184E3,.293189E3,.405188E3,.258618E4,.256618E4,.293618E4/
        DATA PB/.2116217E4,.47277E3,.51979E2,.25155E1,.12181E1,.2108E-1,
        DATA $8.21839E-2,.15562E-1,.7578E-5,.58954E-5,.29759E-5/
        DATA RR/.237632E-2,.7062E-3,.7765E-4,.28324E-5,.139468E-5,
        DATA $8.41149E-7,.4261E-5,.2212E-9,.1845E-11,.1335E-11,.6113E-12/
        DATA CON1,CON2,CON3,CON4,CON5,CON6/.3043,3356756,.49.020576,0.0226      MBL01273
        DATA $388E-05,193.72,93020./      MBL01279
        DATA A/1.,.753511,.975787/
        DATA B/0.,.17416+,.273996/
        DATA C/0.,.22E6,.19E6/
        DATA D/0.,.25E5,.14E6/
30     C
        HGP=CON1*4/(1.+(CON1*H/CON2))
        IF(HGP.LT.0.) HGP=0.
        DO 1002 M=1,11      MBL01282
        IF((HGP-H3(M))1003,1004,1002      MBL01283
35     1002 CONTINUE      MBL01284
        IF ((HGP-HB(12)).GT.0.) GO TO 1052      MBL01285
        M=12      MBL01286
        1003 M=4-1      MBL01287
        1004 TM=T3(4)*(1.+H1(4)*(HGP-HB(4)))      MBL01288
40     IF ((HGP-90300.).GT.0.) GO TO 1006      MBL01289
        T=TM      MBL01290
        30 TO 1070      MBL01291
        1006 IF ((HGP-180000.).GT.0.) GO TO 1009      MBL01292
        I=2      MBL01293
45     GO TO 1007      MBL01294
        1009 I=3      MBL01295
        1007 T=T4*(A(I)-B(I)*ATAN((HGP-C(I))/D(I)))      MBL01296
        1070 IF (H2(M))1011,1020,1011      MBL01297
        1011 TEM=1.+H1(4)*(HGP-HB(4))
        P=PB(M)/TEMP**H2(M)      MBL01298
        R=PB(M)/TEMP** (1.+H2(M))      MBL01299
        GO TO 1030      MBL01300
        1020 TEM=FXP(-H3(M)*(HGP-HB(4)))
        P=PB(M)*TEMP      MBL01301
        R=RR(M)*TEM      MBL01302
        1030 IF ((HGP-CON6).GT.0.) GO TO 1032      MBL01303
        VS=CON3*SQRT(TM)-
        VK=CON4*(T**1.5/(T+CON5)*P)      MBL01304
        RETURN      MBL01305
40     1052 T=0.
        P=0.
        R=0.
        1032 VS=0.
        VK=0.
        RETURN      MBL01306
        END      MBL01307

```

BEST AVAILABLE COPY

```

SUBROUTINE CFRD 74/74 OPT=1 FTN 4.5+414 09/12/77 17.09.

1      SUBROUTINE CFRD                               000000070
C
C SIXDEG 50   C. W. INGRAM, AFRO-SPACE ENGR.        00C000040
C                                     UNIVERSITY OF NOTRE DAME, NOTRE DAME, IND. 000000090
C
5      C READS COEFFICIENTS IN TABULAR FORM AS A FUNCTION OF ANGLE OF 00000100
C ATTACK AND MACH NUMBER 00000110
C MAXIMUM NUMBER OF ANGLES OF ATTACK = 20, MAXIMUM NUMBER OF MACH 00000120
C NUMBERS = 20 00000130

10     C
1001 FORMAT(A4,1X,3I2)                           00000150
1002 FORMAT(1/14X,*ALPHA*, 2X,10F10.4/2IX,10F10.4) 00000160
1003 FORMAT(1/5X,*MACH*,1F10.4,2X,10F10.4/2IX,10F10.4)
1004 FORMAT(1/1X6,3X2C(I2,1H))
1006 FORMAT(1F10.4)
1007 FORMAT(8F10.4)
      COMMON /COEF/ AMCH(20,30),ALPHA(20,30),C(20,20,30),NOA(30),NOM(30) 00000200
      COMMON /COEP1/ NPLY                            00000210
      COMMON /POL/ CE(30), ALPHAR,CMA,CMPA,CZA          00000220
      COMMON /BLK1/ RUN
      DIMENSION AMC(600),ALP(600),CC(12000)           00000230
      EQUIVALENCE (AMC,AMCH),(ALP,ALPHA),(CC,C)
C
20     C SET ARRAY TABLE TO ZERO                   00000240
      NPLY=0                                         00000250
      DO 110 I=1,600                                00000270
      AMC(I)=0.                                     00000290
      110 ALP(I)=0.                                 00000300
      DO 111 I=1,12000                             00000310
      111 CC(I)=0.                                 00000320
      DO 112 I=1,30                                00000330
      NOA(I)=0.                                    00000340
      NOM(I)=0.                                    00000350
      112 CONTINUE
      CZA=0.0.                                     00000360
      CMA=0.0.                                     00000370
      CMPA=0.0.                                     00000390
      C
30     C READ NUMBER OF AERODYNAMIC COEFFICIENTS 00000400
      READ(5,1005) RUN,NC
      1005 FORMAT(A6,4X,I2)
      PRINT 1008,RUN,NC
      1008 FORMAT(1H1,2X,A6,2X,I2 //)
C FOR CONSTANT ANGLE OF ATTACK 40 ANGLE OF ATTACK TABLES ARE READ 00000430
C FOR CONSTANT MACH NUMBER ONE TABLE OF MACH NUMBER IS READ 00000440
      DO 170 M=1,NC                                00000450
      READ(5,1001) NAME,<,NOA(K),NOM(<)
      PRINT 1004, NAME,K                           00000460
      NM=NOM(K)                                    00000470
      IF(NM.EQ.0) NM=1
      NA=NOA(K)                                    00000480
      IF(NA.EQ.0) NA=1
      IF(NA.EQ.1) GO TO 119
      READ(5,1006) (ALPHA(I,K),I=1,NA)
      PRINT 1002, (ALPHA(I,K),I=1,NA)            00000540
      119 DO 120 J=1,NM
      120 READ(5,1007) AMCH(I,K),(C(I,J,K),J=1,NA)
      DO 125 I=1,NM
      125 PRINT 1003,AMCH(I,<),(C(I,J,<),J=1,NA)
      130 CONTINUE
      RETURN
      END

```

# BEST AVAILABLE COPY

SUBROUTINE ED 76/74 OPT=1 FTN 4.5+414 09/12/77 17.09.  
 1           SUBROUTINE ED    00004560  
 2       REAL MASS,IX,IY,L    00004590  
 3       INTEGER PG    00004600  
 4       COMMON /AIRBLK/ TEW,PRFS,RHO,KVIS,VA                          00004610  
 5       COMMON /CODEF/ AMCH(20,30),ALPHA(20,70),C(20,20,70),NOA(30),NOM(70) 00004620  
 6       COMMON /INDBLK/ IDEN,IWIND,ITR,IPRN,IALL,NORG,IPUN,NRODY,ITRST,NT00004630  
 7       IRST  
 8       COMMON /INIT/ TITLE(12),SCALE(30),A(22)                          00004640  
 9       COMMON /THRUST/ T14(15),TRST(15),MASS(15),CG(15),IX(15),IY(15),CGP(100004650  
 10      33)  
 11      COMMON/TSTDAT/EPS,THTC,ETA,L ,RL                                  00004660  
 12      COMMON /WINBLK/ YOH,YH(128),H(128,3)                          00004680  
 13      COMMON/COEP1/ NPLY    00004690  
 14      COMMON /POL/ CE(30), ALPHAP,CMA,CMR,C7A                          00004700  
 15      COMMON/EDBK2/V,D,S,N,ALPHAN,AMCHN,PG,LN                          00004710  
 16      COMMON/EDBK3/AXX,AYX,AXZ,AYX,AYY,AZY,AZX,AZY,AZZ                  00004720  
 17      COMMON/EDBK4/LCOUNT  
 18      COMMON /PLK1/ RUN  
 19      DATA CON0/57.295779/  
 20      1000 FORMAT(5X,--\*)  
 21      1001 FORMAT(1X,T4,\*T14E\*,5X,\*RANGE\*,5X,\*ALT\*,7X,\*Z\*,9X,\*V\*,7X,\*D\*,3X,  
 22        1\*ALP\*D\*,3X,\*H\*,5X,\*PHI\*,2X,\*ALPHAV\*,2X,\*ETA\*,2X,\*L-N\*,3X,\*L-P\*,  
 23        26X,\*H-N\*,4X,\*H-D\*,5X,\*S\*,5X,\*TAU\*,3X,\*K-T\*)  
 24      1002 FORMAT(1X,T4,\*SEC\*,7X,\*FFET\*,5X,\*FEET\*,5X,\*FEET\*,4X,\*FT/SEC\*,2X,  
 25        1\*RAS/SEC\*,2X,\*DEG\*,10X,\*DFG\*,3X,\*DFG\*,4X,\*DFG\*,1X,\*1/SEC\*,1X,  
 26        2\*1/SEC\*,1X,\*RA/SEC\*,1X,\*24/SEC\*,15X,\*DEG\*)  
 27      1003 FORMAT(1X,1F8.4,2F10.2,2F9.2,1E7,1,2F6.2,1E7.2,4F6.2,2,2F7.1,  
 28        11F8.3,1F6.2,1E7.3)  
 29      1010 FORMAT(1H112A4,3)X44PAGFI4)                                  00004840  
 30      1090 FORMAT (10F7.3,2X,1H)  
 31      1091 FORMAT (10F7.3,2X,1H)  
 32       IF (H0DY, EQ. 1) GO TO 921    00004850  
 33       3P=V\*(2.\*AXZ\*D2(2)-2.\*AXX\*D2(4))                                  00004860  
 34       AP=2.\*AXY\*V\*D2(3)\*D1(12)    00004870  
 35       XI=A\*CTAN(BP/AP)    00004880  
 36       BETA=-ALPHAN\*SIN(XI)    00004890  
 37       ALPHM= ALPHAN\*COS(XI)    00004900  
 38       GO TO 841    00004910  
 39      821 ALPH=ATAN(D1(14)/D1(12))\*CON0                                  00004920  
 40       SETA=ATAN(D1(13)/D1(12))\*CON0    00004930  
 41       PP=D2\*CON0    00004940  
 42       IF(MON(LN,50).NE.0) GO TO 2    00004950  
 43       PG=PG+1    00004960  
 44       PRINT 1010,TITLE,PG    00004970  
 45       PRINT 1000    00004980  
 46       PRINT 1001    00004990  
 47       PRINT 1002    00005000  
 48       2 D= D1(5)    00005010  
 49       IF(P.EQ.0.) GO TO 4752    00005020  
 50       SSNC=(D1(5)\*D1(5)\*A(15)\*A(15))/(0\*S\*A(19)\*CMA\*A(16)\*4.)          00005030  
 51       SSNC= (D1(5)\*D1(5)\*A(15)\*A(15))/((0\*S\*A(19)\*CMA\*A(16)\*4.)  
 52       TAU = 1./SORT(1. - 1./SSNC)    00005040  
 53       D2M= A(19)\*A(19)\*A(15)    00005050  
 54       CLAMP = (0\*S)/(2.\*A(15)\*A(19)\*V)\*(C7A\*(1.+TAU)+ D2M/(2.\*A(15))\* (CE(27)  
 55       \* (1.-TAU)) - D2M/A(15)\*CMA\*TAU)                                  00005060  
 56       CLAMP = (0\*S)/(2.\*A(15)\*V)\*(C7A\*(1.-TAU)+ D2M/(2.\*A(15))\* (CE(27)  
 57       \* (1.+TAU)) - D2M/A(15)\*CMA\*TAU)                                  00005070

BEST AVAILABLE COPY

SUBROUTINE ED      74/74      OPT=1      FTH 4.5+414      09/12/77 17.09.00

```

      $*(1.+TAU)) + D24/A(15)*CHPA*TAU)          00005110
      HLAMP= (P*A(15))/(2.*A(15))*(1.- 1./TAU)    00005120
      AA= CLAMN*CLAMP-(P-WLAMN)*(P-WLA+P)        00005130
      WLAMN= (P*A(15))/(2.*A(15))*(1.+ 1./TAU)    00005140
      BB=CLAMP*(P-WLA+P)-CLAMN*(P-WLA+P)         00005150
      AK3=(2*5*A(19)*CE(20)/(4*(15)*SQRT(AA**2 + BB**2)))**COND 00005160
      GO TO 4763                                     00005170
  60      4762 CLAMP=0.                                00005190
          CLAMN=0.                                00005190
          WLAMP=0.                                00005200
          WLAMN=0.                                00005210
  65      AK3=1.                                    00005220
          TAU=0.                                    00005230
          SS9C=0.0                                 00005230
  70      4763 CONTINUE
          PRINT 1003, (D1(I),I=1,4),V,D1(5),ALPHAN,AMCHN,PP,ALPH,BETA, 00005250
          1CLAMN,CLAMP,WLAMN,WLAMP,SS9C,TAU,AK3           00005260
  75      IF(IPUN.EQ.0) GO TO 1113                  00005270
          LCOUNT=LCOUNT+1                            00005280
          IF(LCOUNT.EQ.10) GO TO 1112                00005290
          DAL(LCOUNT)=ALPH                         00005300
          DBE(LCOUNT)=BETA                         00005310
          GO TO 1113                                00005320
  80      1112 DAL(LCOUNT)=ALPH                     00005330
          DBE(LCOUNT)=BETA                         00005340
          LCOUNT=0                                  00005350
  85      1113 LN=LH+1                               00005360
          RETURN                                     00005390
          END                                         00005400
                                              00005410

```

BEST AVAILABLE COPY

	SUBROUTINE INIT6	76/74 OPT=1	FTN 4.5+614	89/12/77 17.09.0
1	SUBROUTINE INIT6			
C	C SIXDEG 100 C. W. INGRAM, AERO-SPACE ENGR.		00000610	
C	UNIVERSITY OF NOTRE DAME, NOTRE DAME, IND.		00000620	
S	C INITIALIZATION PROGRAM FOR N-DEGREE OF FREEDOM MOTION (3+N*6)		00000630	
C	REAL MASS,IX,IY,L		00000640	
1001	FORMAT(12A4)		00000650	
1002	FORMAT (//1X,29HINITIALIZATION INPUT'//)		00000660	
1003	FORMAT (4(6(1X,2HA(,I2,4H) = ,F11.4)/))		00000670	
1004	FORMAT (1X,7HNORC = ,I1,3X,7HTPRV = ,I2,3X,7HNALL = ,I1,3X,		00000680	
	7THIPIN = ,I1,3X,7HN900Y = ,I1,3X,9HISCALE = ,I1,3X,6HITRST = ,I1,/00000730			
	\$/)		00000690	
1005	FORMAT (//5(6(1X,6HSCALE(,I2,4H) = ,E8.2)/))		00000700	
1006	FORMAT(1,5X,6HTIME,5X,6HTHRUST,7X,4HMASS,5X,11HCG POSITION,7X,5HCG POSITION,		00000710	
	8-A5,2HIX,7X,2HIY,1)		00000720	
1007	FORMAT(4X,F5.2,5X,-5.0,5X,F5.3,5X,F8.2,8X,F6.2,4XF6.3,4X,F5.3)		00000730	
1008	FORMAT(5X,13HTHRUST DATA *,3X,6HEPS = ,F5.2,3X,9HTHETAC = ,F5.2,3X00000790			
20	S,6HETA = ,F5.2,3X,1HL = ,F5.2,/,/)		00000740	
1009	FORMAT(//,5X,14H300Y LENGTH = ,F4.2,/,/)		00000750	
1010	FORMAT(7I10)		00000760	
1011	FORMAT(I10,3E10.4,I10,E10.4)		00000770	
1012	FORMAT(8E10.4 / 9E10.4 / 6E10.4)		00000780	
25	1013 FORMAT(6E10.4)		00000790	
	1014 FORMAT(2E10.4)		00000800	
1015	FORMAT(3(8E10.4 /), 6E10.4)		00000810	
	LOGICAL LSCALE,IALL,LTRST			
	COMMON /WINBLK/ V0H,YH(128),W(128,3)		00000820	
30	COMMON /AIRBLK/ TE4,PRES,RHO,KVIS,VA		00000830	
	COMMON /DENBLK/ V0D,YD(128),DEN(128),TEMP(128)		00000840	
			00000850	
	COMMON/COPP1/ NPLY			
	COMMON /POL/ CE(30), ALPHAR,CMA,CMRA,C7A		00000860	
35	COMMON /INDBLK/ IDEN,IWIND,ITER,IPRN,IALL,NORC,IPUN,NBODY,ITRST,NT		00000870	
	8RST		00000880	
	COMMON/INIT/TITLE(12),SCALE(30),A(22)		00000890	
	COMMON/THRUST/TIM(15),TPST(15),4ASS(15),CG(15),IX(15),IV(15),CGP(100000910			
40	85)		00000900	
	COMMON/TSTDAT/EPS,THTC,ETA,L ,RL		00000910	
	READ(5,1001) TITLE		00000920	
C			00000930	
	DO 10 I=1,15		00000940	
45	TIM(I)=0.0		00000950	
	TRST(I)=0.0		00000960	
	MASS(I)=0.0		00000970	
	CG(I)=0.0		00000980	
	IX(I)=0.0		00000990	
	IV(I)=0.0		00001000	
50	CGP(I)=0.0		00001010	
10	CONTINUE		00001020	
	IDEN=0		00001030	
	IWIND=0		00001040	
55	DO 11 J=1,3			
	DO 11 I=1,128		00001050	
	W(I,J)=0.0		00001060	
	VW(I)=0.0		00001070	
			00001080	

BEST AVAILABLE COPY

	SUBROUTINE INITG	74/74	OPT=1	FTN 6.5+414	09/12/77 17.09
	V0(I)=0.0 DEN(I)=0.0 TEHP(I)=0.0				00001090 00001100 00001110 00001120 00001130
60	11 CONTINUE				
	C				
65	C READ CONTROL PARAMETERS READ(5,1010) NORC,IPRN,NALL,IPUN,NBODY,ISCALE,ITRST LSCALE=ISCALE.EQ.1 IALL=NALL.EQ.1 LTRST=ITRST.EQ.0				00001140 00001160 00001170 00001180 00001190
70	C READ INITIAL CONDITIONS IF(LTRST) GO TO 4 READ(5,1011) NTRST,EPS,THTC,ETA,L,BL EPS=EPS/57.295779 THTC=THTC/57.295779				00001200 00001210 00001230 00001240 00001250
75	4 GO TO 7 CONTINUE NTRST=1				00001260 00001270 00001280
	7 CONTINUE				
80	READ(5,1012) (A(I),I=1,22) IF(LSCALE) GO TO 1 DO 2 I=1,30 2 SCALF(I)=1. GO TO 3				00001300 00001310 00001320 00001330
85	3 READ(5,1015) (SCALE(I),I=1,30) CONTINUE IF(LTPST) GO TO 5 READ(5,1013) TIM(1),MASS(1),CG(1),IX(1),IY(1),CGP(1)				00001350 00001360
90	READ(5,1013) TT(I,D),MASS(D),CG(I),IX(D),IY(D),CGP(D) READ(5,1014) (TIM(I),TRST(I),I=1,NTRST)				
	5 CONTINUE				00001400
	C ECHO OUTPUT				00001410 00001420 00001430
95	PRINT 1002 PRINT 1004, NORC,IPRN,NALL,IPUN,NBODY,ISCALE,ITRST PRINT 1003, (I,A(I),I=1,22)				00001440 00001450
	PRINT 1005, (I,SCALE(I),I=1,30)				00001460
100	IF(LTPST) GO TO 5 EEPS=EPS*57.295779 TTHTC=THTC*57.295779				00001470 00001480 00001490
	PRINT 1006,EEPS,TTHTC,ETA,L				00001500
	PRINT 1009 ,BL				00001510
	PRINT 1006				00001520
105	PRINT 1007,(TIM(I),TRST(I),MASS(I),CGP(I),CG(I),IX(I),IY(I),I=1,NTSRST)				00001530 00001540
	6 CONTINUE				00001550
	RETURN				00001560
	END				00001570

BEST AVAILABLE COPY

	SUBROUTINE SIXDEG	74/74 OPT=1	FTN 4.5+414	09/12/77 17.09.
1	SUBROUTINE SIXDEG(ATMOS)			00001550
	UNIVERSITY OF NOTRE DAME, NOTRE DAME, IND.			00001590
2	2004 FORMAT(12H ALPHA ERROR2XE14.3)			00001600
3	2005 FORMAT(11H WIND EPP99)			00001610
4	2006 FORMAT(11H MACH ERROR2XE14.3)			00001620
5	2157 FORMAT (IX,TF20.3)			00001630
6	2089 FORMAT(//5X,*----ALPHA *,1F10.4,* DEGREES EXCEEDS MAXIMUM*, 1* ALPHA IN ARRAY----*)			
7	1666 FORMAT(//5X,*----MACH *,1F10.4,* EXCEEDS MAXIMUM MACH *, 1*NUMBER IN ARRAY----*)			
8	REAL MASS,IX,IY,MTX,MTY,MTZ,L,YYJD,YZJD			00001640
9	REAL MDOT			00001650
10	INTEGER PG			00001660
11	LOGICAL LCZA,LCHM,LCHPA			00001670
12	LOGICAL LTRST			00001680
13	COMMON /AIRPLK/ TE4,PRES,RHO,KVIS,V4			00001690
14	COMMON /COEF/ AMCH(20,30),ALPHA(20,30),C(20,20,30),NOA(30),NOH(30)			00001700
15	COMMON /INDBLK/ IDEN,IWIND,ITER,IPRN,IALL,NORC,IPUN,NBODY,ITRST,NT			00001710
16	SRST			00001720
17	COMMON /INIT/ TITLE(12),SCALE(30),A(22)			00001730
18	COMMON/THRUST/TIM(15),TRST(15),MASS(15),CG(15),IX(15),IY(15),CGP(100001740			
19	COMMON/TSTODAT/EPS,THTC,ZTA,L,RL			00001740
20	COMMON/WINPLK/ NOW,YH(128),W(129,3)			00001750
21	COMMON/COEP1/ NP_Y			00001760
22	COMMON/POLY/CE(10),ALPHAR,CNA,CMPA,CZA			00001770
23	COMMON/DENBLK/YD(128),DN(128),TEMP(128)			00001780
24	COMMON/E09K/ D1(14),D2(14),D3(14),WIN(3),DAL(10),DRE(10)			00001790
25	COMMON/E09K2/V,0,S,OP,ALPHAN,AMCN,PG,LN			00001800
26	COMMON/E09K3/AXX,AZY,AXZ,AYY,AYZ,AZX,AZY,AZZ			00001810
27	COMMON/E09K4/ LCOUNT			
28	DATA CONO,RAD/57.235779,.017453233/			00001820
29	LTRST=ITRST.EQ.0			00001830
30	ITER=0			00001840
31	LW=0			00001850
32	PG=0			00001860
33	KOUNT=0			00001870
34	LCOUNT=0			00001880
35	44=1			00001890
36	D2(1)=1.			00001900
37	S=3.1415927*A(19)**2/4.			00001910
38	DO 20 I=1,14			00001920
39	20 D1(I)=A(I)			00001930
40				00001940
41				00001950
42	RAD2=RAD/2.			00001960
43	D=D1(8)*RAD2			00001970
44	E=D1(9)*RAD2			00001980
45	F=D1(10)*RAD2			00001990
46	CP=COS(E)			00002000
47	SP=SIN(E)			00002010
48	CT=COS(D)			00002020
49	ST=SIN(D)			00002030
50	CS=COS(F)			00002040
51	SS=SIN(F)			00002050
52	C VEPSOR COMPONENTS (54)			00002060
53	D1(A)=-CP*ST*SS+SP*CT*CS			00002070

BEST AVAILABLE COPY

SUBROUTINE SIXDEG	74/76	OPT=1	FTN 4.5+414	09/12/77 17.09.0
60	D1(9)=-CP*CT*SS+SP*ST*CS D1(10)=CP*ST*CS+SP*CT*SS D1(11)=CP*CT*CS+SP*ST*SS AMP=A(18)		00002080 00002090 00002100 00002110 00002120 00002130 00002140	
25	M=A(20) IF(A(20)*(D1(1)-A(21)).GT.-0.1) GO TO 597			
41	I1=1			
65	55 Y=D1(3) IF(X>T1) GO TO 56 X=D1(1) IF(X.GT.TIM(NTRST)) GO TO 56		00002150 00002160 00002170 00002180 00002190 00002200 00002210 00002220	
70	I=1 IF(X.LT.TIM(I+1)) GO TO 57			
75	I=I+1 GO TO 58 57 CONTINUE V1=TRST(I) V2=TRST(I+1) Y=Y1+(X-TIM(I))*((Y2-Y1)/(TIM(I+1)-TIM(I))) &TRST=Y		00002230 00002240 00002250 00002260 00002270	
80	V1=MASS(1) V2=MASS(NTRST) Y=Y1+(X-TIM(1))*((Y2-Y1)/(TIM(NTRST)-TIM(1))) A(18)=Y M00T=(AMP-A(18))/A(20)		00002280 00002290 00002300 00002310 00002320 00002330	
85	AMP=A(18) Y1=D1(1) V2=CG(NTRST) Y=Y1+(X-TIM(1))*((Y2-Y1)/(TIM(NTRST)-TIM(1))) &CG=Y		00002340 00002350 00002360 00002370	
90	V1=IX(1) V2=IK(NTRST) Y=Y1+(X-TIM(1))*((Y2-Y1)/(TIM(NTRST)-TIM(1))) A(15)=Y V1=IY(1) V2=IV(NTRST)		00002380 00002390 00002400 00002410 00002420 00002430	
95	Y=Y1+(X-TIM(1))*((Y2-Y1)/(TIM(NTRST)-TIM(1))) A(16)=Y V1=CGP(1) V2=CGP(NTRST) Y=Y1+(X-TIM(1))*((Y2-Y1)/(TIM(NTRST)-TIM(1))) CGP=Y		00002440 00002450 00002460 00002470 00002480 00002490	
100	100 CONTINUE IF(X.GT.TIM(NTRST)) M00T=0. SCL=1./SQR(D1(8)**2+D1(9)**2+D1(10)**2+D1(11)**2)		00002500 00002510 00002520	
105	D1(8)=SCL*D1(8) D1(9)=SCL*D1(9) D1(10)=SCL*D1(10) D1(11)=SCL*D1(11) CALL ATMS(Y)		00002530 00002540 00002550 00002560 00002570	
110	C MATRIX OF DIRECTION COSINES AXX=D1(8)**2+D1(11)**2-.5 AYX=D1(8)*D1(9)+D1(10)*D1(11) AZX=D1(8)*D1(10)-D1(11)*D1(9) AYZ=D1(8)*D1(9)-D1(11)*D1(10)		00002580 00002590 00002600 00002510 00002620	

BEST AVAILABLE COPY

	SUBROUTINE SIXOEG	74/74	OPT=1	FTN 4.5+414	09/12/77 17.09.0
115	$\text{AY} = \text{D1}(9)^{*}2 + \text{D1}(11)^{*}2 - .5$ $\text{AY} = \text{D1}(9)^{*}\text{D1}(10) + \text{D1}(11)^{*}\text{D1}(5)$ $\text{AZ} = \text{D1}(8)^{*}\text{D1}(10) + \text{D1}(11)^{*}\text{D1}(9)$ $\text{AZ} = \text{D1}(9)^{*}\text{D1}(10) - \text{D1}(11)^{*}\text{D1}(5)$ $\text{AZ} = \text{D1}(10)^{*}2 + \text{D1}(11)^{*}2 - .5$ $\text{IF}(\text{WIND.EQ.0}) \text{ GO TO } 2104$				00002630 00002640 00002650 00002660 00002670 00002680 00002690 00002700 00002710 00002720 00002730 00002740 00002750 00002760 00002770 00002780 00002790 00002800 00002810 00002820 00002830 00002840 00002850 00002860 00002870 00002880 00002890 00002900 00002910
120	<b>C COMPUTE WIND</b> $\text{IF}(\text{Y.LT.YH}(1)) \text{ GO TO } 101$ $\text{I}=2$ $100 \text{ IF}(\text{YH}(1).GE.\text{Y}) \text{ GO TO } 210$ $\text{I}=\text{I}+1$ $\text{GO TO } 100$				00002700 00002710 00002720 00002730 00002740 00002750 00002760 00002770 00002780 00002790 00002800 00002810 00002820 00002830 00002840 00002850 00002860 00002870 00002880 00002890 00002900 00002910
125	101 <b>PRINT 1005</b> <b>RETURN</b> $210 \text{ FASE} = (\text{Y}-\text{YH}(\text{I}-1)) / (\text{YH}(\text{I})-\text{YH}(\text{I}-1))$ $\text{DO } 220 \text{ K=1,3}$ $220 \text{ WIN}(\text{K}) = \text{W}(\text{I}-1,\text{K}) + \text{FASE} * (\text{W}(\text{I},\text{K}) - \text{W}(\text{I}-1,\text{K}))$				00002700 00002710 00002720 00002730 00002740 00002750 00002760 00002770 00002780 00002790 00002800 00002810 00002820 00002830 00002840 00002850 00002860 00002870 00002880 00002890 00002900 00002910
130	<b>C WIND COMPONENTS</b> $\text{WX} = 2.^{*}(\text{WIN}(1)^{*}\text{AXX} + \text{WIN}(2)^{*}\text{AYX} + \text{WIN}(3)^{*}\text{AZX})$ $\text{WY} = 2.^{*}(\text{WIN}(1)^{*}\text{AYX} + \text{WIN}(2)^{*}\text{AYY} + \text{WIN}(3)^{*}\text{AYZ})$ $\text{WZ} = 2.^{*}(\text{WIN}(1)^{*}\text{AZX} + \text{WIN}(2)^{*}\text{AYZ} + \text{WIN}(3)^{*}\text{AZZ})$				00002800 00002810 00002820 00002830
135	<b>C VELOCITY VECTOR</b> $\text{D1}(12) = \text{D1}(12) - \text{WX}$ $\text{D1}(13) = \text{D1}(13) - \text{WY}$ $\text{D1}(14) = \text{D1}(14) - \text{WZ}$				00002840 00002850 00002860 00002870
140	<b>C SPEED</b> $2104 \text{ V} = \text{SQR}(\text{D1}(12)^{*}2 + \text{D1}(13)^{*}2 + \text{D1}(14)^{*}2)$ <b>C ALPHA PRIME - YAH - ARCTAN(SQR(V*V+W*W)/U))</b> $\text{ALPHAR} = \text{ARCTAN}(\text{SQR}(\text{D1}(13)^{*}2 + \text{D1}(14)^{*}2), \text{D1}(12))$				00002880 00002890 00002900 00002910
145	<b>C DYNAMIC PRESSURE</b> $\text{Z} = 5.^{*}\text{RHO}^{\text{*}}\text{V}^{\text{*}}\text{V}$				00002920 00002930 00002940
150	<b>C CROSS-SPIN</b> $\text{QPP} = \text{SQR}(\text{D1}(6)^{*}2 + \text{D1}(7)^{*}2)$				00002950 00002960 00002970
155	<b>C ROLL ANGLES</b> $\text{OP} = \text{ARCTAN}(\text{D1}(13), \text{D1}(14))$ $\text{OPP} = \text{ARCTAN}(-\text{D1}(7), \text{D1}(6))$				00002980 00002990
160	<b>C PD/2V AND DD/2V</b> $\text{IF}(\text{V.GT.0}) \text{ GO TO } 2214$				00003000 00003010 00003020
165	2 <b>CONTINUE</b> $\text{PD} = 0.$ $\text{DD} = 0.$ $\text{AMHN} = 0.$ $\text{GO TO } 2215$				00003030 00003040 00003050 00003060
170	2214 $\text{PD} = (\text{D1}(5)^{*}\text{A}(19)) / (2.^{*}\text{V})$ $\text{DD} = (\text{DPP}*\text{A}(19)) / (2.^{*}\text{V})$ $\text{AMHN} = \text{V}/\text{VA}$ $2215 \text{ DS} = 0.^{*}\text{S}^{\text{*}}\text{A}(19)$ $\text{DS} = (\text{D}^{\text{*}}\text{S})^{\text{*}}1./\text{A}(19)$				00003070 00003080 00003090 00003100 00003110
175	<b>C INTERPOLATE COEFFICIENT TABLES</b> $\text{DO } 150 \text{ K=1,30}$ $\text{IF}(\text{NOA}(\text{K}).EQ.0) \text{ GO TO } 145$ $\text{I}=1$ $\text{J}=1$ $\text{IF}(\text{NOA}(\text{K}).EQ.0) \text{ GO TO } 120$ $\text{IF}(\text{ALPHAN.LT.ALPHA}(1,\text{K})) \text{ GO TO } 111$				00003120 00003130 00003140 00003150 00003160 00003170 00003180 00003190

BEST AVAILABLE COPY

SUBROUTINE SIXDEG 74/74 OPT=1 FTM 4.5+614 09/12/77 17.09.

```

N=NDA(K)
IF(ALPHAN.GT.ALPHA(N,K)) GO TO 8888
J=?
175   110 IF(ALPHA(J,K).GE.ALPHAN) GO TO 115
      J=J+1
      GO TO 110
111 PRINT 1004,ALPHAN
      RETURN
180   8888 PRINT 6889, ALPHAN
      RETURN
115 FRA=(ALPHAN-ALPHA(J-1,K))/(ALPHA(J,K)-ALPHA(J-1,K))
120 IF(NOM(K).EQ.0) GO TO 140
      IF(AMCHN.LT.AMCH(I,K)) GO TO 131
      M=NOM(K)
145   IF(AMCHN.GT.AMCH(N,K)) GO TO 1131
      I=2
130   IF(AMCH(I,K).GE.AMCHN) GO TO 135
      I=I+1
      GO TO 130
131 PRINT 1006,AMCHN
      RETURN
145   1131 PRINT 1665, AMCHN
      RETURN
135 FRA=(AMCHN-AMCH(I-1,K))/(AMCH(I,K)-AMCH(I-1,K))
      CE(K)=C(I-1,J,K)+FRA*(C(I,J,K)-C(I-1,J,K))
      IF(NOM(K).EQ.0) GO TO 150
      T1=C(I-1,J-1,K)+FRA*(C(I,J-1,K)-C(I-1,J-1,K))
      LCZA=K.EQ.6
      LCMA=K.EQ.13
      LCMPA=K.EQ.19
      IF(LCZA) CZA=(CE(K)-T1)/(ALPHA(J,K)-ALPHA(J-1,K))*COND*
      $SCALE(K)
      IF(LCMA) CMA=(CE(K)-T1)/(ALPHA(J,K)-ALPHA(J-1,K))*COND*
      $SCALE(K)
      IF(LCMPA) CMPA=(CE(K)-T1)/(ALPHA(J,K)-ALPHA(J-1,K))*COND*
      $SCALE(K)
      CE(K)=T1+FRA*(CE(K)-T1)
      GO TO 150
140 CE(K)=C(I,J-1,K)+FRA*(C(I,J,K)-C(I,J-1,K))
      GO TO 150
145 CE(K)=C(I,1,K)
150 CF(K)=E(K)*SCALE(K)
210   C COMPUTE COEFFICIENTS CX, CY, CZ, CL, CM, CN (TABLE 3)
1511 CONTINUE
      IF(NPLY.NE.1) GO TO 1512
      DO 1513 KK=1,30
1513 CE(KK)=CE(KK)*SCALE(KK)
1512 CONTINUE
      SP=SIN(OP)
      CP=COS(OP)
      SP4=SIN(4.*OP)
      CP4=COS(4.*OP)
      SPP4=SIN(4.*OPP)
      CPP4=COS(4.*OPP)
      CX=CE(1)
      00003200
      00003210
      00003220
      00003230
      00003240
      00003250
      00003260
      00003270
      00003280
      00003290
      00003300
      00003310
      00003320
      00003330
      00003340
      00003350
      00003360
      00003370
      00003380
      00003390
      00003400
      00003410
      00003420
      00003430
      00003440
      00003450
      00003460
      00003470
      00003480
      00003490
      00003500
      00003510
      00003520
      00003530
      00003540
      00003550
      00003560
      00003570
      00003580
      00003590
      00003600
      00003610
      00003620
      00003630
      00003640
      00003650
      00003660
      00003670
      00003680

```

BEST AVAILABLE COPY

SUBROUTINE SIXOES 76/74 OPT=1

FTN 4.5+614

09/12/77 17.09.

```

230      SY=(CF(2)+CE(3)*SP4+CE(4)*CP4+P0*CE(5))*CP+(CE(6)+CE(7)*SP4+CE(8)*
          00003590
          SCP1)*SP+CE(22)          00003700
          CZ=(CE(2)+CE(3)*SP4+CE(4)*CP4+P0*CE(5))*(-SP)+(CE(6)+CE(7)*SP4+CE(8)*
          00003710
          SP4)*CP+CE(23)          00003720
          CL=CF(9)+CE(30)+CE(10)*SP4+CE(11)*CP4+P0*CE(12)+ALPHAR*(CE(24)+CE(25)*
          00003730
          CE(26)*CP)          00003740
          CM=(CF(13)+CE(14)*SP4+CE(15)*CP4)*CP+(CE(16)+CE(17)*SP4+CE(18)*CP4)*
          00003750
          SP3*CF(19)*SP+(CE(24)*SP4+CE(29)*CP4)*QD*COS(OPP)+CE(20)*
          00003760
          CN=(CE(13)+CE(14)*SP4+CE(15)*CP4)*(-SP)+(CE(16)+CE(17)*SP4+CE(18)*
          00003770
          CP4)*QD*CE(19)*CP+(CE(27)+CE(28)*SP4+CE(29)*CP4)*QD*(-SIN(OPP))+
          00003780
          SCE(21)          00003790
          IF(IWIND.EQ.0) GO TO 151          00003800
C ADD WIND BACK          00003810
          D1(12)=D1(12)+WX          00003820
          D1(13)=D1(13)+WY          00003830
          D1(14)=D1(14)+WZ          00003840
245      C KINEMATICAL RELATIONSHIPS          00003850
C * VELOCITY (9)          00003860
          151 D2(2)=2.*(D1(12)*AXX+D1(13)*AYX+D1(14)*AZX)          00003870
          D2(3)=2.*(D1(12)*AYX+D1(13)*AYY+D1(14)*AZY)          00003880
          D2(4)=2.*(D1(12)*AZX+D1(13)*AYZ+D1(14)*AZZ)          00003890
C * MOMENTS          00003900
          D2(5)=1./A(15)*(2S*CL)          00003910
          D2(6)=1./A(16)*(2S*CY+D1(5)*D1(7)*(A(16)-A(15)))          00003920
          D2(7)=1./A(16)*(2S*CN-D1(5)*D1(5)*(A(16)-A(15)))          00003930
255      C * VERSOR (10)          00003940
          D2(8)=-.5*(D1(5)*D1(11)-D1(7)*D1(9)+D1(5)*D1(10))          00003950
          D2(9)=-.5*(D1(6)*D1(11)+D1(7)*D1(8)-D1(5)*D1(10))          00003960
          D2(10)=-.5*(D1(7)*D1(11)-D1(5)*D1(9)+D1(5)*D1(10))          00003970
          D2(11)=-.5*(D1(5)*D1(8)+D1(6)*D1(9)+D1(7)*D1(10))          00003980
          IF(NORG.NE.0) GO TO 230          00003990
          G=2.* (A(17)-.30783368E-5*D1(3))          00004000
          GO TO 250          00004010
265      230 G=2.*A(17)          00004020
C * FORCE          00004030
          250 D2(17)=QSM*CX-G*AYY-(D1(6)*D1(14)-D1(7)*D1(13))          00004040
          D2(18)=QSM*CY-G*AYX-(D1(7)*D1(12)-D1(5)*D1(14))          00004050
          D2(19)=QSM*CZ-G*AZY-(D1(5)*D1(13)-D1(6)*D1(12))          00004060
          IF(LTPST) GO TO 251          00004070
          TX=ATRST*COS(EPS)          00004080
          TY=ATRST*SIN(EPS)*SIN(THTC)          00004090
          TZ=-ATRST*SIN(EPS)*COS(THTC)          00004100
          QT=ETA*TX          00004110
          HTY=(RL-CGL)*TZ          00004120
          QTZ=(RL-CGL)*TY          00004130
          MYJD=HDOT*D1(6)*L**2          00004140
          QZJD=HDOT*D1(7)*L**2          00004150
          D2(5)=D2(5)+MTX          00004150
          D2(6)=D2(6)+(HTY+MYJD+Q*S*CZ*ACG)/A(16)          00004170
          D2(7)=D2(7)+(HTZ+HZJD+Q*S*CY*ACG)/A(16)          00004180
          D2(12)=D2(12)+TX/A(18)          00004190
          D2(13)=D2(13)+TY/A(18)          00004200
          D2(14)=D2(14)+TZ/A(18)          00004210
285      251 CONTINUE          00004220
          IF(LN.EQ.0) CALL ED          00004230

```

BEST AVAILABLE COPY

	SUBROUTINE SIXDEG	74/74	0DT=1	FTN 4.5+414	89/12/77 17.09.0
	C RUNGE-KUTTA CONSTANTS			80004240	
	DO 298 I=1,14			80004250	
	GO TO (294,295,296,297,70),41			80004260	
294	DE1(I)=D1(I)			80004270	
	DE2(I)=D2(I)*H			80004280	
	E1=DE2(I)*.5			80004290	
	GO TO 298			80004300	
295	E1=D2(I)*.5*H			80004310	
	DE2(I)=DE2(I)+4.*E1			80004320	
	GO TO 298			80004330	
296	E1=D2(I)*H			80004340	
	DE2(I)=DE2(I)+E1+E1			80004350	
	GO TO 298			80004360	
297	E1=(DE2(I)+D2(I)*H)/5.			80004370	
300	D1(I)=DE1(I)+E1			80004380	
	I1=M1+1			80004390	
	GO TO 55			80004400	
	70 GO TO (540,550),44			80004410	
305	540 KOUNT=KCUNT+1			80004420	
	IF(D1(I)-A(22)) 550,597,580			80004430	
	550 IF(A9S(D1(3)-A(22)).LT..01) GO TO 597			80004440	
	4=-D1(3)-A(22))/D2(3)			80004450	
	44=2			80004460	
	41=1			80004470	
310	C NEXT TIME LINE			80004480	
	50 TO 55			80004490	
	380 IF(MOD(KOUNT,TPR4).NE.0) GO TO 25			80004500	
	CALL ED			80004510	
	50 TO 25			80004520	
315	597 CALL ED			80004530	
	RETURN			80004540	
	END			80004550	

BEST AVAILABLE COPY

	FUNCTION ARCTAN      74/74      OPT=1	FTN 4.5+414	09/12/77 17.09.
1	FUNCTION ARCTAN(P1,P2)		
	IF(P2) 2,1,2	ARC00090	
	1 IF(P1) 3,8,4	ARC00010	
	3 ARCTAN=4.7123890	ARCJ0020	
5	RETURN	ARC00030	
	4 ARCTAN=1.5707963	ARC00040	
	RETURN	ARC00050	
	2 IF(P1) 5,6,5	ARCJ0050	
	6 IF(P2.GT.0.) GO TO 8	ARC00070	
10		ARC00090	
	ARCTAN=3.1415927	ARC00110	
	RETURN	ARC00120	
	8 ARCTAN=.0	ARC00130	
	RETURN	ARC00140	
15	5 ARC=ATAN(P1/P2)	ARC00150	
	IF(P2) 10,9,9	ARC00170	
	10 ARCTAN=ARC+3.1415927	ARC00190	
	RETURN	ARC00200	
	9 IF(ARC) 11,12,12	ARC00210	
20	11 ARCTAN=ARC+6.2831853	ARC00220	
	RETURN		
	12 ARCTAN=ARC		
	RETURN		
	END		

BEST AVAILABLE COPY

## Appendix G

Coefficient Arrays Input

100005 12

cx	c( 1 )	cx	c( 1 )	cx	c( 1 )	cx	c( 1 )
		ALEMA	0.0000	2.0000	5.0000	10.0000	15.0000
MACH	0.0300	-0.2730	-0.2735	-0.2746	-0.2915	-0.2660	-0.2725
MACH	-0.300	-0.2730	-0.2735	-0.2766	-0.2585	-0.2860	-0.2725
MACH	0.100	-0.2916	-0.2930	-0.3010	-0.3225	-0.3175	-0.3110
MACH	-0.100	-0.3090	-0.3110	-0.3200	-0.3650	-0.3689	-0.3630
MACH	1.0100	-0.3690	-0.3965	-0.4200	-0.4520	-0.4610	-0.4550
MACH	1.1100	-0.5060	-0.5055	-0.5120	-0.5420	-0.5700	-0.5660
MACH	1.2100	-0.5210	-0.5216	-0.5260	-0.5560	-0.5840	-0.5790
MACH	2.0100	-0.5210	-0.5216	-0.5260	-0.5560	-0.5840	-0.5790
cyt	c( 1 )						
		ALPHA	0.0000	2.0000	4.0100	8.0000	10.0000
MACH	0.0100	.0213	.0043	.0028	.0461	.0631	.1343
MACH	.1100	.0213	.0043	.0298	.0441	.0631	.1343
MACH	.1000	.0012	.0013	.0033	.0112	.0170	.0270
MACH	.0100	-.0001	-.0036	-.0025	.0029	.0067	.0114
MACH	1.1100	-.0009	-.0012	-.0013	.0061	.1129	.2161
MACH	1.1100	-.0050	-.0051	-.0109	.0570	.1141	.2395
MACH	1.2100	-.0056	-.0023	-.0076	.0546	.1031	.2235
MACH	2.0100	.0056	.0023	.0076	.0366	.1031	.2170

BEST AVAILABLE COPY

CYR	21 5)								
MACH	0.0000	2.0000	4.0000	6.0000	8.0000	10.0000	15.0000	20.0000	25.0000
MACH	0.2100	0.0000	-0.0300	-0.1350	-0.5350	-0.7750	-2.1630	-5.9130	-12.5000
MACH	.4100	0.0000	-0.0300	-0.1350	-0.5350	-0.7750	-2.1630	-5.9160	-12.5000
MACH	.6100	0.0000	-0.0300	-0.1750	-0.6100	-0.4600	-1.1650	-2.8900	-6.1500
MACH	.8100	0.0000	-0.0300	-0.1050	-0.3500	-0.4400	-1.1000	-2.8000	-5.0000
MACH	1.0100	0.0000	-0.0700	-0.1670	-0.2950	-0.3300	-0.7800	-2.3720	-3.4570
MACH	1.2100	0.0000	-0.0800	-0.1600	-0.3120	-0.2540	-0.6000	-2.4630	-3.4000
MACH	1.4100	0.0000	-0.0800	-0.1600	-0.3100	-0.2650	-0.6750	-1.7700	-2.3500
MACH	1.6100	0.0000	-0.0800	-0.1600	-0.3100	-0.2650	-0.6750	-1.7700	-2.3500
C2	21 6)								
MACH	0.0000	5.0000	10.0000	15.0000	20.0000	25.0000	27.0000	50.0000	
MACH	0.2100	0.0000	-3.600	-7.500	-1.1900	-1.7100	-2.4600	-2.7800	-2.7800
MACH	.4100	0.0000	-3.600	-7.500	-1.1900	-1.7100	-2.4600	-2.7400	-2.7500
MACH	.6100	0.0000	-4.190	-8.000	-1.2900	-1.8750	-2.5400	-2.9150	-2.9150
MACH	.8100	0.0000	-3.600	-7.500	-1.3800	-1.9600	-2.6700	-3.0900	-3.0900
MACH	1.0100	0.0000	-4.100	-8.000	-1.4600	-2.1600	-3.0600	-3.6600	-3.6600
MACH	1.2100	0.0000	-4.100	-8.000	-1.4600	-2.1600	-3.0600	-3.6600	
MACH	1.4100	0.0000	-4.100	-8.000	-1.4600	-2.1600	-3.0600	-3.6600	
MACH	1.6100	0.0000	-4.100	-8.000	-1.4600	-2.1600	-3.0600	-3.6600	
MACH	2.0100	0.0000	-4.100	-8.000	-1.4600	-2.1600	-3.0600	-3.6600	

BEST AVAILABLE COPY

CLON CFS 91

	21.000	2.0000	6.0000	9.0000	10.0000	15.0000	20.0000	25.0000	25.0000
MACH	0.7100	+0.070	+0.070	+0.060	+0.065	+0.050	+0.060	+0.071	+0.045
MACH	0.710	+0.070	+0.070	+0.060	+0.065	+0.050	+0.060	+0.071	+0.045
MACH	0.710	+0.0552	+0.0627	+0.0634	+0.0665	+0.0690	+0.0704	+0.0677	+0.0596
MACH	0.710	+0.0567	+0.0562	+0.0561	+0.0585	+0.0606	+0.0610	+0.0602	+0.0561
MACH	1.0700	+0.0525	+0.0552	+0.0542	+0.0574	+0.0593	+0.0622	+0.0560	+0.049
MACH	1.0700	+0.0536	+0.0546	+0.0541	+0.0555	+0.0565	+0.0604	+0.0576	+0.0500
MACH	1.2100	+0.0546	+0.0543	+0.0547	+0.0552	+0.0567	+0.0582	+0.0530	+0.0446
MACH	2.0100	+0.0545	+0.0543	+0.0547	+0.0552	+0.0567	+0.0582	+0.0530	+0.0446
CLG64 C100									
	21.000	2.0000	6.0000	9.0000	10.0000	15.0000	20.0000	25.0000	25.0000
MACH	0.7100	+0.0000	+0.0000	+0.0060	+0.0123	+0.0251	+0.0343	+0.0311	+0.0314
MAR4	0.7100	+0.0000	+0.0000	+0.0060	+0.0123	+0.0251	+0.0343	+0.0311	+0.0314
MACH	0.7100	+0.0000	+0.0031	+0.0055	+0.0147	+0.0246	+0.0544	+0.0962	+0.1486
M2CH	0.7100	+0.0000	+0.0031	+0.0068	+0.0166	+0.0246	+0.0543	+0.1043	+0.1725
M2CH	1.0700	+0.0000	+0.0042	+0.0099	+0.0187	+0.0274	+0.0496	+0.0895	+0.1459
M1CH	1.0700	+0.0000	+0.0040	+0.0084	+0.0217	+0.0265	+0.0574	+0.0907	+0.1060
MATH	1.2100	+0.0000	+0.0050	+0.0059	+0.0166	+0.0259	+0.0543	+0.0860	+0.0940
MACH	2.0100	+0.0000	+0.0050	+0.0059	+0.0166	+0.0259	+0.0543	+0.0860	+0.0940

BEST AVAILABLE COPY

BEST AVAILABLE COPY

CNGA	C(17)	ALPHA	0.0000	2.0000	4.0000	6.0000	8.0000	10.0000	12.0000	14.0000	16.0000	18.0000	20.0000	22.0000	24.0000	26.0000	28.0000	30.0000
MACH	0.0700	0.0000	.0025	.0269	.1364	.2146	.5069	.9436	.9261	1.0669	1.0669	1.0669	1.0669	1.0669	1.0669	1.0669	1.0669	1.0669
MACH	.0100	0.0000	.0025	.0249	.1364	.2146	.5069	.9436	.9261	1.0569	1.0569	1.0569	1.0569	1.0569	1.0569	1.0569	1.0569	1.0569
MACH	.0100	0.0000	.0035	.0037	.1727	.3312	.7229	.9509	.5036	.2629	.2629	.2629	.2629	.2629	.2629	.2629	.2629	.2629
MACH	.0100	0.0000	.0031	.0057	.2021	.3780	.8345	1.0400	.6267	.3916	.3916	.3916	.3916	.3916	.3916	.3916	.3916	.3916
MACH	1.0700	0.0000	.0009	.0073	.2511	.4546	1.0030	1.2660	.4860	.3869	.3869	.3869	.3869	.3869	.3869	.3869	.3869	.3869
MACH	1.1700	0.0000	.0261	.0450	.2755	.4570	1.0010	1.2840	.8332	.6664	.6664	.6664	.6664	.6664	.6664	.6664	.6664	.6664
MACH	1.2700	0.0000	.0000	.0176	.2233	.3931	.9091	1.0051	.5373	.6214	.6214	.6214	.6214	.6214	.6214	.6214	.6214	.6214
MACH	2.0700	0.0000	.0000	.0176	.2233	.3931	.9091	1.0051	.5373	.6214	.6214	.6214	.6214	.6214	.6214	.6214	.6214	.6214
CND		C(19)																
MACH	0.0000	5.0000	8.0100	10.0000	12.0000	14.0000	16.0000	18.0000	20.0000	22.0000	24.0000	25.0000	25.0000	25.0000	25.0000	25.0000	25.0000	25.0000
MACH	0.0100	0.0000	.2309	.5300	.9200	1.5200	2.6000	4.6000	12.5000	19.5000	19.5000	19.5000	19.5000	19.5000	19.5000	19.5000	19.5000	19.5000
MACH	.0100	0.0000	.2300	.5300	.9200	1.5200	2.6000	4.6000	12.5000	19.5000	19.5000	19.5000	19.5000	19.5000	19.5000	19.5000	19.5000	19.5000
MACH	.0100	0.0000	.4700	.5900	.5000	.9300	1.5500	2.7000	6.6000	9.5000	15.4000	15.4000	15.4000	15.4000	15.4000	15.4000	15.4000	15.4000
MACH	.0100	0.0000	.5500	.4200	.2400	.5000	1.1400	2.2000	5.6000	8.0000	12.0000	12.0000	12.0000	12.0000	12.0000	12.0000	12.0000	12.0000
MACH	1.0100	0.0000	.1400	.1100	.0000	.0000	.4610	1.3500	5.0000	6.0000	6.7000	6.7000	6.7000	6.7000	6.7000	6.7000	6.7000	6.7000
MACH	1.1100	0.0000	.3000	.3300	.3200	.3000	.3000	.6900	4.1500	5.4100	6.7100	6.7100	6.7100	6.7100	6.7100	6.7100	6.7100	6.7100
MACH	1.2100	0.0000	.4500	.3200	.3000	.0000	.0000	.8000	3.3000	4.1000	4.7400	4.7400	4.7400	4.7400	4.7400	4.7400	4.7400	4.7400
MACH	2.0100	0.0100	.4500	.3200	.3000	.0000	.0000	.8000	3.3000	4.1000	4.7400	4.7400	4.7400	4.7400	4.7400	4.7400	4.7400	4.7400

BEST AVAILABLE COPY

CHINE 6 (200)

	$\Delta\text{MHA}$	0.0000	50.0000
MACH	0.0100	0.0714	0.0714
MACH	-0.100	0.0714	0.0714
MACH	-0.200	0.0618	0.0618
MACH	-0.300	0.0900	0.0900
MACH	-0.400	0.0973	0.0973
MACH	-0.500	0.0800	0.0800
MACH	-0.600	0.0727	0.0727
MACH	-0.700	0.0727	0.0727

卷之二

ALWMA	0.0003	2.0000	4.0000	8.0000	15.0000	25.0000	50.0000
MACH	0.111-3300	-115.0000	-119.0000	-126.0000	-136.5000	-154.0000	-194.0000
MACH	0.111-3300	-115.0000	-119.0000	-126.0000	-139.5000	-154.0000	-194.0000
MACH	0.111-3200	-161.0000	-162.4000	-165.5000	-164.0000	-176.3000	-178.3000
MACH	0.111-3200	-145.0000	-156.5000	-169.5000	-167.5000	-210.0000	-213.0000
MATH	1.0700	-130.0000	-147.0100	-169.5000	-192.0000	-215.3000	-215.0000
MATH	1.1100	-120.0000	-134.0000	-144.4000	-158.4000	-175.0000	-175.0000
MATH	1.27100	-131.0000	-123.0000	-111.0000	-97.4000	-83.5000	-83.5000
MATH	2.07100	-121.0000	-123.0000	-111.5000	-97.4000	-93.5000	-93.5000

BEST AVAILABLE COPY

Vita

James D. Schneider graduated from Oklahoma State University in 1962 with a Bachelor of Science degree in Mechanical Engineering. He entered pilot training, after receiving his commission through Officer Training School, and earned his aeronautical rating in February 1964. He accumulated twelve years of flying experience including instructor pilot in both the T-37 and T-38 trainers, aircraft commander in the F-4D, and operations pilot in the T-39. After completing an assignment to Headquarters Air Training Command as Operations Center Staff Officer, Major Schneider entered the Air Force Institute of Technology for study in Astronautical Engineering.

Permanent address: Fargo, Oklahoma 73840

SECURITY CLASSIFICATION OF THIS PAGE (When Data Entered)

REPORT DOCUMENTATION PAGE		READ INSTRUCTIONS BEFORE COMPLETING FORM
1. REPORT NUMBER AFIT/GA/AA77D-8 ✓	2. GOVT ACCESSION NO.	3. RECIPIENT'S CATALOG NUMBER
4. TITLE (and Subtitle)  MAGNUS EFFECT ON A BALLISTIC TRAJECTORY		5. TYPE OF REPORT & PERIOD COVERED  AFIT Thesis
7. AUTHOR(s)  James D. Schneider Major USAF		6. PERFORMING ORG. REPORT NUMBER
9. PERFORMING ORGANIZATION NAME AND ADDRESS  Air Force Institute of Technology (AU) ✓ Wright-Patterson AFB, Ohio 45433		10. PROGRAM ELEMENT, PROJECT, TASK AREA & WORK UNIT NUMBERS
11. CONTROLLING OFFICE NAME AND ADDRESS		12. REPORT DATE December, 1977
		13. NUMBER OF PAGES
14. MONITORING AGENCY NAME & ADDRESS(if different from Controlling Office)  Air Force Institute of Technology (AU) Wright-Patterson AFB, Ohio 45433		15. SECURITY CLASS. (of this report)  Unclassified
		15a. DECLASSIFICATION/DOWNGRADING SCHEDULE
16. DISTRIBUTION STATEMENT (of this Report)  Approved for public release; IAW AFR/190-17  Approved for public release, distribution unlimited.		
17. DISTRIBUTION STATEMENT (of the abstract entered in Block 20, if different from Report)		
18. SUPPLEMENTARY NOTES  Approved for public release; IAW AFR/190-17  JERRAL F. GUESS, CAPT, USAF Director of Information		
19. KEY WORDS (Continue on reverse side if necessary and identify by block number)  Ballistic Trajectory Magnus Lift Trajectory Simulation		
20. ABSTRACT (Continue on reverse side if necessary and identify by block number)  → The effect of Magnus coefficients, projectile spin rate, and pitching motion on lateral displacement of a ballistic trajectory is investigated by use of a six degree of freedom simulation. The coefficients had no significant effect. Increased spin rate extends the projectile impact point both down range and cross range. Oscillations induced by rate motion increased the lateral deviation but oscillations induced by an initial displacement did not. ←		